SONAR IMAGING OF BAY BOTTOM SEDIMENTS AND ANTHROPOGENIC IMPACTS IN GALVESTON BAY, TEXAS

A Thesis

by

DONALD SHEA MADDOX

Submitted to the Office of Graduate Studies of
Texas A&M University
in partial fulfillment of the requirements for the degree of

MASTER OF SCIENCE

December 2005

Major Subject: Geophysics

SONAR IMAGING OF BAY BOTTOM SEDIMENTS AND ANTHROPOGENIC IMPACTS IN GALVESTON BAY, TEXAS

A Thesis

by

DONALD SHEA MADDOX

Submitted to the Office of Graduate Studies of
Texas A&M University
in partial fulfillment of the requirements for the degree of

MASTER OF SCIENCE

Approved by:

Chair of Committee,	William W. Sager
Committee Members,	Thomas W.C. Hilde
	William R. Bryant
	Timothy M. Dellapenna
Head of Department,	Richard L. Carlson

December 2005

Major Subject: Geophysics

ABSTRACT

Sonar Imaging of Bay Bottom Sediments and Anthropogenic Impacts

in Galveston Bay, Texas. (December 2005)

Donald Shea Maddox, B.S., Millsaps College

Chair of Advisory Committee: Dr. William W. Sager

Knowledge of surface sediment distribution in Galveston Bay is important because it allows us to better understand how the bay works and how human activities impact the bay and its ecosystems. In this project, six areas of bay bottom were surveyed using acoustic techniques to make maps of bay bottom types and to investigate the types and extent of anthropogenic impacts. A total of 31 km^2 was surveyed in six areas, one in Bolivar Roads (6.1 km^2), one near Redfish Bar (3.1 km^2), two in East Bay (12 km^2), one southeast of the Clear Lake entrance (5.3 km^2), and one in Trinity Bay (4.3 km^2). Side-scan sonars (100 kHz and 600 kHz) were used to image the bay bottom, and a chirp sonar (2-12 kHz) was used to image subsurface sediment layers and bottom topography. In the side-scan records, objects as small as a few meters in extent were visible, whereas the chirp sonar records show a vertical resolution of a few tens of centimeters. The side-scan images display strong backscatter in some areas due to coarse sediments in addition to weak backscatter in areas of fine sediment. The bay bottom was classified using three levels of sonar backscatter ranging from high to low. Areas of differing sonar backscatter intensity were sampled with cores and grab-samples. High backscatter corresponded to coarse shell debris and oyster reefs, medium backscatter corresponded

to a sand-silt-shell mixture, and low backscatter corresponded to silty loam. Chirp sonar records were classified as one of nine different bottom reflection types based on changes in amplitude and stratigraphy. Parallel, layered sediments are seen filling the bay valley and resting atop a sharp contact at which the acoustic signal fades out. Along the flanks of the valley fill the acoustic response revealed an absent or weakly laminated stratigraphy, whereas areas of high oyster productivity produced mounds, strong surface returns, and strong, shallow subsurface reflectors surrounding current oyster reefs. Anthropogenic features imaged with the sonar included sediment disruptions, such as the ship channels, dredge holes, gouges, and trawl marks, as well as debris, such as submerged boats, pipes, and unidentified objects.

ACKNOWLEDGMENTS

I would like to thank Texas A&M University, the Department of Geology and Geophysics, the Department of Oceanography, NOAA (National Oceanic and Atmospheric Administration), and the Texas General Land Office (TGLO) for their support during this research project. Funding for this research was provided by the Coastal Management Program of the TGLO and Coastal Coordination Council pursuant to NOAA grants NA-02-009 and NA-03-11. I am indebted to the staff and students from the Department of Geology and Geophysics and Department of Oceanography at Texas A&M and the Department of Marine Science at Texas A&M Galveston who assisted in collecting the geophysical data. I also appreciate Dr. John Anderson and the Department of Earth Sciences for allowing me to use their laboratory equipment.

TABLE OF CONTENTS

LIST OF FIGURES

FIGURE Page

FIGURE Page

INTRODUCTION

Few studies have focused on anthropogenic impacts on the bay bottom and large scale sedimentation patterns in Galveston Bay. These types of data are important for geologists, engineers, and biologists because knowledge of surface sediment distributions and anthropogenic perturbations on the bay bottom have an effect on sedimentation, potential hazards, and biological production within the bay. Because Galveston Bay is partly surrounded by major cities and industrial areas, it is widely used and modified in order to keep channels and passages clear for commercial use.

The objective of this project was to map bay bottom sediment distribution, examine anthropogenic impact types and distribution in the bay. Studies of this type have been done in other bays, such as a survey in Chesapeake Bay that revealed 10 different bottom types (Wright et al. 1987), a survey in Monterey Bay displaying complex outcrop patterns and large sand bodies (Eittreim et al. 2001), a survey in the Northern Channel Islands where benthic habitats were mapped (Cochrane and Lafferty, 2002), and a similar survey in Chesapeake Bay to study pre-Holocene and recent oyster beds (Smith et al. 2003).

Similar surveys were also conducted in Galveston Bay. Powell et al. (1995) described an acoustic survey mapping oyster reefs using a dual frequency (27 and 300 kHz) acoustic profiler. While Powell's survey covered much of the bay, it used track lines spaced 0.4 km (¼ mi) apart and did not incorporate side-scan sonar, therefore gaps between prof[1]iles limited details and resolution that a high-resolution survey can provide.

This thesis follows the style of AAPG Bulletin.

In the present study, side-scan and chirp sonar were used to collect acoustic images of the bay bottom, and sediment samples were collected to correlate these images with sediment types. Due to the size of the bay, funding and time would not permit a complete survey, therefore small survey sites were spread throughout the bay, targeting different geological and utilization settings (Figure 1). Two surveys sites are situated astride the Houston Ship Channel, one located at Bolivar Roads, between Bolivar Peninsula and Galveston Island, and the other located southeast of Redfish Island. These two survey sites lie in the most utilized parts of the bay. The entrance of the Houston Ship Channel and the Galveston Island-Bolivar Peninsula ferry lane is located in the Bolivar Roads area and the Redfish Island area is located where the Trinity Ship Channel intersects the Houston Ship Channel and is also an area of numerous oyster farming leases. The other four sites are located ~4-7 km from the ship channel, and were chosen to examine whether anthropogenic impacts exist away from the ship channel and what changes occurred in sediment distribution in these areas. Two are in East Bay, one is outside of the Clear Lake entrance, and in Trinity Bay. One East Bay survey site is located north of Bolivar Peninsula whereas the other is located over the northwestern part of Hannah's Reef. The other survey sites are located in the northern bay, one is located several km east of the Clear Lake entrance and the other is located in the center of Trinity Bay.

The major hypothesis tested is that the majority of the anthropogenic impacts will center on the ship channels and docks (the most frequented sections of the bay) and that bottom types will vary depending upon the sedimentary influences and energy environments most active in the study areas.

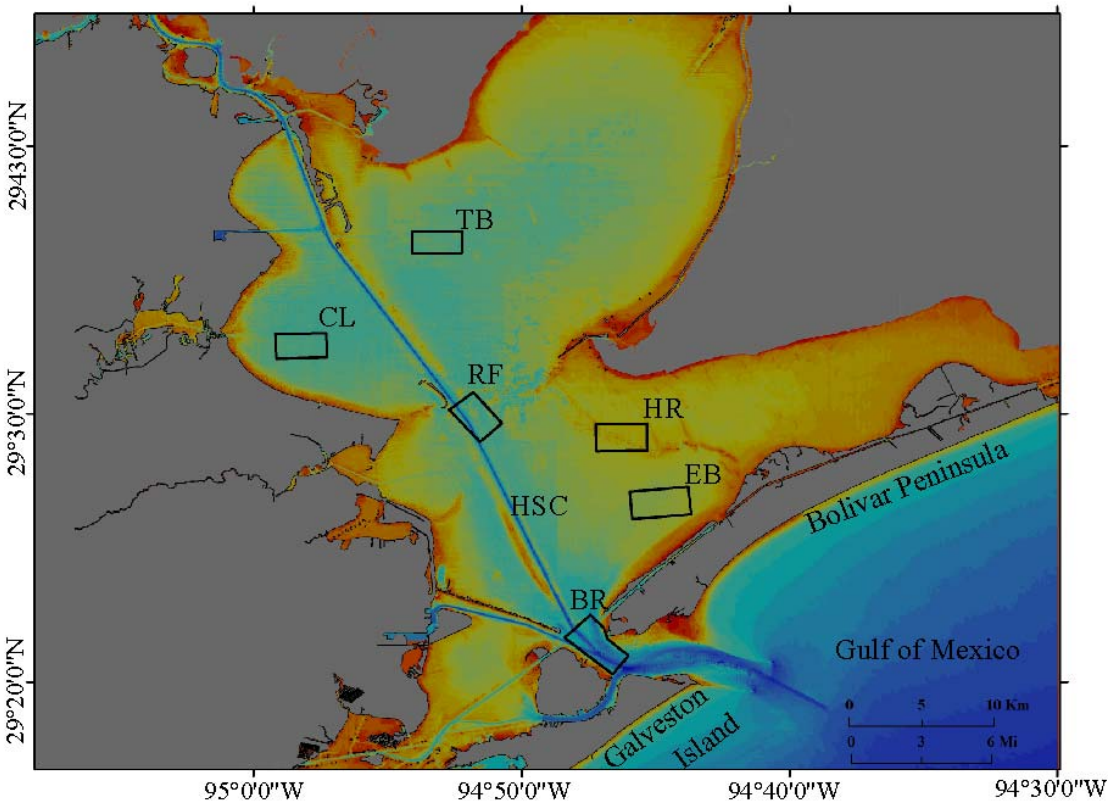

Figure 1. Bathymetry map of Galveston Bay, Texas. Map shows locations of the six survey sites: Bolivar Roads (BR), East Bay (EB), Hannah's Reef (HR), Redfish Island (RF), Clear Lake entrance (CL), Trinity Bay (TB), and Houston Ship Channel (HSC). Warm colors represent shallow water while cooler colors represent deeper water.

BACKGROUND

The geologic history of Galveston Bay is closely tied to the rise in sea level that flooded the Trinity River incised valley starting 18,000 years ago (Rodriguez et al. 1998). During the last glacial maximum, the Trinity and San Jacinto rivers incised the shelf and deposited sediment into the Gulf of Mexico at the shelf edge. After sea level rose and stabilized at the present level, these rivers deposited sediment in the bay, giving the bay its shallow depth and relatively flat bottom (Lankford and Rogers, 1969).

The bathymetry of the bay has been modified over the years by channel dredging, spoil bank construction, artificial island construction, and shell removal (Lankford and Rogers, 1969). Because of this extensive modification and high use we expected to find many anthropogenic impacts on the bay bottom, some of which may affect sediment distribution. The bathymetry map displays a shallow, relatively flat topography and numerous large-scale, man made features such as the ship channel, dredge spoil islands, and jetties (Figure 1). The Houston Ship Channel dissects the bay, starting between the north (NJ) and south jetties (SJ) off of Galveston Island and Bolivar Peninsula and ending in the northern section of the San Jacinto river mouth at the Port of Houston. Depths in the HSC average 14 m. Other ship channels visible are the Texas City Channel and the Intercoastal Waterway. The Texas City Channel averages ~12m in depth and connects the HSC to the refineries in Texas City. The Intercoastal Waterways runs parallel with Bolivar Peninsula and Galveston and averages ~4m in depth. The ship channels are displayed on the bathymetry map as blue to blue-green, linear features cutting through shallower sections of the bay.

Dredge spoils and jetties are also visible on the bathymetry image and as warm colors surrounded by cold colors. The dredge spoils are located along the immediate flanks of the HSC and as man-made islands throughout the bay. Jetties are displayed as linear features formed along the ship channel in order to keep sediment from collecting in the channels. Examples of these are the Texas City Dike north of the Texas City Channel, South Jetty off of Galveston Island, and North Jetty off of Bolivar Peninsula.

Oyster reefs and large oyster beds are visible in East Bay, west of Redfish Island, and near Smith Point. These are depicted as red highs surrounded by shallower colors on the bathymetry map. These areas existing in shallow waters of the bay and represent productive areas within the bay.

Two side-scan sonars were used in the study. Side-scan sonars emit a high frequency (100 kHz or 600 kHz) acoustic pulse through the water column. As the acoustic wave contacts the bay bottom the majority of the energy is reflected away, however a small amount is scattered back to the towfish and is converted into an electrical signal. This returning pressure wave is referred to as “backscatter” and is a function of the properties of sediment and surficial materials, particularly the physical roughness of the marine bottom and objects on the bottom, and the angle of incidence of the sonar beam as it encounters the surface (Barnhardt et al. 1998). The side-scan sonar insonifies the seabed on both sides of the towfish, imaging a swath of bottom as it moves forward. For this survey, hard, stiff materials yield a strong surface return which is displayed as a dark backscatter while soft materials yield a weak return and are displayed as light backscatter (Barnhardt et al. 1998). There is also contrast of shade depending on topography and shadows of objects lying on the bay bottom. The resulting image resembles an aerial

photograph and is interpreted by examining different areas of contrasting shades and patterns.

Chirp sonar is used to study the shallow subsurface geology of marine environments. It releases a pulse of continuous frequencies from 2 kHz to 12 kHz, which penetrates into the subsurface and is reflected back to the towfish. The return wave is converted into electrical signals represented by pixels, and is displayed in sonar pulse travel time versus distance. The chirp data allow interpretation of the layers of sediment beneath the estuary bottom, giving detail equivalent to a scale of 10-20 cm (Lee et al. 2002). By examining the layering and amplitude of the seismic return it is possible to differentiate between hard material, such as an oyster reef, and soft material, such as estuarine mud.

METHODS

Because of logistical and financial constraints, field work was divided into two phases. The Bolivar Roads and Redfish Island survey sites were completed during the first phase, whereas the remaining four survey sites were completed during the second. The swath width used for all surveys was 100 m. The survey areas total 31 km^2 and contain 228 survey lines oriented in an N-S and E-W direction (Appendix A).

The survey lines for the first two survey sites were spaced 50 meters apart, imaging all of the bay bottom twice and therefore providing 100% overlap of data. The last four survey sites consisted of lines spaced 75 meters apart, providing 50% overlap of data. The lesser coverage for the last four survey sites was a compromise to allow for greater area coverage.

For the Bolivar Roads and Redfish Island survey area, the side-scan sonar was towed ~20 m behind the boat from an A-frame. Deeper water in these areas allowed the sonar to be towed below the area of high surface noise in the bay. The side-scan sonar was towed from a davit on the starboard side of the boat (submerged ~1.5 m beneath the hull) during the other four surveys. This allowed me to image the bay bottom in the shallow water while keeping the sonar away from the noise of the propellers at the rear of the boat. Because the survey was conducted in shallow water, surface noise from choppy water, schools of fish, and passing ship wakes was often imaged and appears as "spotty" high backscatter and linear high backscatter features that are not observed on overlapping records (i.e. is not a fixed object). The chirp sonar was towed from a davit on the port

side of the ship on all six surveys. The sonar hydrophones were submerged ~1 m below the water surface and the instrument was kept forward of the boat engines.

Side-scan sonar data from the Bolivar Roads and Redfish Island survey areas were collected, processed, and mosaicked using CodaOctopus *Geosurvey Office* software. Side-scan data from the remaining survey sites was collected using Marine Sonic *Sea Scan PC* acquisition software and were processed and mosaicked using Chesapeake Technologies *SonarWeb Pro*. The mosaics were interpreted by examining different levels of backscatter. Backscatter intensity was then classified as high, medium and low. In the images presented from this study, high return is imaged as black or dark gray and represents coarse, angular material whereas low return is displayed as light gray or white and likely represents finer material. The mosaic was then examined in detail for visible bay bottom textures and features.

Chirp data from Bolivar Roads and Redfish Island survey areas were interpreted from paper records printed from Edgetech's *X-star* software. Chirp data from the remaining four survey sites were processed and interpreted using Triton Elics *DelphMap* and *SGIS* software. The chirp data were interpreted by examining different bottom reflection returns and changes in stratigraphy over the survey area.

Short cores and grab samples were collected after the side-scan and chirp data were processed and interpreted. Core and grab sample locations were chosen by examining differences in bay bottom backscatter from the side-scan mosaics. The cores were then processed and correlated to the geophysical data. Twenty-six gravity cores and eighty-two grab samples were collected in order to compare the seismic data with sediment texture and content. Three different sediment collection techniques were used to collect

the samples. In water deeper than 3 m, samples were collected using a gravity corer, in shallower sections of the bay cores were collected by pushing them into the bay bottom. A clam-shell grab sampler was used to obtain surface samples from all sections of the survey area. Cores were cut along the long axis and physically described for grain-size, color, visible structures, and composition. Selected cores were later sectioned and x-rayed to examine internal structure, non-visible to the naked eye. Grab samples were photographed and correlated with areas of different backscatter in the side-scan records.

Surface sediment was later placed in a 100 ml beaker with distilled water and one unmeasured scoop of sodium hexametaphosphate in order to disaggregate the clay particles. The samples were then mixed using a magnetic stirrer. Using a pipette, ~6 ml of sample were withdrawn from the beaker and placed in a Malvern APA2000 particle size detection unit, which passes the sample in front of a laser and measures the grain size spectrum. This data were then used to determine percentages of sand, silt, and clay in the survey areas.

The surveys used differential global positioning satellites (DGPS) in order to determine location in the bay. DGPS recorded the ship's position with a resolution of ~5 m. A layback correction was later applied to the sonar records during processing to account for the difference between the recorded position of the boat and the actual position of the sonar.

All data and results were placed into an ESRI *ArcGIS* project displaying locations, mosaics, sediment types, bay bottom types, bottom reflection types, anthropogenic impact locations, and oyster bed locations, allowing for the integration and interpretation of all data and for detailed map creation.

RESULTS

Side-scan Sonar Data

Side-scan sonar data from Bolivar Roads were divided into three levels of backscatter: high, medium, and low. High backscatter was found in the ship channel, along the immediate sides of the ship channel, and to the north of the ferry lane (Figure 2). Medium backscatter was imaged along the northwest, southwest, and northeast sides of the mosaic in shallower water along the sides of the ship channel. Low backscatter was observed in the southeast section of the mosaic in an area where extensive sand dunes were visible (Figure 3).

The sonar records also showed a wide variety of anthropogenic impacts in this area (Figure 4). In the west-central section of the survey area, to the north of the ferry lane, the bay bottom displayed numerous linear sediment disturbances and gouges. These gouges are most likely made as shrimp trawlers drag their drag their otter boards along the bay bottom. The majority of objects located in the survey area were seen adjacent to the ship channel and varied in size and shape. The largest object seen in this area was a cylindrical object surrounded by pipes in the south-west section of the survey area. Other objects that scattered the bay bottom in this survey area were pipes, small vessels, and numerous unidentified items (Figure 5) (Appendix B).

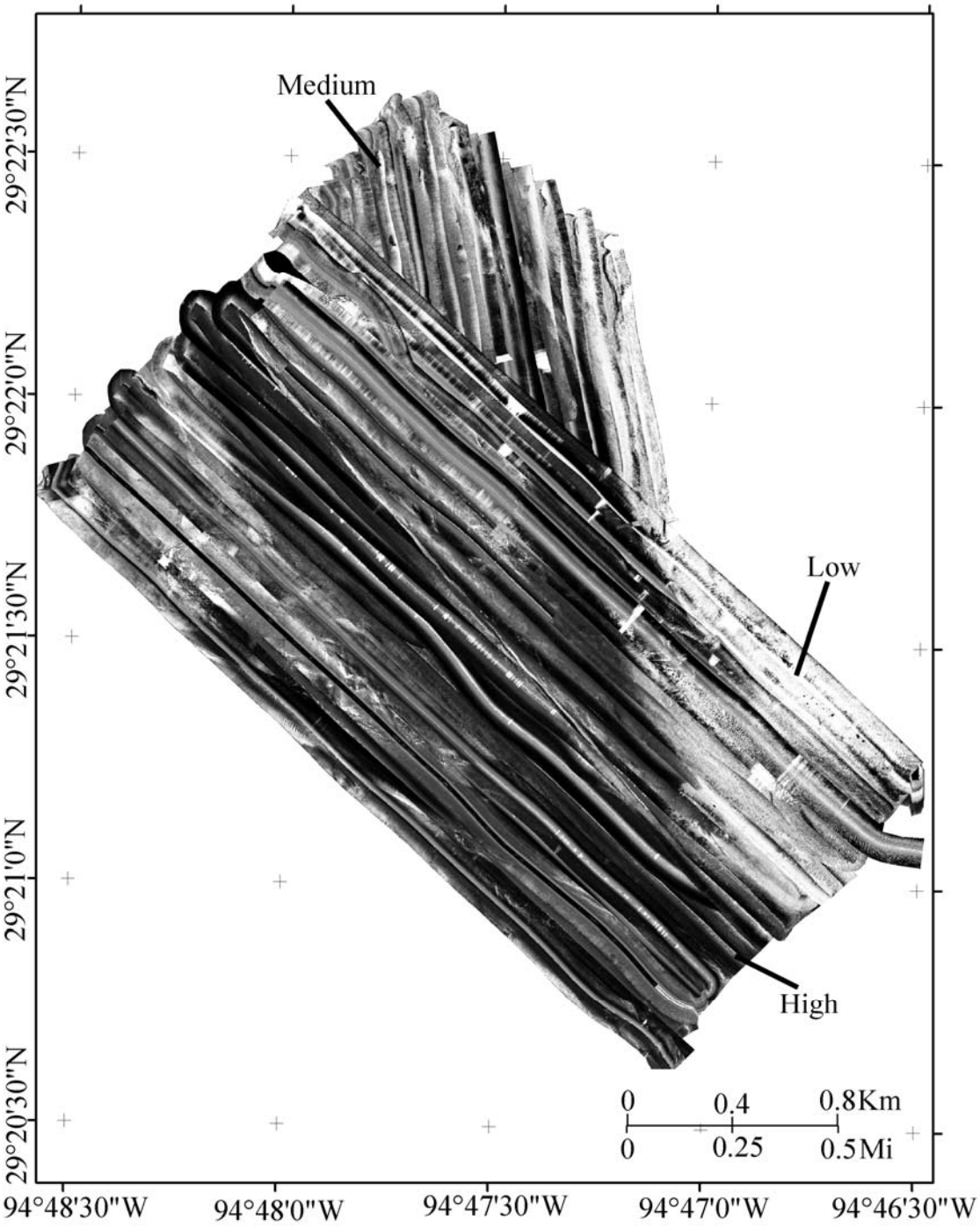

Figure 2. Side-scan sonar mosaic of the Bolivar Roads survey area. Mosaic displays locations of high, medium, and low acoustic return. High backscatter is shown as dark shades whereas low backscatter appears as light shading.

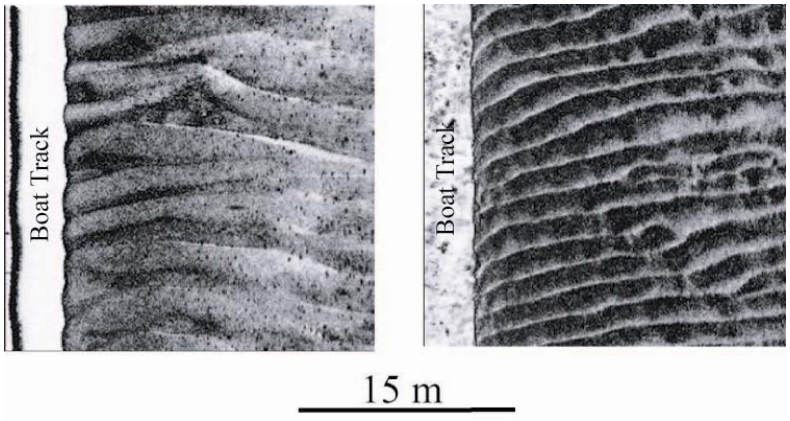

Figure 3. Side-scan sonar image of sediment waves located in the Bolivar Roads area. High backscatter is shown as dark shades whereas low backscatter appears as light shading.

The side-scan sonar records from Bolivar Roads also showed a variation in bay bottom textures. The alternating high low bands in the southeastern section of the survey area are the most widespread bedforms found in the survey area. The features cover ~ 1 km^2 of the southeastern section of the survey area. The distance between alternating bands of backscatter is between 5-10 m, increasing from south to north. In the northern area of the banded section, the banding trends from north-south. In the northeast, northwest, and southwest, chaotic, alternating bands are seen. These features are usually linear and trend in different directions depending on which area of the survey they are found. More consistent high-low amplitude banding was imaged in the center of the ship channel. These areas of banding are aligned perpendicular with the ship channel and the distance between banding is ~7 m. In the east central section of the survey site there were north-south trending vertical furrows as the side-scan sonar backscatter transitioned from low backscatter to medium backscatter (Figure 6). Similar features were interpreted as furrows caused by neap tidal currents as described by Dellapenna et al. (1998) in Chesapeake Bay using a similar side-scan sonar system.

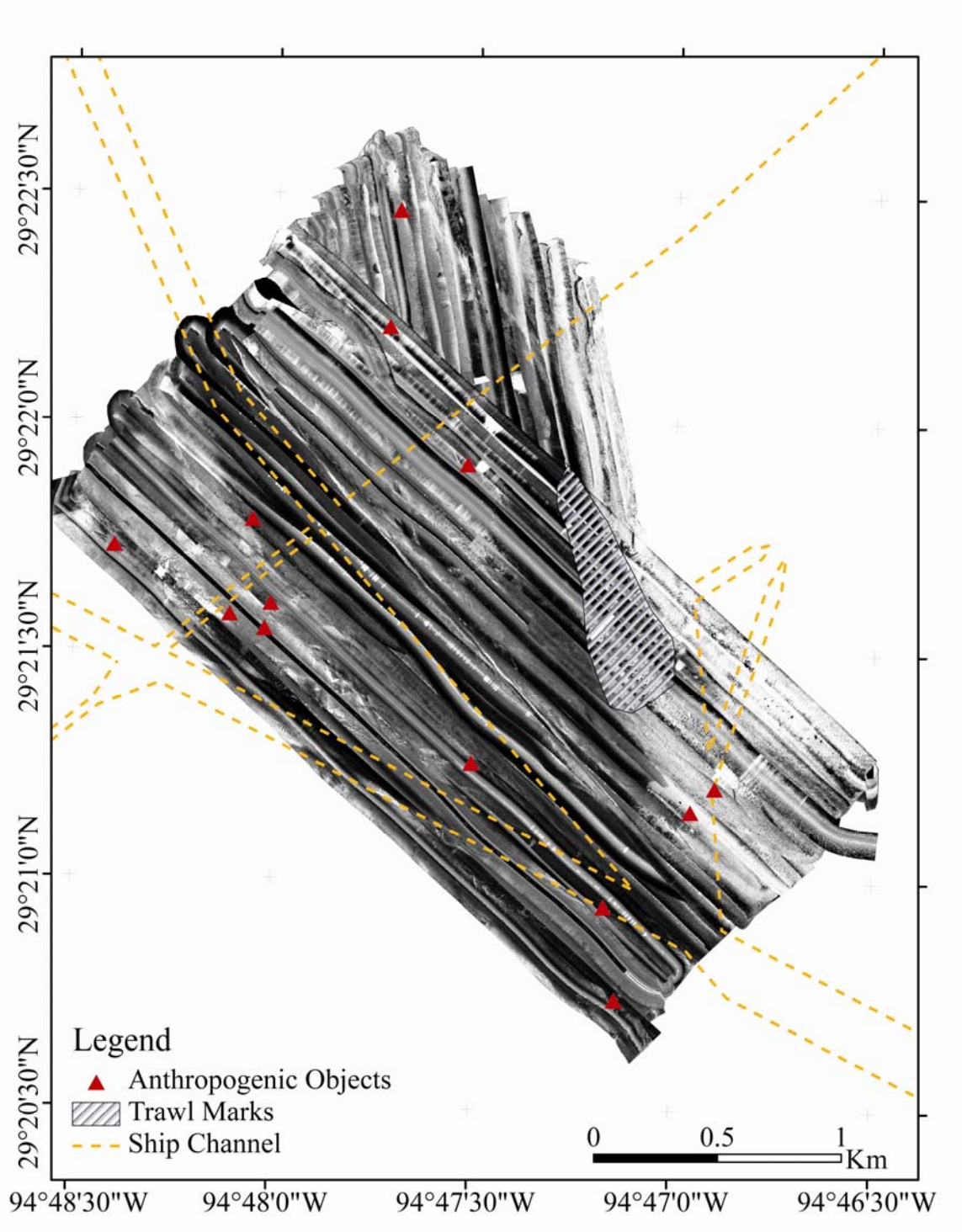

Figure 4. Anthropogenic impacts in the Bolivar Roads survey area. High backscatter is shown as dark shades whereas low backscatter appears as light shading.

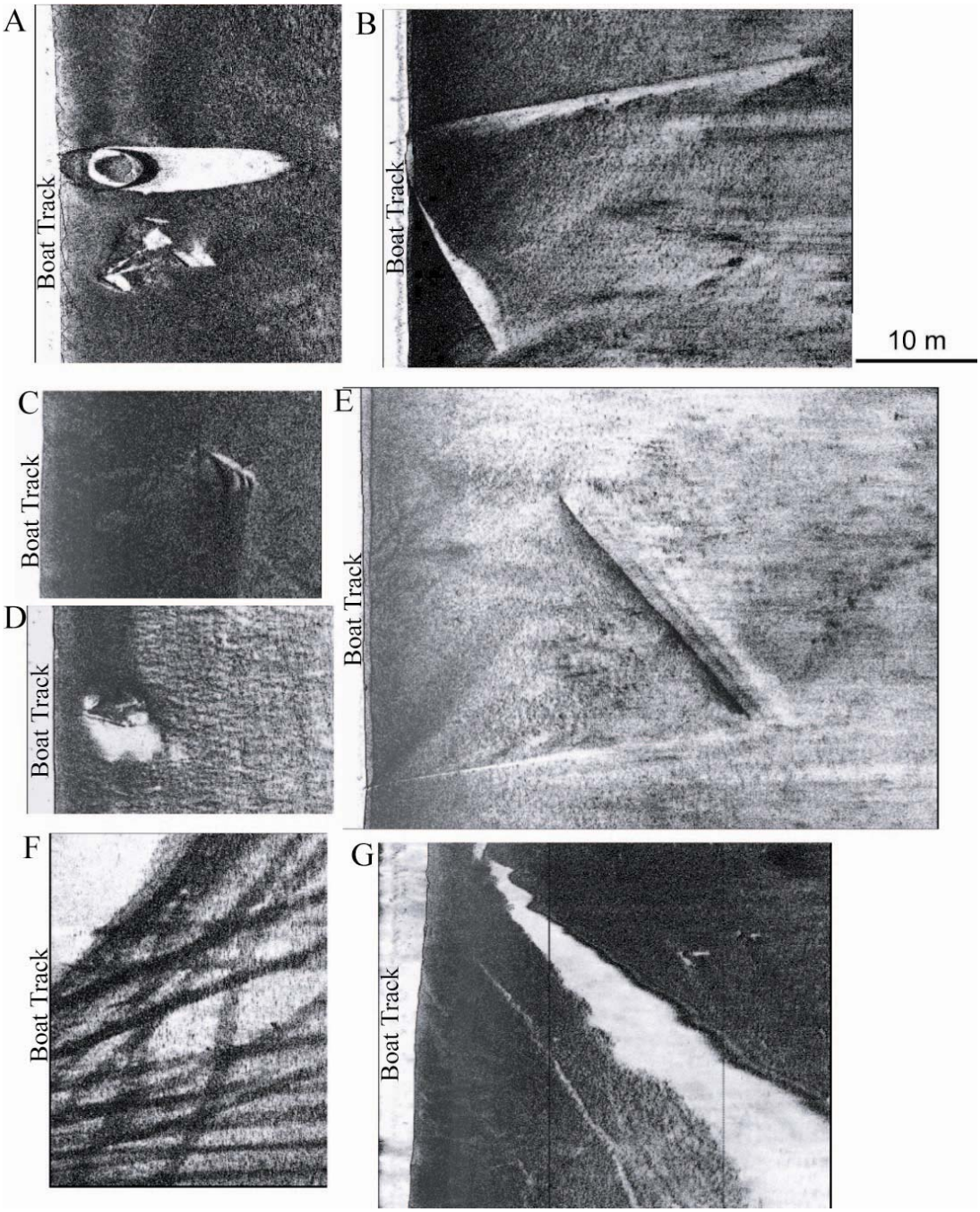

Figure 5.Sonar images of anthropogenic impacts in the Bolivar Roads survey area. **A** shows a large cylindrical object; **B** shows a large bent pipe; **C**, **D**, and **E** display various unidentified objects; **F** shows bay bottom gouges from shrimp trawls; **G** displays the edge of the Houston Ship Channel. High backscatter is shown as dark shades whereas low backscatter appears as light shading.

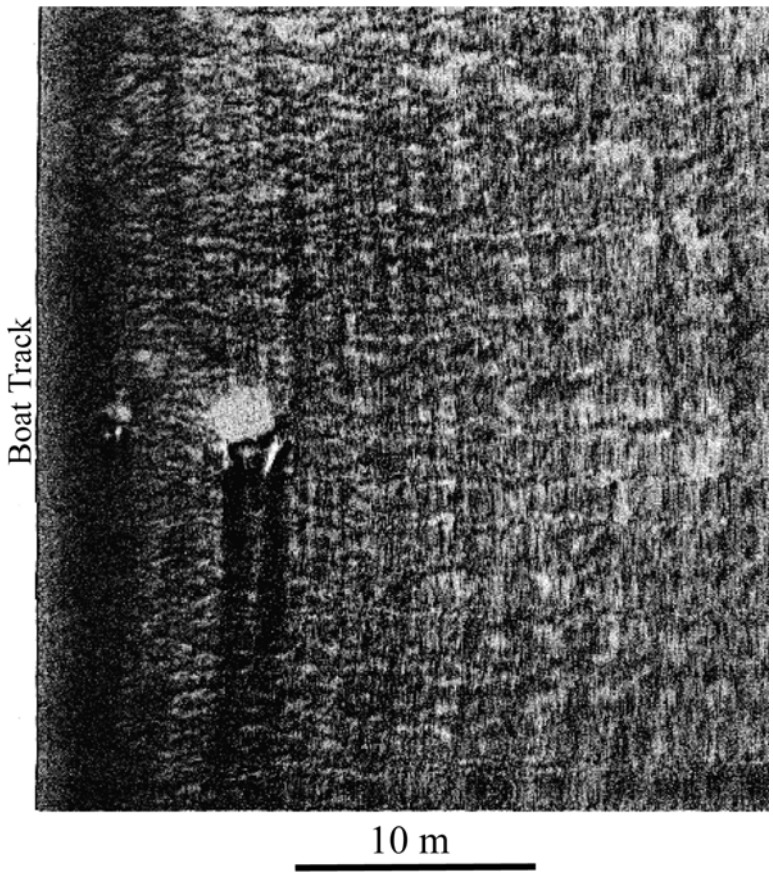

Figure 6. Side-scan sonar image of furrows in the Bolivar Roads survey area. High backscatter is shown as dark shades whereas low backscatter appears as light shading.

Side-scan sonar data from Redfish Island also display three levels of backscatter that were classified as high, medium, and low (Figure 7). High backscatter was seen in the eastern section of the survey area where there is a large concentration of oyster reefs. Medium backscatter is seen along the western section of the survey area. Low backscatter is observed as semi-circular features in the eastern and north-central sections of the mosaic.

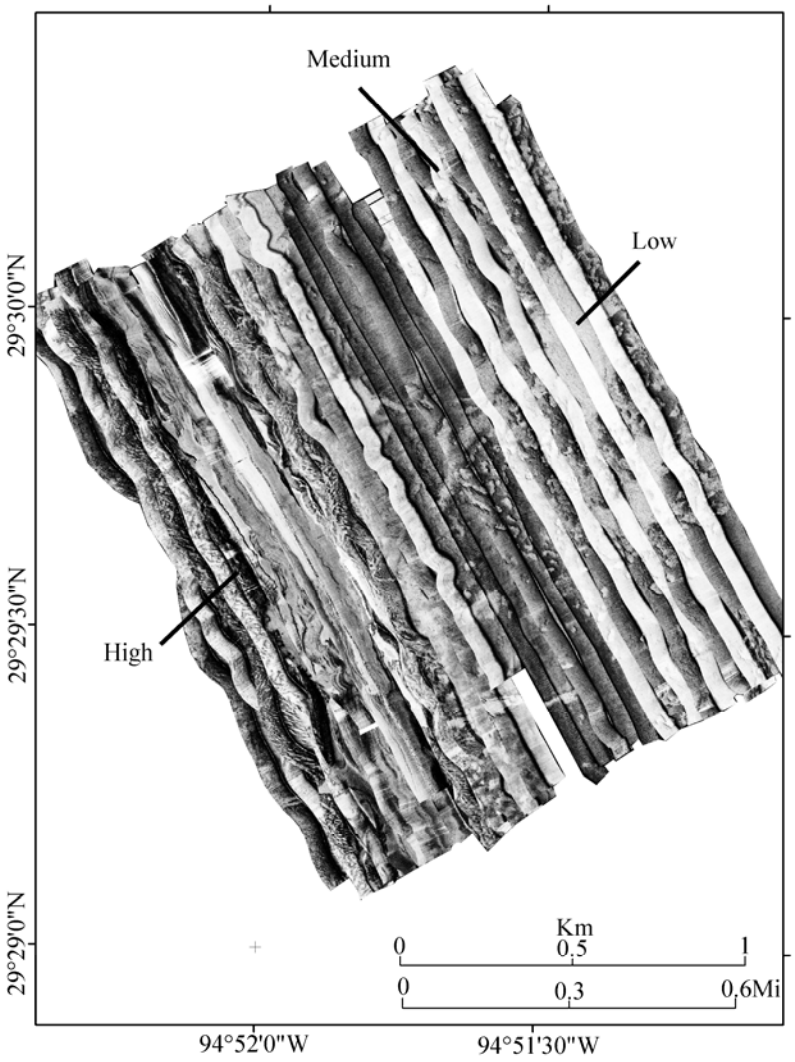

Figure 7. Side-scan sonar mosaic of the Redfish Island survey area. High backscatter is shown as dark shades whereas low backscatter appears as light shading.

Sonar data displayed several anthropogenic impacts in the Redfish Island survey area (Figure 8). Numerous circular bay bottom gouges were seen on the bay bottom in this area, probably due to oyster dredging. Oysters are harvested by dragging a metal dredge along the bay bottom while piloting the boat in circles. The dredge may create large grooves in the bay bottom as it displaces sediment and picks up oysters. Other anthropogenic impacts found in this area are depressions and dredge spoil banks. The

large depressions were probably created between 1935 and 1945 when the U.S. Army removed shell to build military bases (Powell et al. 1995). These were imaged by the side-scan as low amplitude circular returns with high backscatter along the edge of the depression farthest from the towfish (Figure 9). The dredge spoil banks were built up on the sides of the ship channel by the Army Corps of Engineers after removing sediment from the ship channels. Two spoil banks in this area were imaged by the side-scan sonar and are displayed as low backscatter returns tapering off to the west. These show signs of failure and flow which is depicted by westward thinning of the low amplitude acoustic return (Figure 10). Anthropogenic impacts are also seen in the western side of the survey area as vertical, linear high returns resembling pipes or circular or linear sediment disruptions resembling dredge marks and pipes (Figure 11) (Appendix B).

Bottom features in the Redfish Island survey area were difficult to interpret due to the weaving of the boat during the collection of data as we were forced to avoid numerous oyster boats during the survey. The most obvious bottom texture in this survey area is located in the center of the ship channel as alternating high-low amplitude backscatter similar to those found in Bolivar Roads and chaotic, spotty returns.

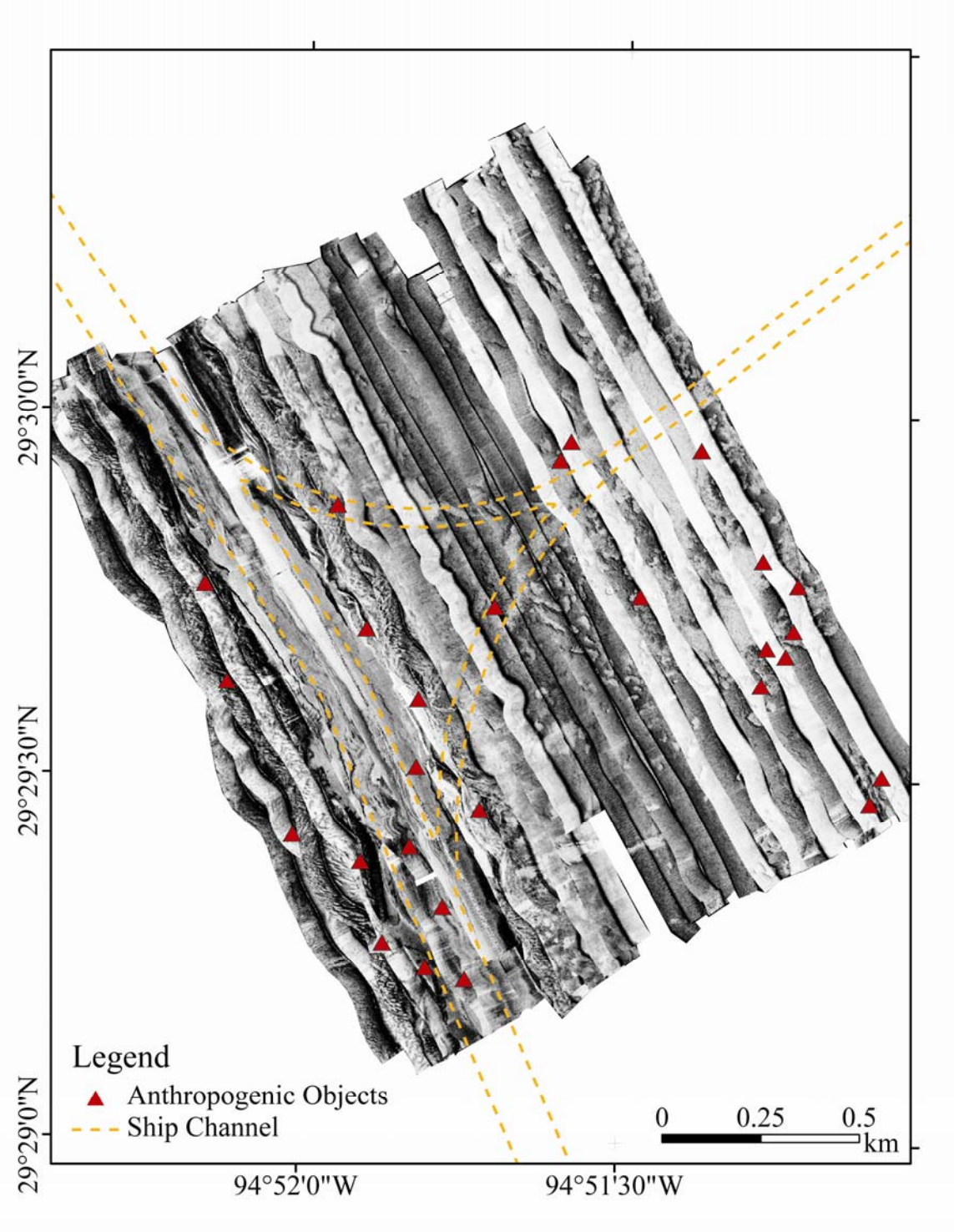

Figure 8. Anthropogenic impacts in the Redfish Island survey area. High backscatter is shown as dark shades whereas low backscatter appears as light shading.

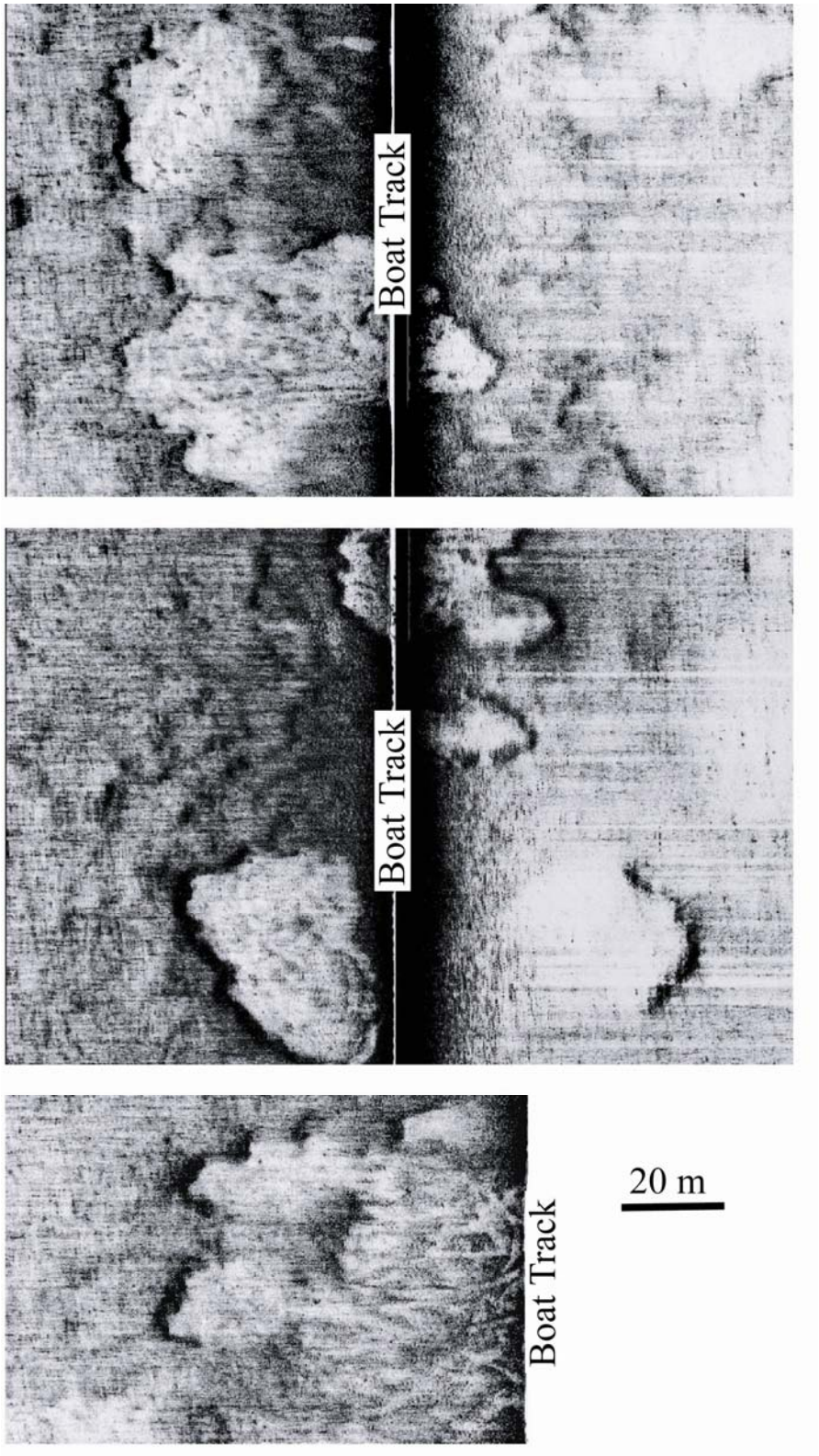

Figure 9. Side-scan sonar images of depressions in the Redfish Island survey area. High backscatter is shown as dark shades whereas low backscatter appears as light shading.

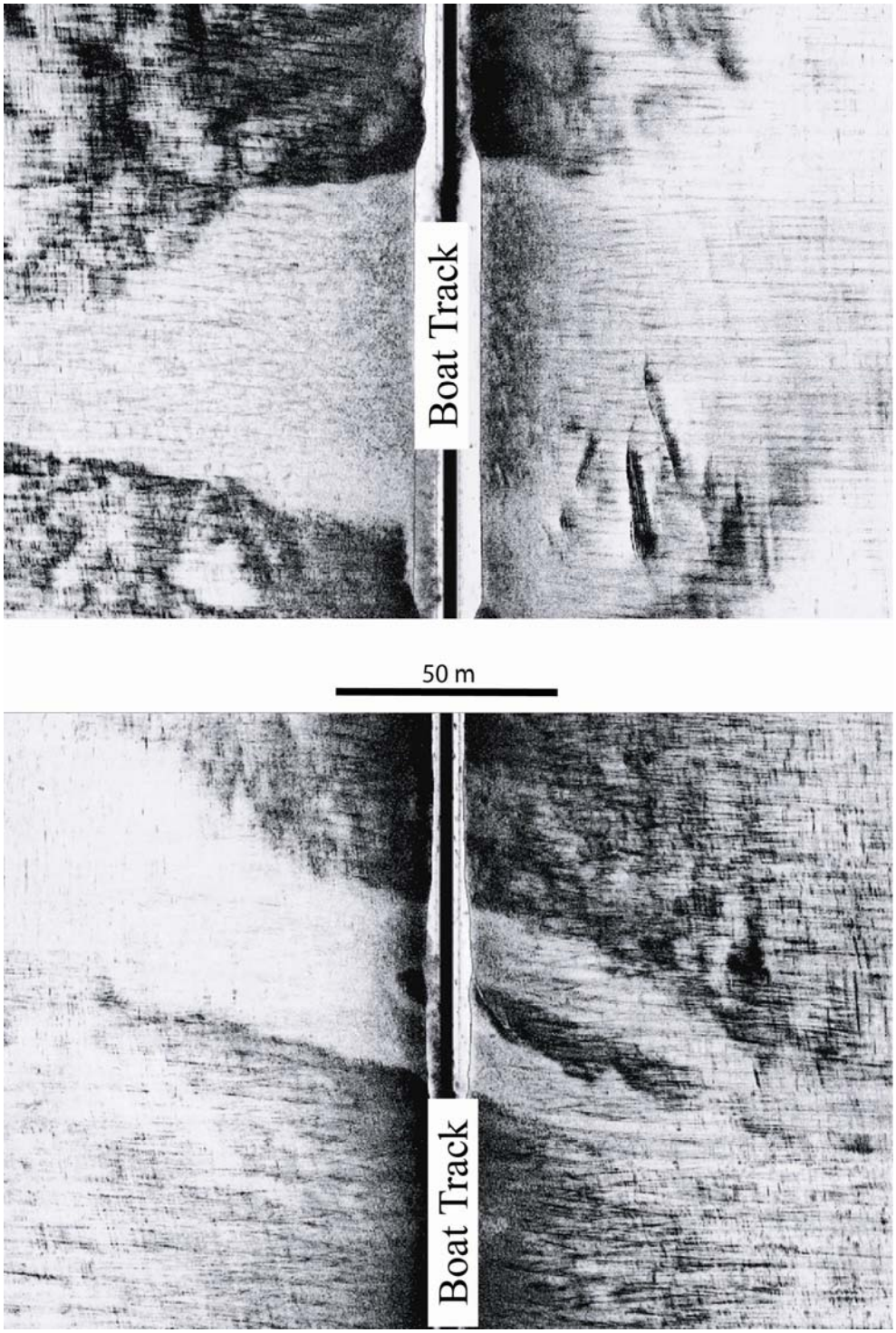

Figure 10. Side-scan sonar images of spoil banks in the Redfish Island survey area. High backscatter is shown as dark shades whereas low backscatter appears as light shading.

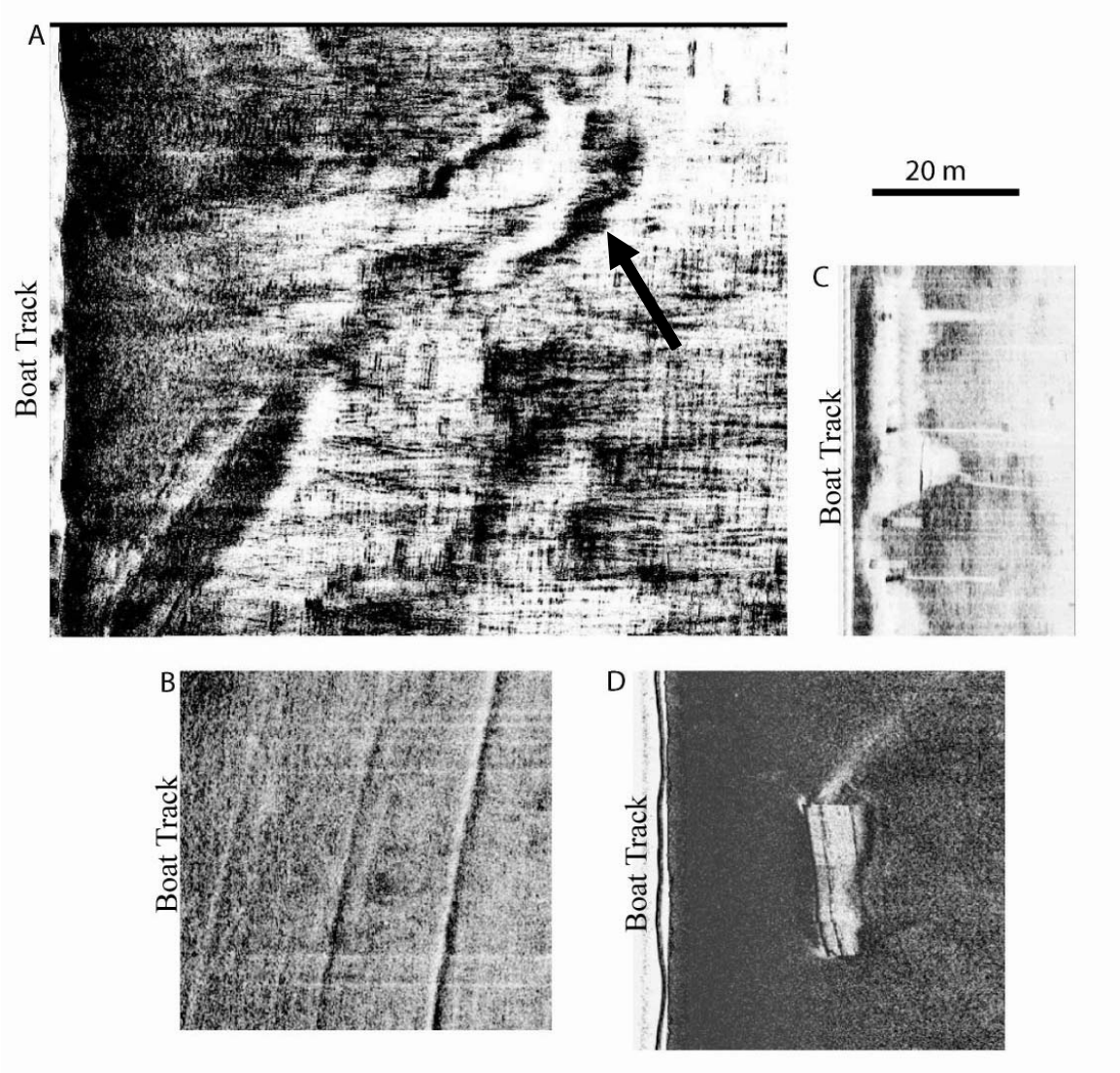

Figure 11. Side-scan images of anthropogenic impacts in the Redfish Island area. **A** shows a circular gouge mark on the bay bottom possible caused by oyster dredging; **B** shows parallel gouges from shrimp trawling; **C** shows a row of vertical pipes delineated by shadows perpendicular to sonar track; **D** shows a large unknown object lying on the bay bottom. High backscatter is shown as dark shades whereas low backscatter appears as light shading.

Side-scan sonar data in southern East Bay survey site revealed a single, uniform, low backscatter (Figure 12). The mosaic displayed few anthropogenic impacts in this area. The majority of the impacts in the area consisted of long, linear grooves or disruptions which have been interpreted as shrimp trawl marks. The mosaic also displayed boat wakes from shrimp fisherman trawling in the survey area during the survey and numerous small, and inconsistent, dark spots which are thought to be surface noise from choppy water or schools of fish.

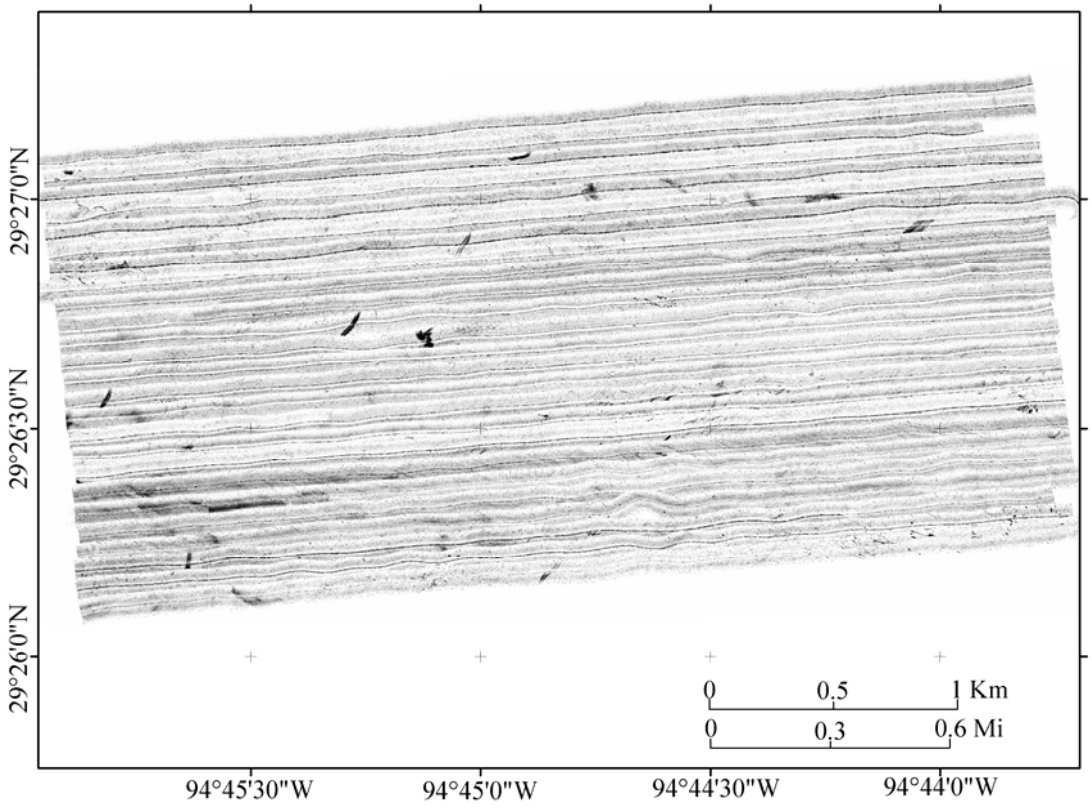

Figure 12. Side-scan sonar image of the East Bay survey site. Mosaic shows a relatively uniform acoustic return. Many of the larger dark spots on the mosaic represent boat wakes from passing shrimp trawlers working in the area during the survey.

Side-scan sonar data from the Clear Lake entrance, Hannah's Reef, and Trinity Bay survey sites each show mainly two bay bottom types consisting of high and low backscatter (Figures 13, 14, 15). In each of these sites, high backscatter is seen as sub-circular patches on the mosaic surrounded by areas of low backscatter. Like other areas of the bay, the majority of the anthropogenic impacts at these survey areas are linear bay bottom gouges (Figure 16).

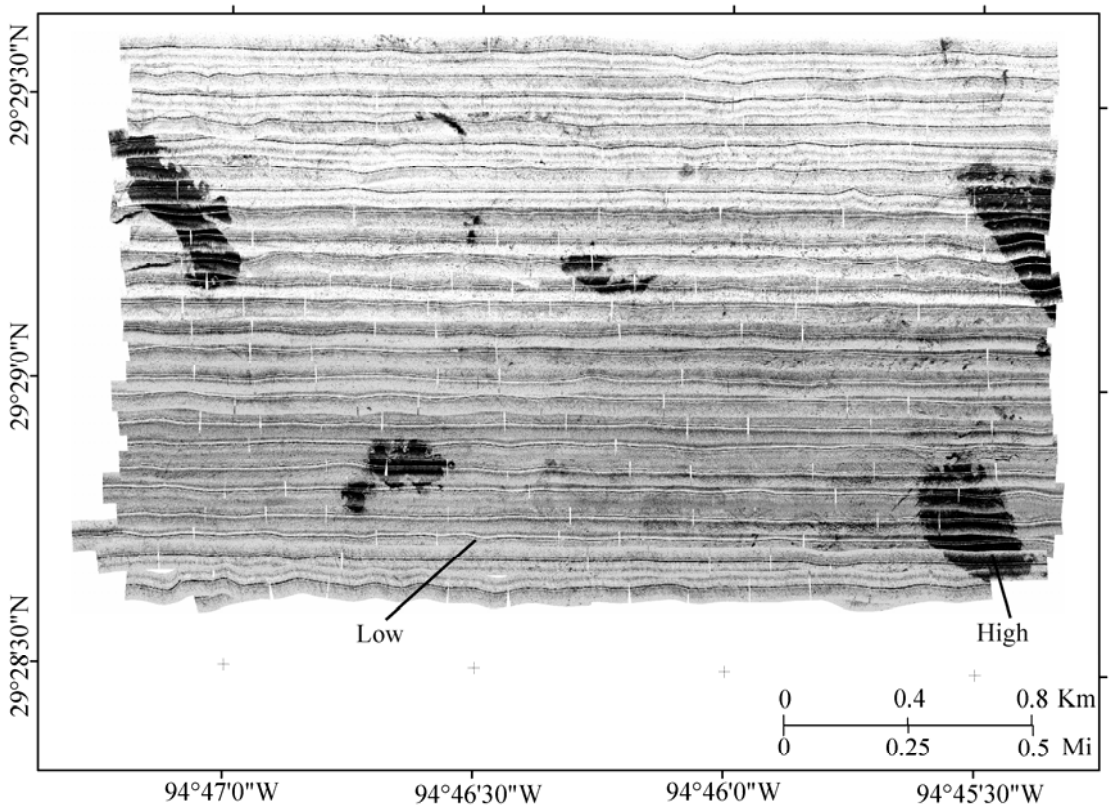

Figure 13. Side-scan sonar mosaic of the Hannah's Reef survey area. Light shades represent low backscatter while dark shades represent high backscatter.

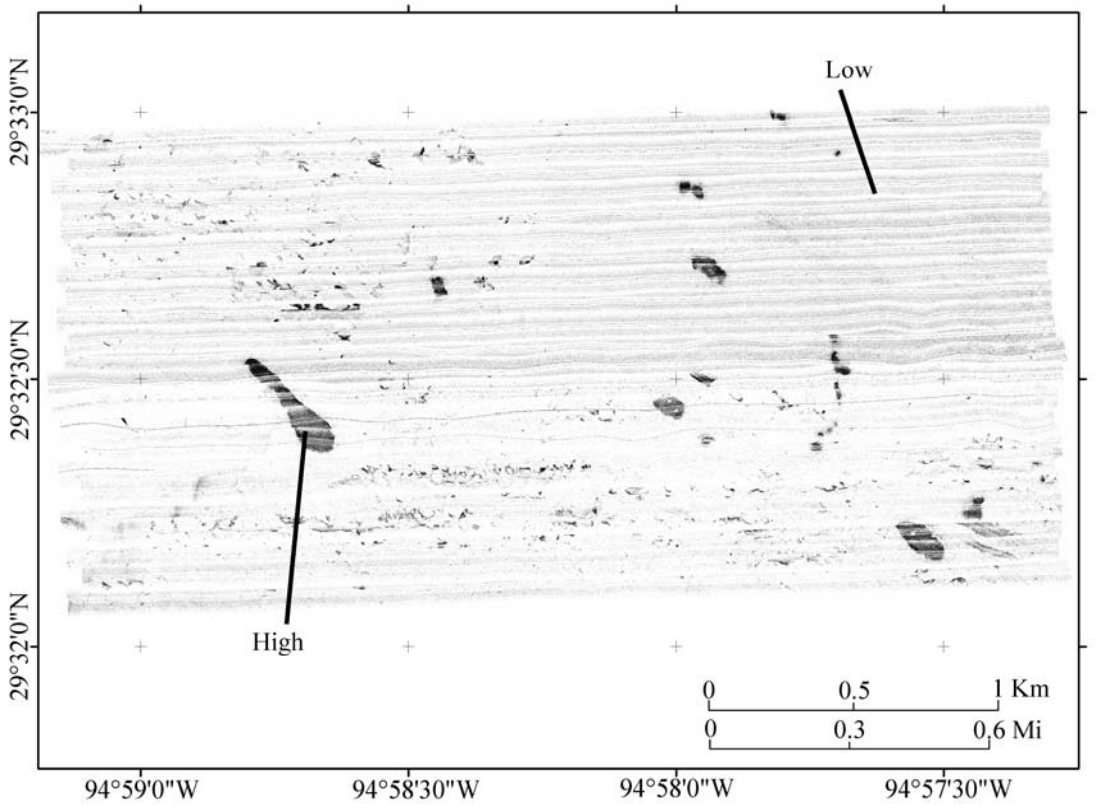

Figure 14. Side-scan sonar mosaic of the Clear Lake entrance survey area. Light shades represent low backscatter while dark shades represent high backscatter.

Chirp Sonar Data

A total of 9 seismic reflection types were classified in the survey areas (Figure 17). The change in seismic reflection corresponds to different sediment properties and disturbances (Figure 18). Seismic Reflection Type (SRT) 1 displays deep penetration and horizontal strata layering until the acoustic signal comes into contact with an irregular horizon. SRT 1 is found in the Redfish Island site in the shallower sections of the survey area along the sides of the ship channel, and in the southwestern section of the Hannah's Reef site (Figure 19, 20).

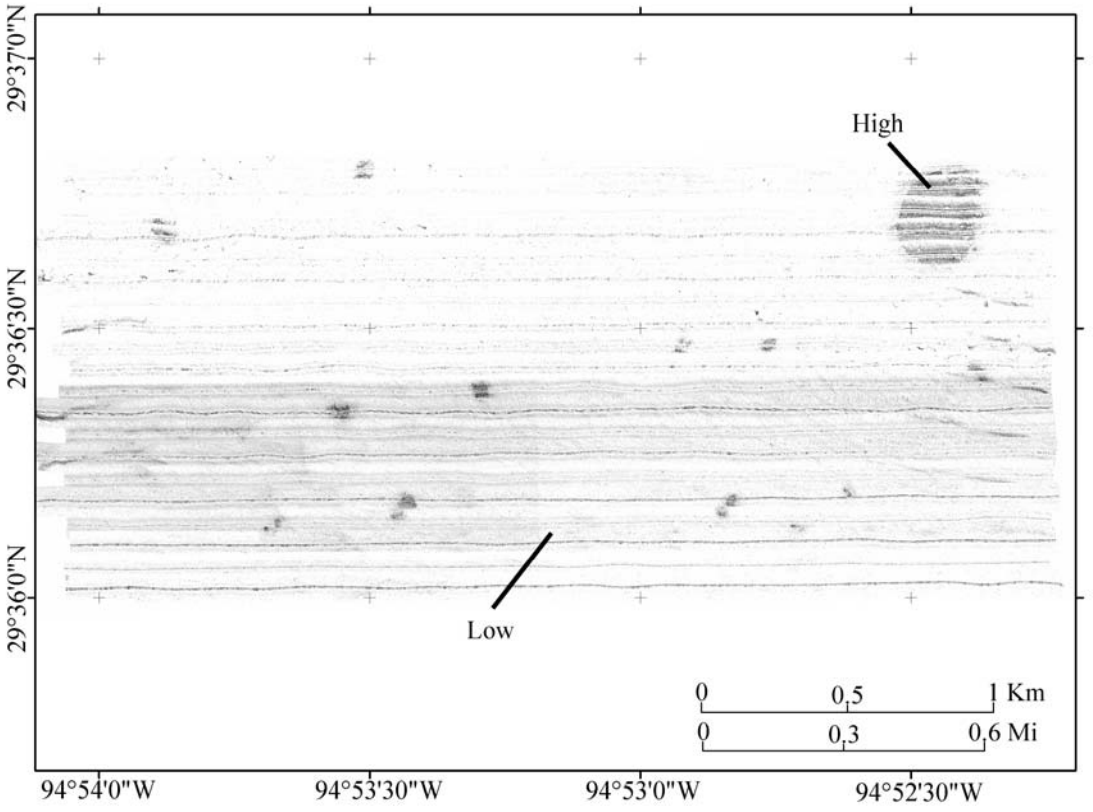

Figure 15. Side-scan sonar mosaic of the Trinity Bay survey area. Light shades represent low backscatter while dark shades represent high backscatter.

Seismic reflection type 2 displays shallow penetration and chaotic bedding. This reflection type is located in the south-east portion of Bolivar Roads and in the ship channel of the Redfish Island survey site (Figure 21).

SRT 3 displays shallow penetration and acoustic reverberation (a prolonged echo), which shows no internal structure in the subsurface. In Bolivar Roads this reflection type is located in the southwest, northwest, and northeast sections of the survey area and in the northcentral section of the Redfish Island survey area.

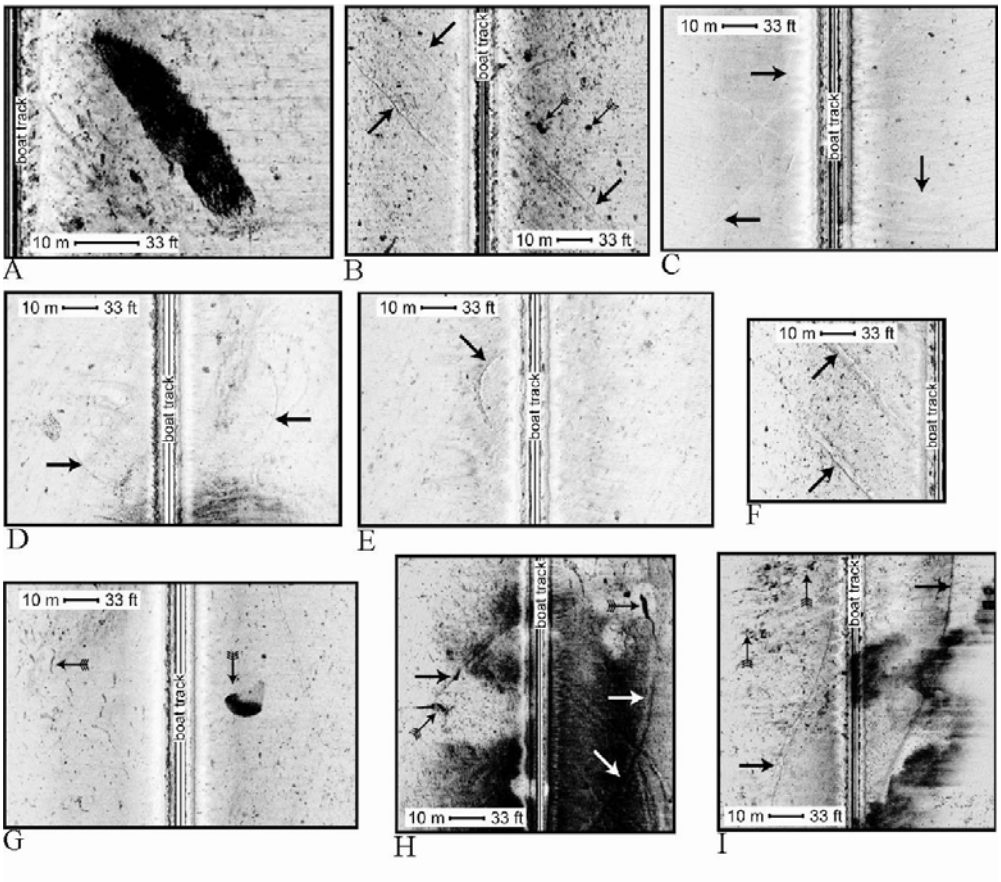

Figure 16. Side-scan sonar images of impacts in the four off-channel survey sites. The dark return in **A** is thought to represent a sunken boat; dark arrows in **B-I** show trawl marks on the bay bottom, while light arrows with tails in **B, G, H,** and **I** point to high backscatter events from the water column.

SRT 4-8 are closely related, generally located in close proximity to one another. Each type displays strong reflectors at the bay bottom or below surrounding SRT 4. The classification of each therefore relied on the shape and character of that reflector.

SRT 4 shows elevated, mounded bay bottom topography with acoustic wipeout below. It is prevalent in areas of high side-scan backscatter. This return is imaged throughout the Hannah's Reef, Clear Lake entrance, and Trinity Bay survey areas (Figures 22 and 23). The mounds vary in size in each location ranging from a few meters to tens of meters in diameter.

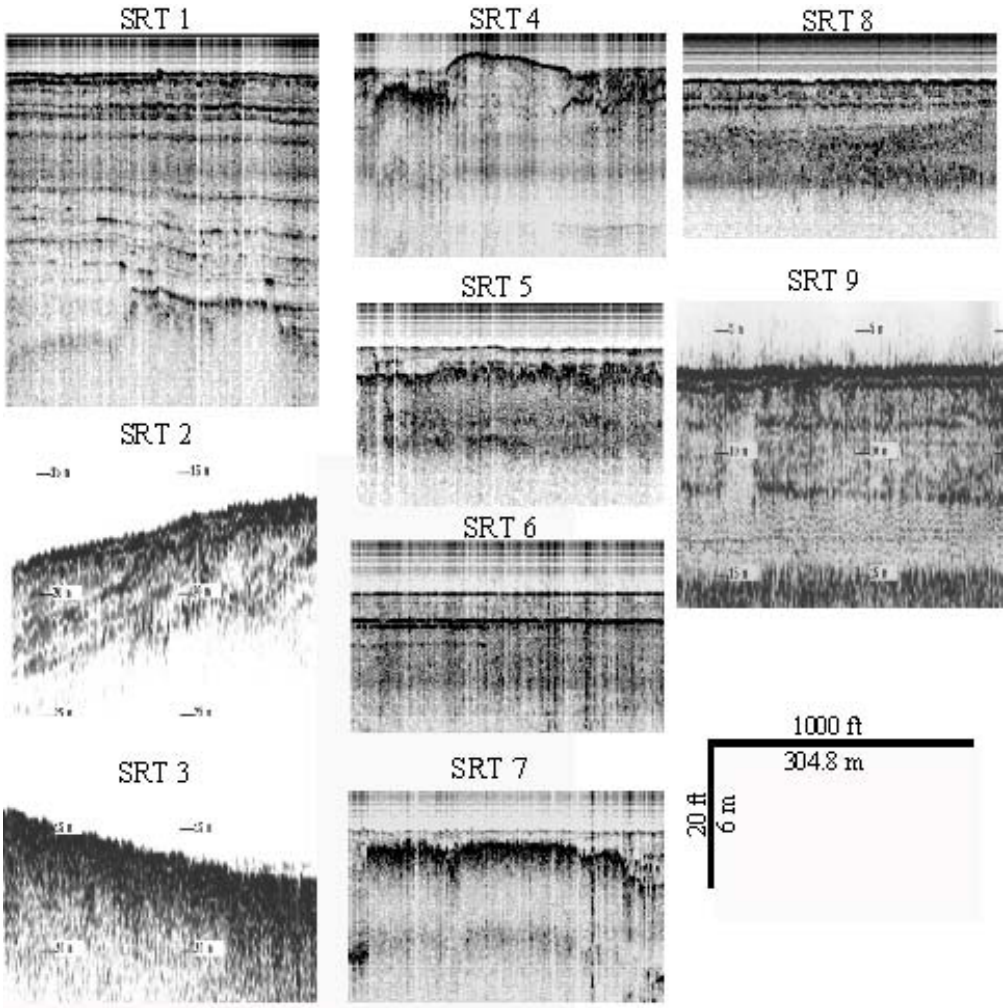

Figure 17. Examples of chirp seismic reflection types. Samples define seismic reflection types in the bay used to classify the bay sediments.

SRT 5 shows an acoustically transparent layer below the bay bottom, followed by a strong, jagged reflector at depth. This reflector is found in the Hannah's Reef, Clear Lake entrance, and Trinity Bay survey areas. It is representative of a hard subsurface layer and is often located in areas surrounding high side-scan sonar return.

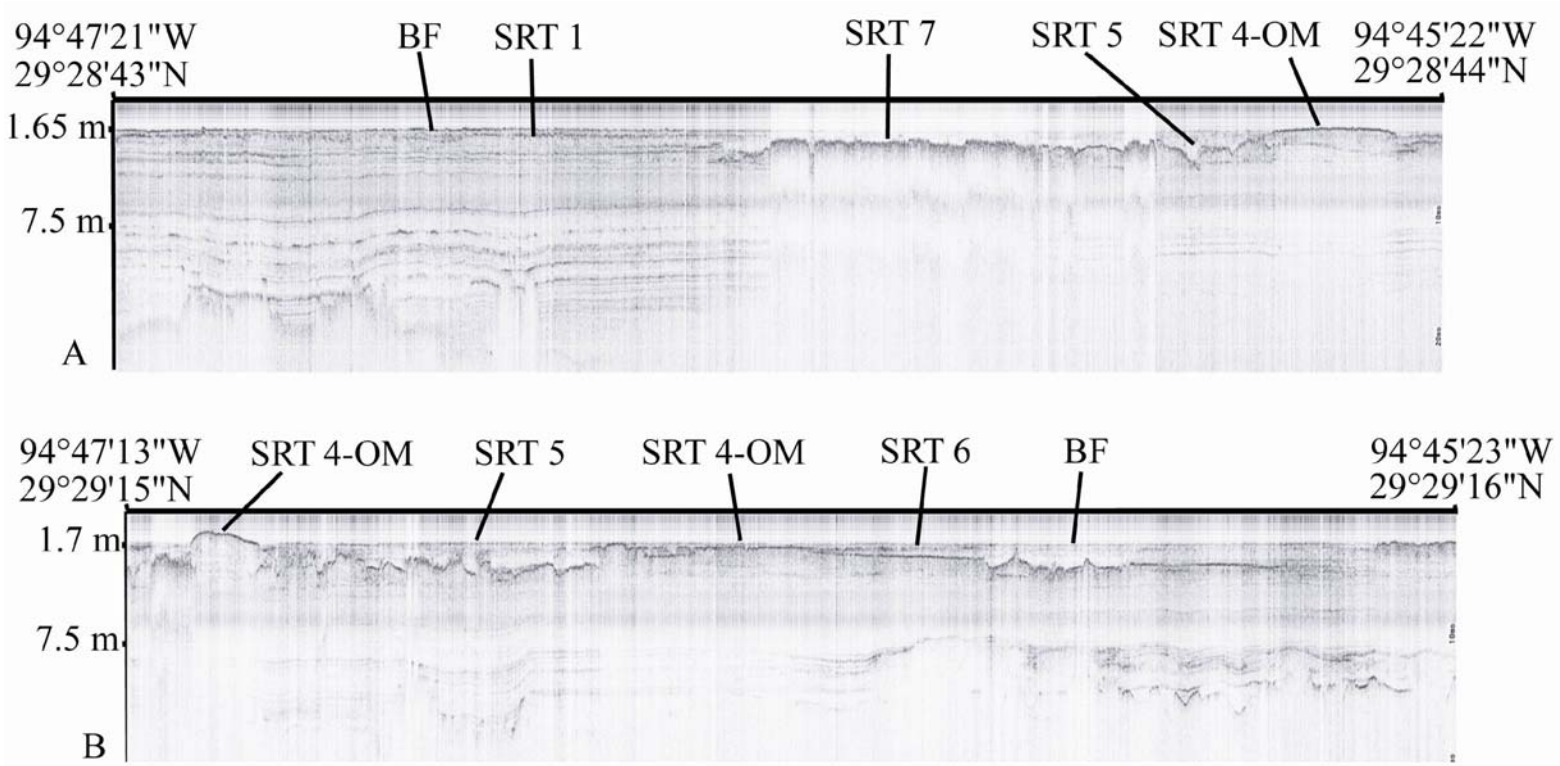

Figure 18. Chirp sonar lines from the Hannah's Reef survey site. Records show changes in stratigraphy, seismic reflection, and oyster reefs (OR). BF marks the location of the bav floor.

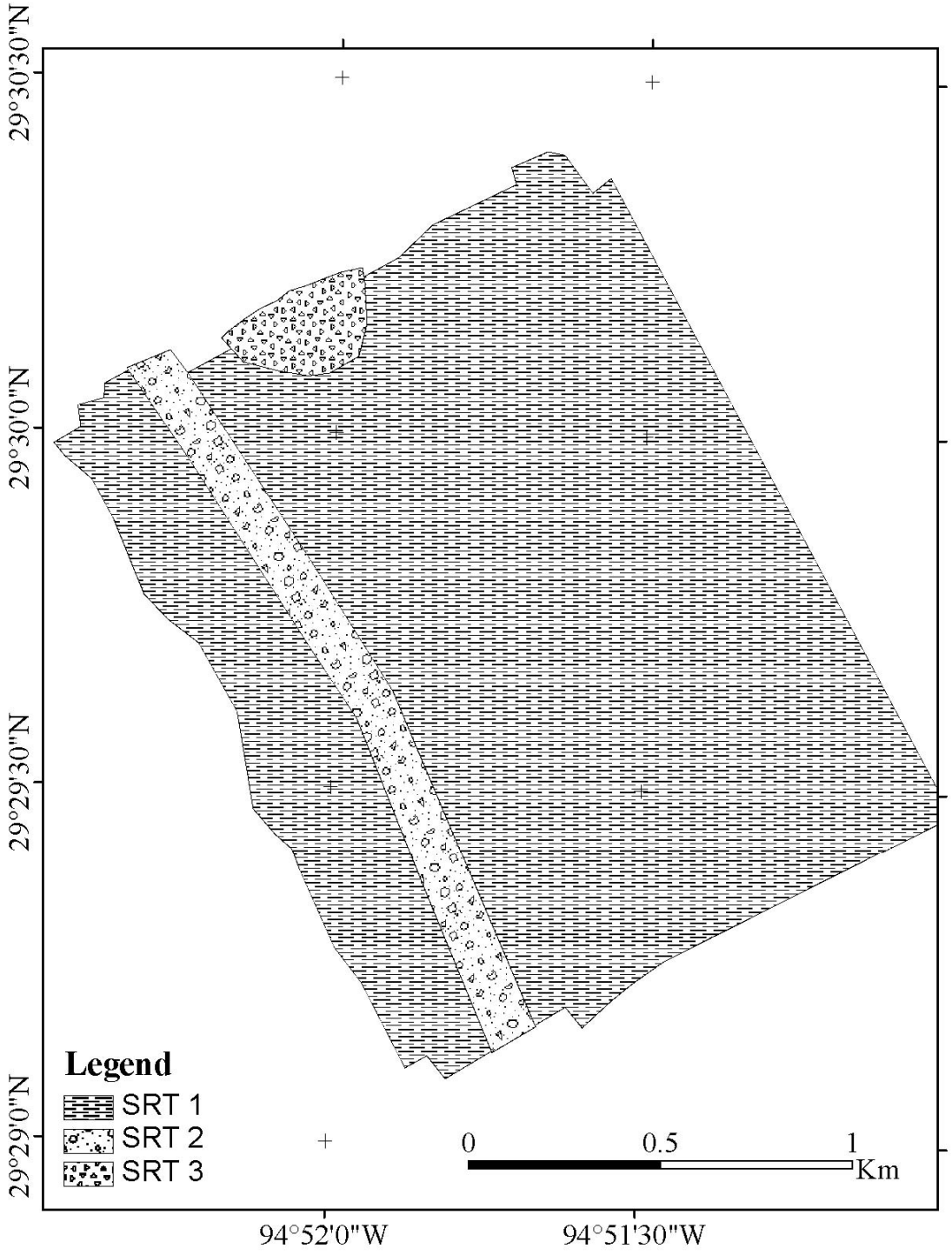

Figure 19. Seismic reflection type map of the Redfish Island survey area. Map shows seismic reflection characterization of the bay bottom in the Redfish Island survey area.

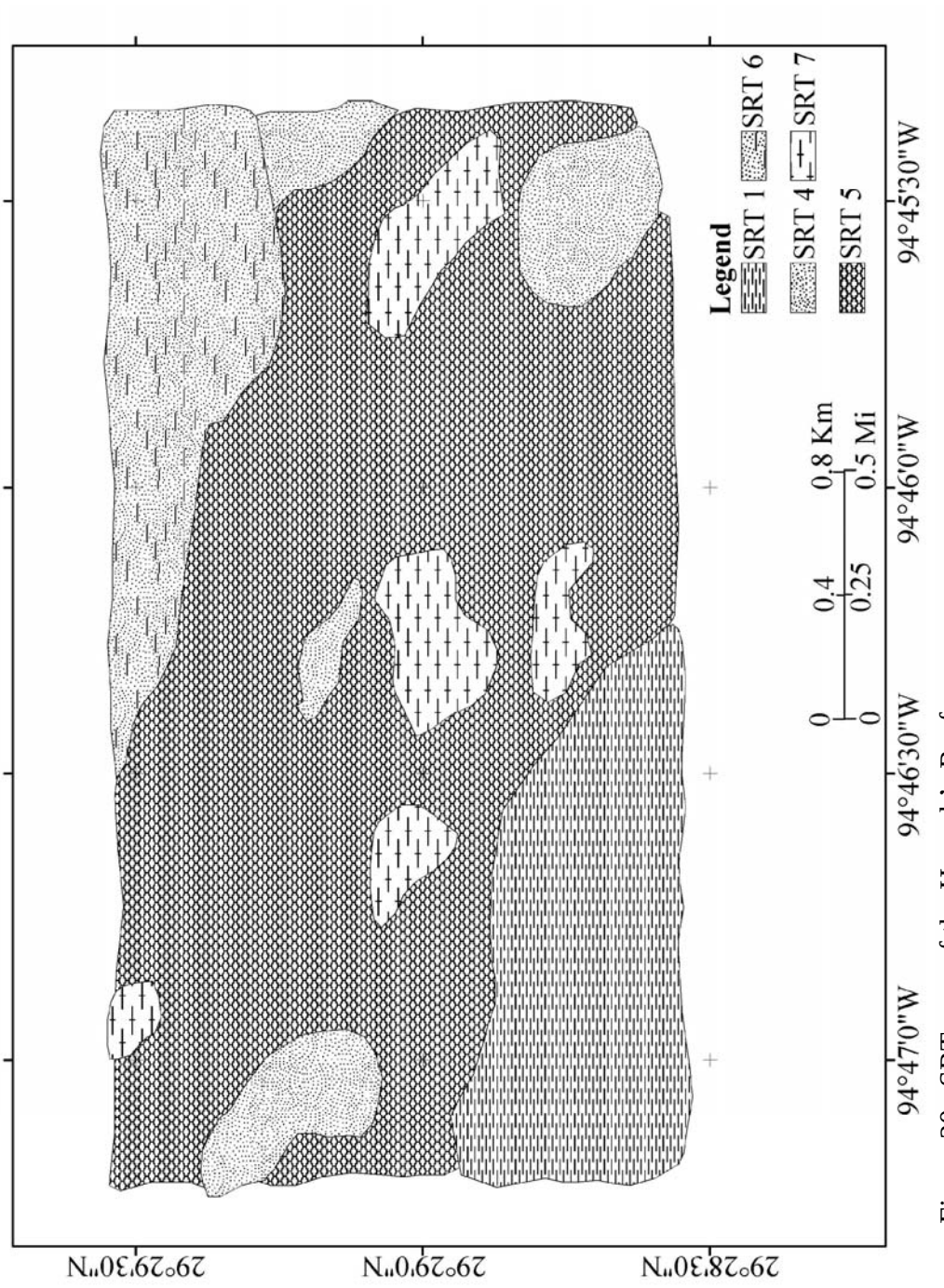

Figure 20. SRT map of the Hannah's Reef survey area.

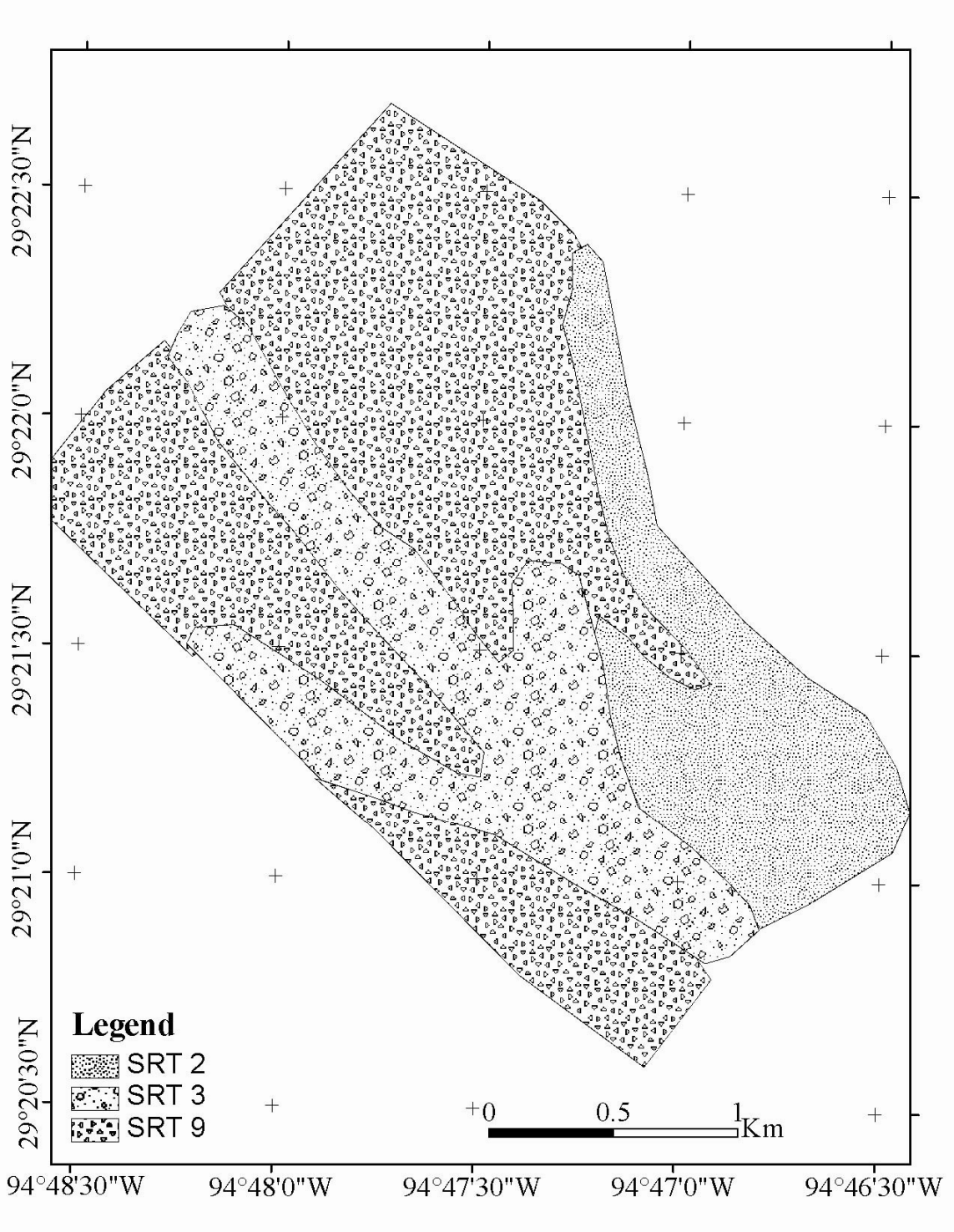

Figure 21. SRT map of the Bolivar Roads survey area.

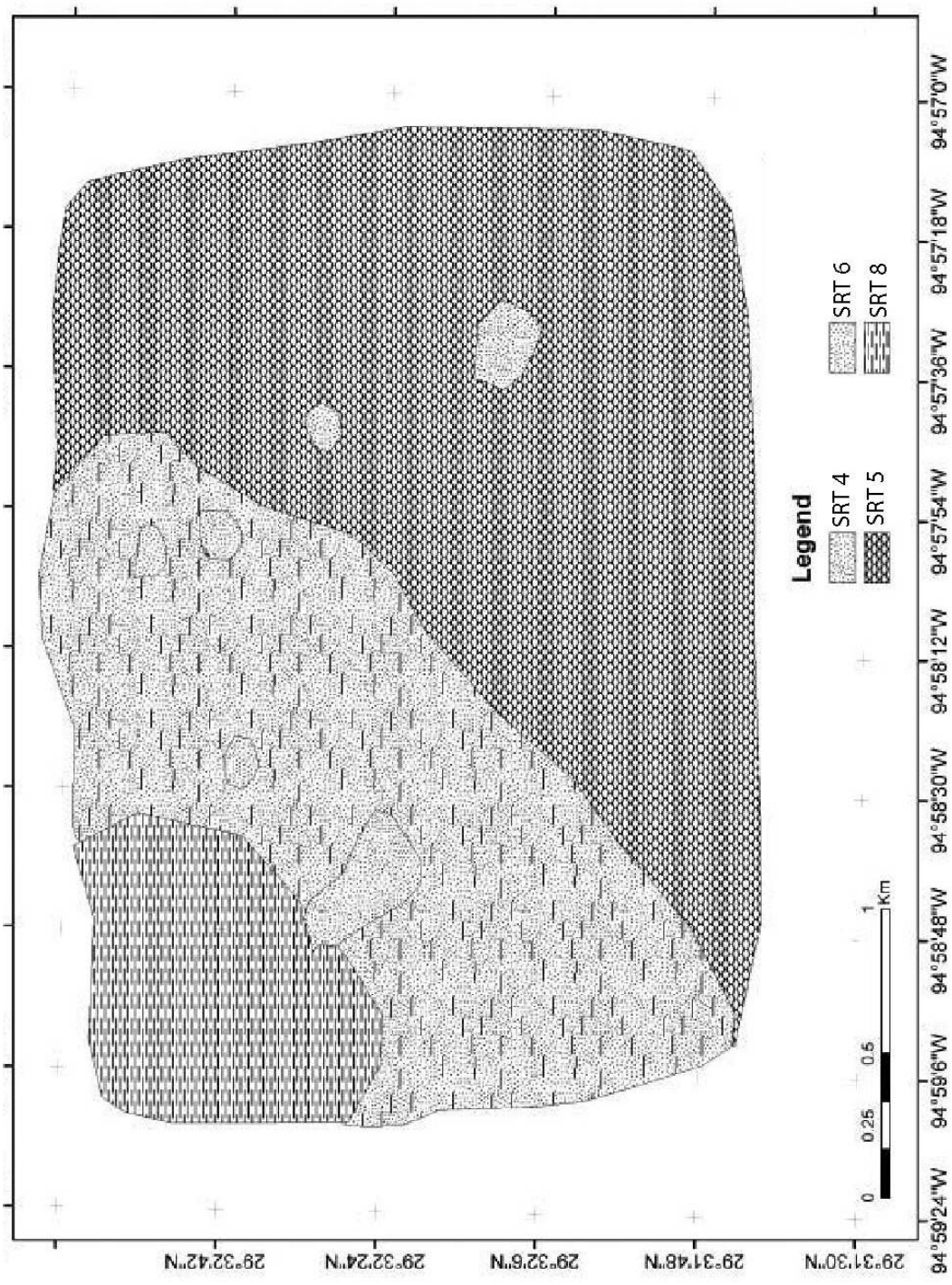

Figure 22. SRT map of the Clear Lake entrance survey area.

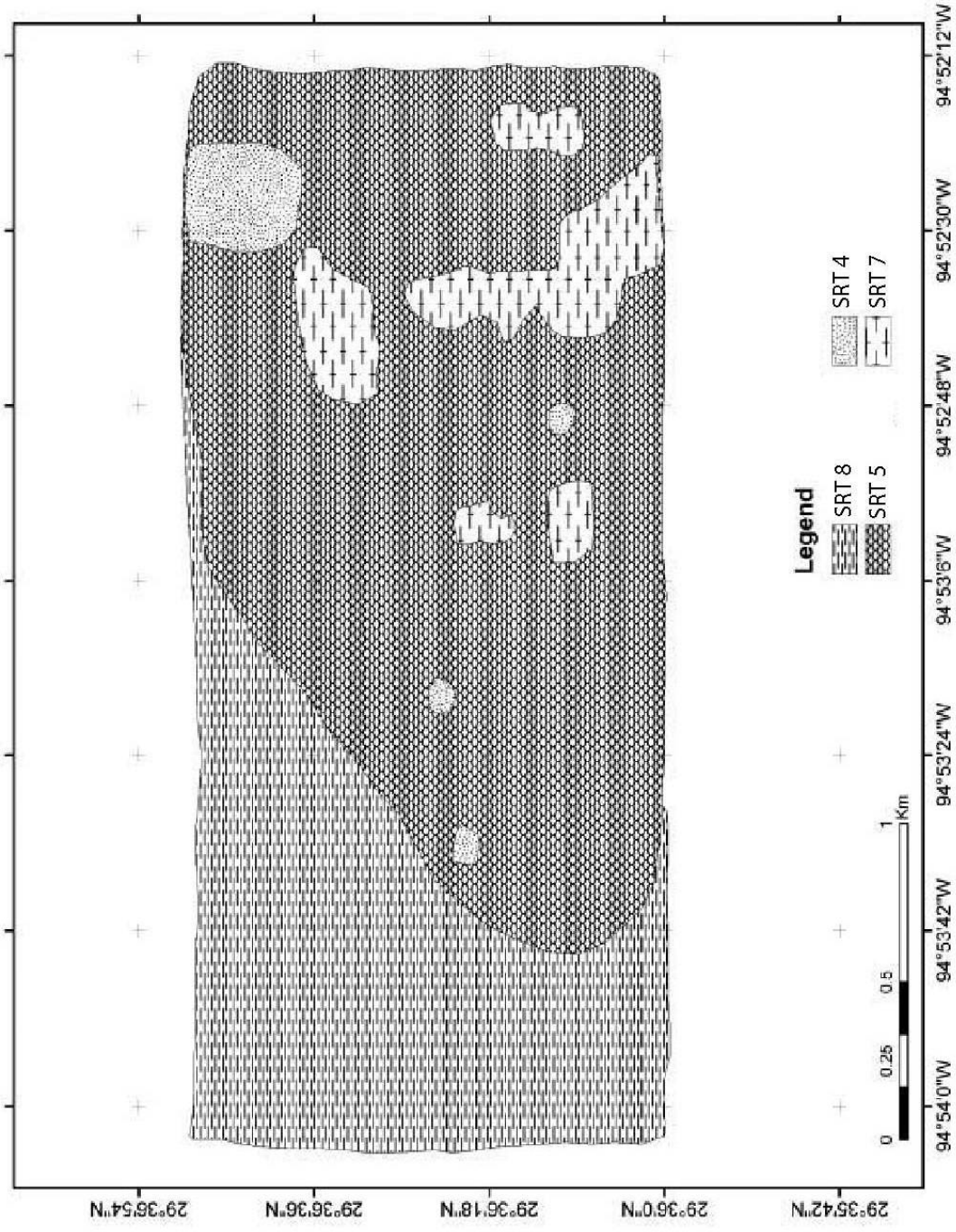

Figure 23. SRT map of the Trinity Bay survey area.

SRT 6 shows light reflectors, immediately below the bay bottom, followed by a strong horizontal reflector and weak horizontal strata below at depth. It is seen in the Hannah's Reef and Clear Lake survey areas in locations of high side-scan sonar return.

SRT 7 displays areas of acoustic wipeout, which resembles a strong, shallow reflection with no penetration below, representing gassy sediments. This bottom type is seen in the Hannah's Reef and Trinity Bay survey areas, surrounded by SRT 5.

SRT 8 shows weak to absent reflectors below the bay bottom and represent coarser material. This reflector is found only in the northeastern section of the Hannah's Reef survey area and in the northwestern section of the Clear Lake entrance survey area.

SRT 9 shows a strong bay bottom return followed by weak parallel reflectors and a shallow multiple. This reflector is found in the Bolivar Roads survey sight along the southwestern, northwestern, and northeastern sides of the ship channel. The presence of a strong bay floor return and shallow multiple is indicative of a hard substrate covering the bay bottom.

Chirp seismic data also showed numerous anthropogenic impacts in the survey area. The largest impact imaged is the ship channel and is displayed as ~19 m channel with parallel strata on either side (Figure 24). Other impacts visible in the chirp records are hyperbolic reflectors thought to be buried pipelines (Figure 25), slight increases in elevation with sudden weakening of the acoustic symbol thought to be dredge spoils (Figure 26), and small holes, ~2m deep, along the eastern side of the ship channel (Figure 27).

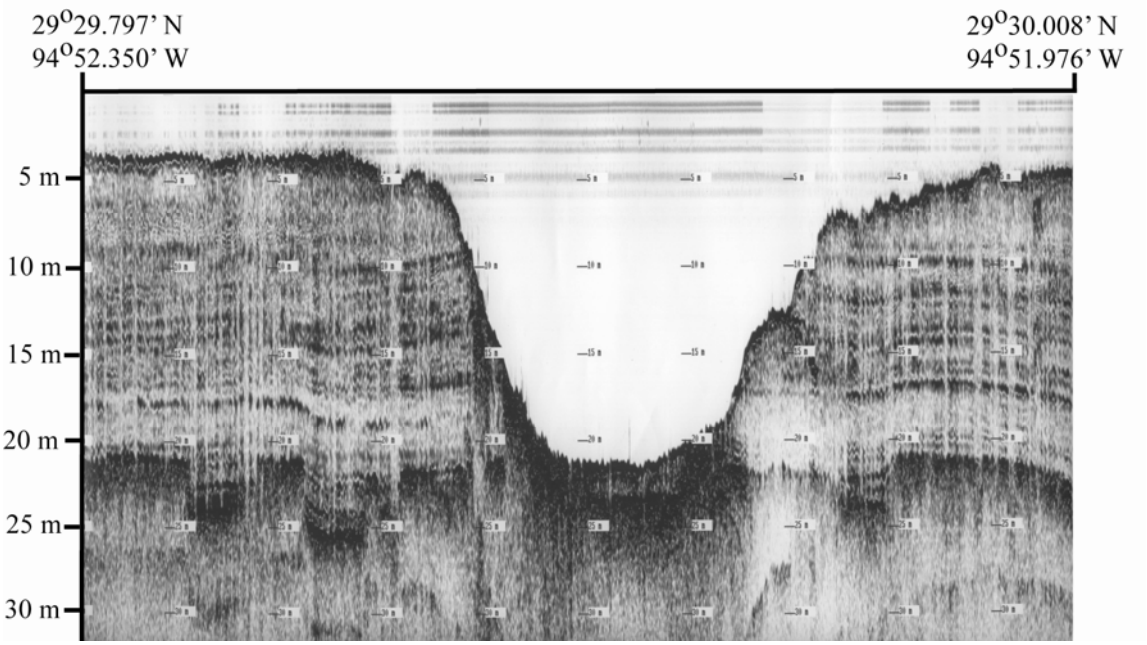

Figure 24. Chirp sonar record showing the HSC in the Redfish Island survey area.

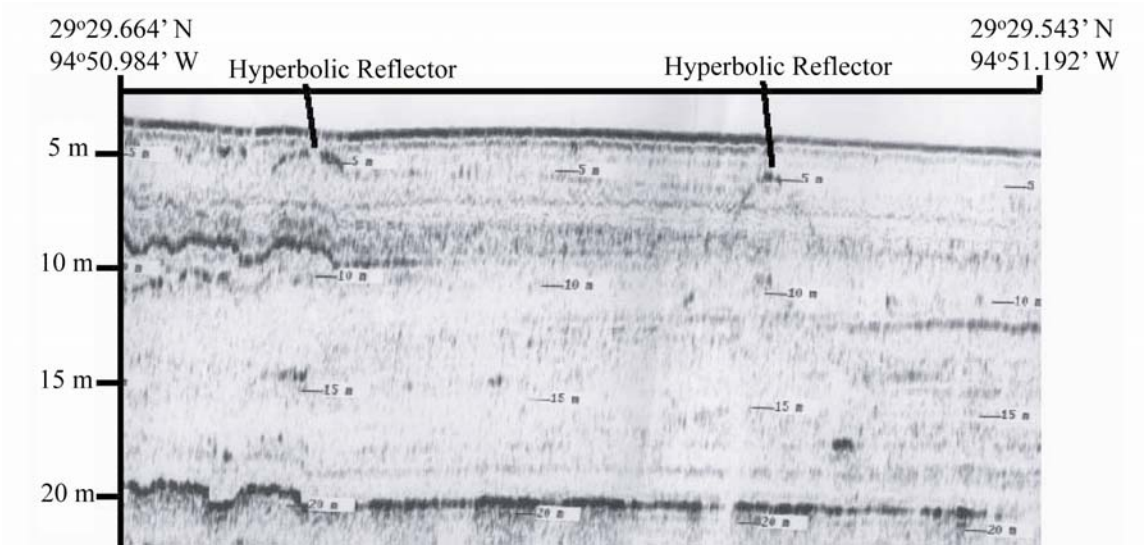

Figure 25. Chirp sonar record showing hyperbolic reflectors in the Redfish Island area.

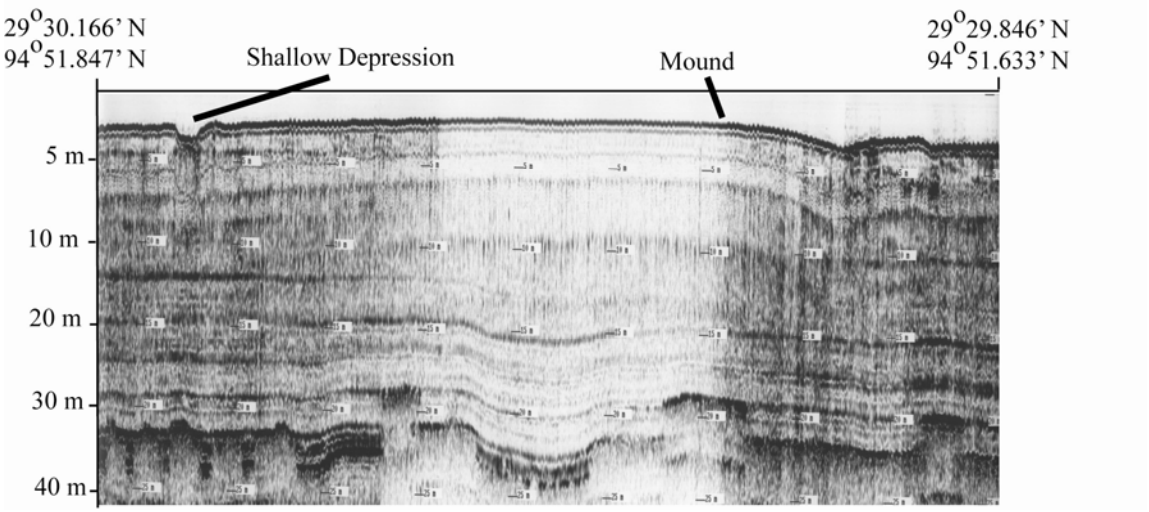

Figure 26. Chirp record showing increase in topography in the Redfish Island area.

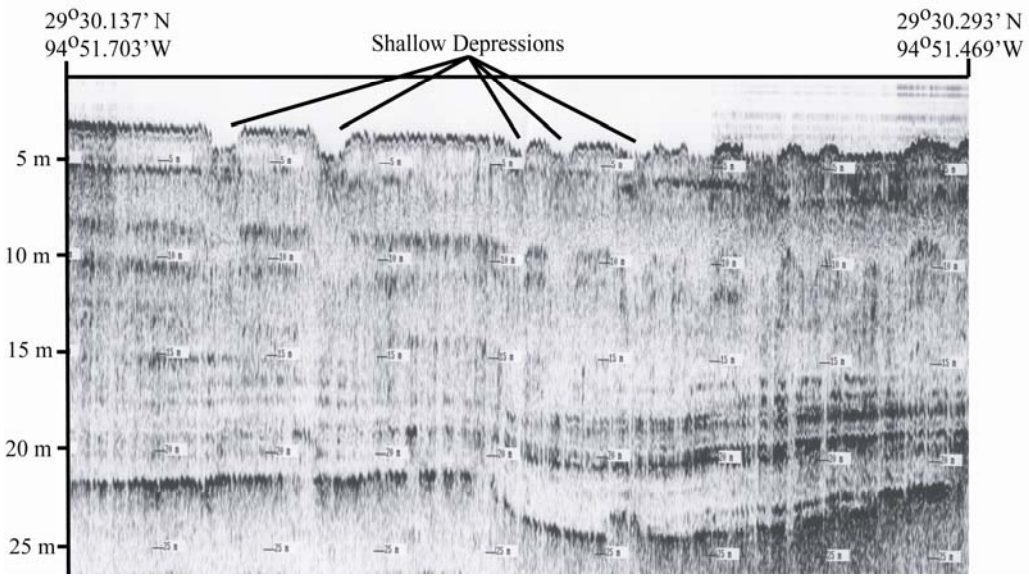

Figure 27. Chirp sonar record showing shallow depressions in the Redfish Island area.

Grab and Core Samples

Eight gravity cores and thirty-two grab samples were collected in the Bolivar Roads survey area in order to ground truth the geophysical data. The gravity cores varied from 12 cm to 42 cm in length. Coring in this area was hindered by a coarse layer of shell debris covering the bay bottom. Surface sediment from the cores contained mud, mud-shell mixture, and sand (Figure 28). Cores from the southeast section of the survey area contained a sandy mud layer, ~6 cm in thickness, overlain by a 7 cm thick layer of sand. Other cores displayed a dark gray stiff mud and shell mixture or tan stiff mud and/or shell mixture. The thirty-two grab samples collected in the Bolivar Roads area helped create a better understanding of the side-scan sonar mosaic. Nearly all grab samples infer a hard bay bottom covered with shell debris and stiff mud (Figure 29) (Appendix C, D, and E). This coarse layering is likely responsible for the strong return on the side-scan sonar mosaic and shallow penetration from the chirp sonar. Surface sediment size varied widely in Bolivar Roads, with an average sand percentage ~72%, silt percentage ~24%, and ~4% clay (Figure 30 and 31).

Ten gravity cores and ten grab samples were collected in the Redfish Island survey area. The gravity cores varied from 13 cm to 78 cm in length. Coring this area produced longer cores due to the soft sediment located in this area. Surface sediment from the cores contained silty sediments, silt-shell mixture, and shells (Figure 28). Cores from the eastern section of the survey area were generally short and contained large shell fragments and silty sediment, whereas those from the western section of the survey area were longer and contained organic-rich fine-grained sediments with lesser shell fragments. Ten grab samples collected in the survey area recovered mostly silty sediment

and silt-shell mixtures, although one grab sample from the ship channel contained fine sand (Figure 32) (Appendix C, D, and E). Surface sediment size displayed mostly silty sand in this area, with an average sand percentage ~41%, silt percentage ~48%, and ~11% clay (Figure 30 and 31).

Two push cores and seven grab samples were collected at each of the remaining survey sites. The push cores averaged ~50 cm length and consisted mostly of silty, laminated sediment with a high organic content. The grab samples from each site contained organic rich silt or oyster shell fragments. Fine grained sediments were correlated in areas of low return on the side-scan sonar mosaics, whereas oyster shell fragments were located in areas of high return (Figures 33- 36).

Surface sediment in the East Bay survey site displayed ~75% silt, ~13% sand, and ~12% clay. Surface sediment in the Hannah's Reef survey site also displayed mostly silt, ~75%, with 15% sand, and 10% clay (Figure 30). Grab samples of oyster shells in the Hannah's Reef, Clear Lake entrance, and Trinity Bay survey site only collected limited amounts of shell fragments because the grabs usually did not penetrate owing to the shells (Figure 28). As a result, it was not possible to determine the underlying sediment type accurately.

Surface sediments in the Clear Lake entrance survey site contained mostly silt, with a sand percentage of ~12%, silt percentage of ~77%, and a clay percentage of ~11% (Figures 28 and 30). Surface sediment in the Trinity Bay survey site also contained mostly silty sediment with a sand percentage of ~20%, a silt percentage of ~70%, and a clay percentage of ~10% (Figures 28 and 30).

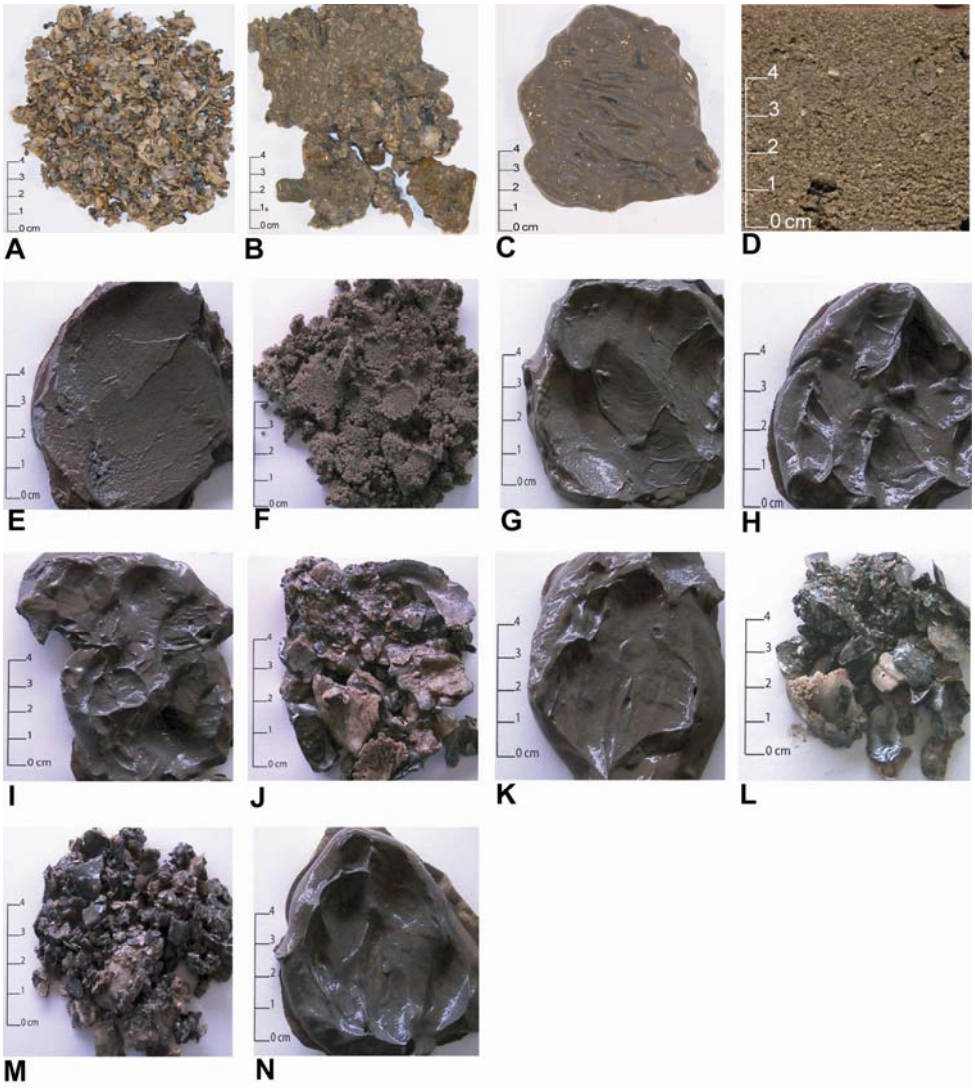

Figure 28. Surface sediment from the survey areas. **A** is a sample of marine shell debris collected from the Bolivar Roads survey area; **B** is a sample of marine shell debris/silt mixture from the Bolivar Roads survey area; **C** is a sample of stiff fine grained mixture from the Bolivar Roads area; **D** is a sample of sand collected from the Bolivar Roads survey area; **E** is a sample of silty sediment collected from the Redfish Island area; **F** is a sample of sand collected from the Redfish Island area; **G** and **H** are samples of silty sediment collected from the East Bay survey site; **I** is a sample of bay fill mud (silty sediment) collected from the Hannah's Reef site; **J** is a sample of oyster shell debris collected from the Hannah's Reef site; **K** is a sample of silty sediment from the Clear Lake entrance site; **L** is a sample of oyster shell debris collected in the Clear Lake entrance site; **M** is a sample of oyster shell debris from the Trinity Bay site, and **N** is a sample of fine grained sediment from the Trinity Bay site.

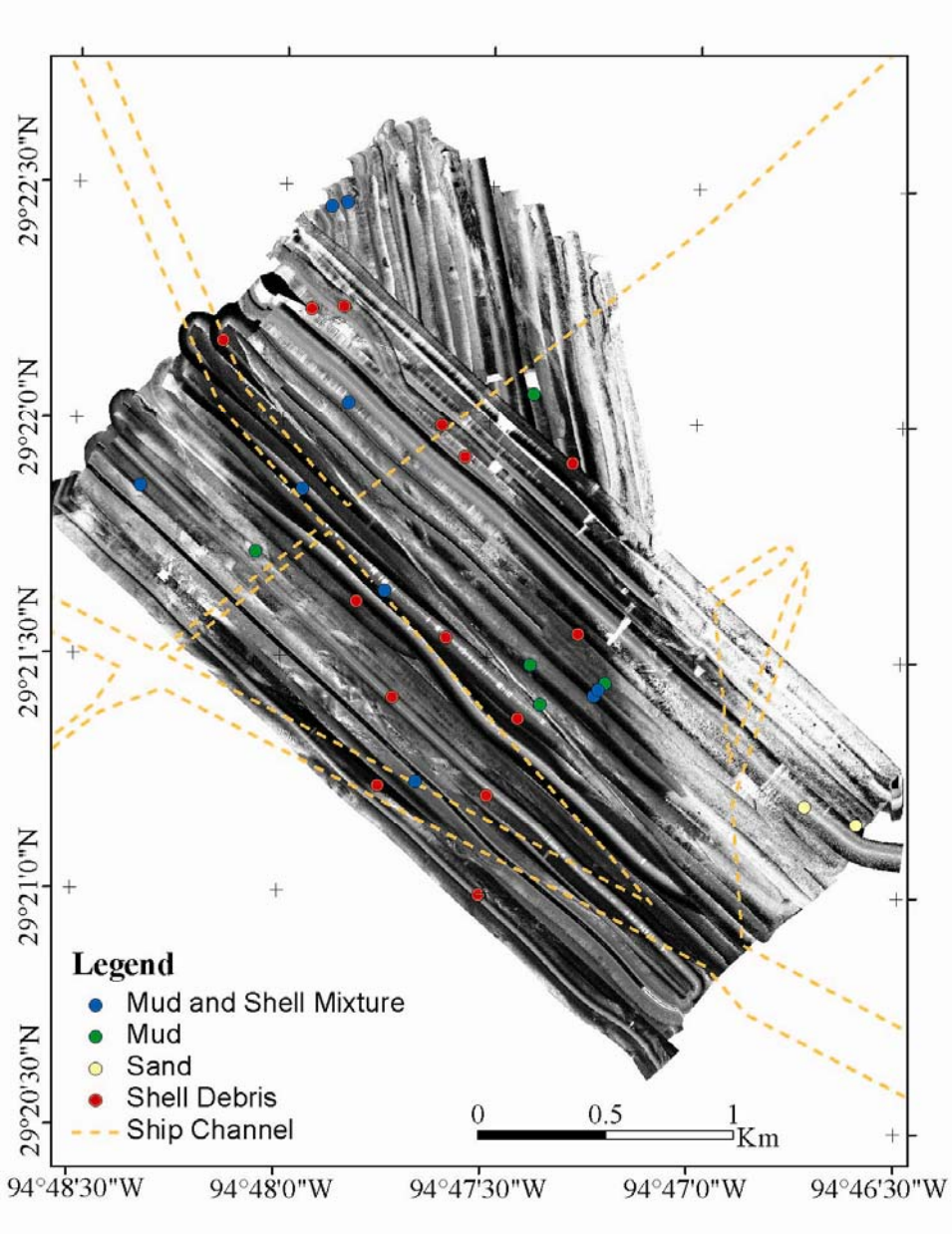

Figure 29. Surface sediment types sampled from the Bolivar Roads survey area.

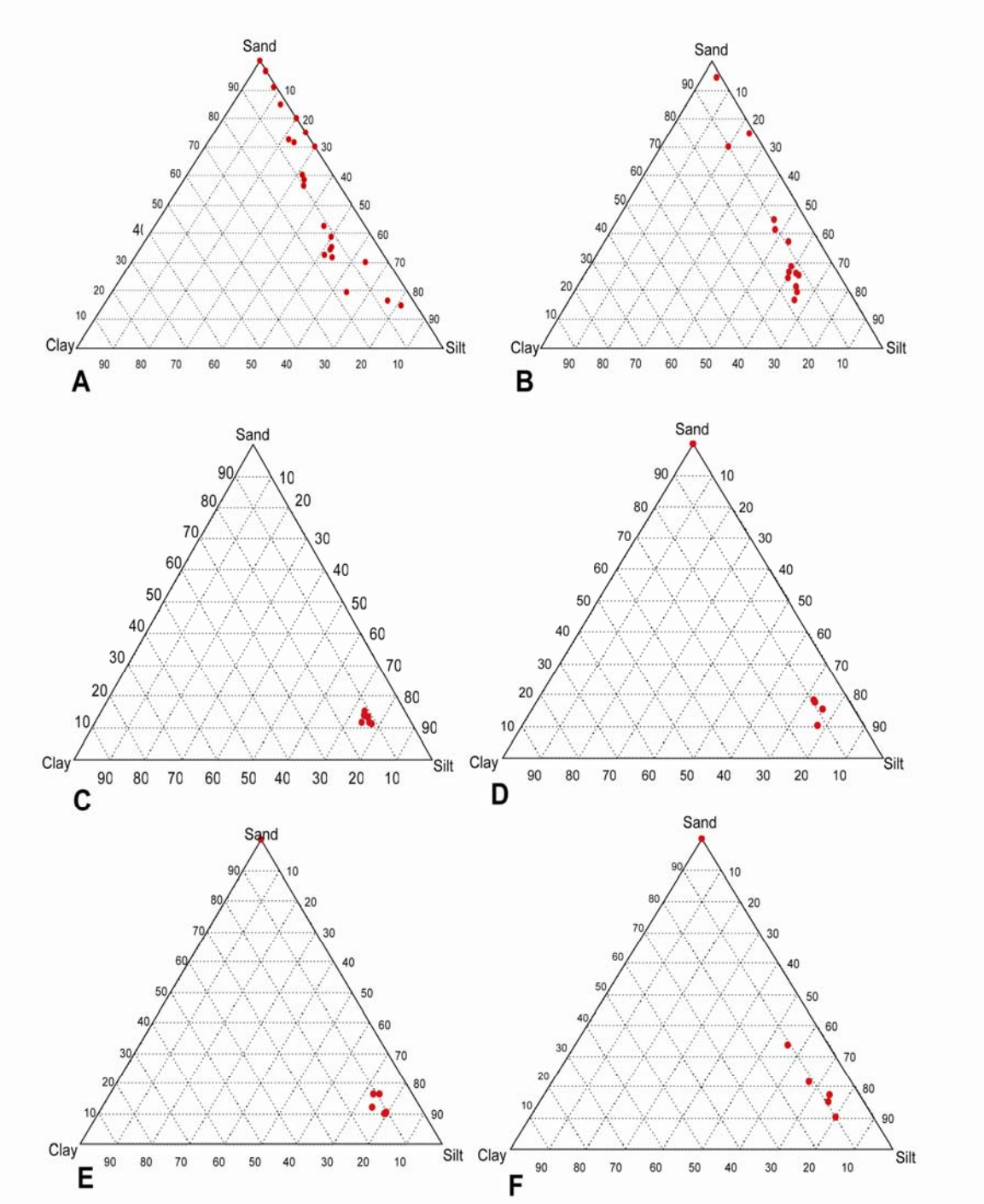

Figure 30. Ternary diagrams showing sand/silt/clay percentages as each survey site. **A** shows percentages at the Bolivar Roads survey site; **B** shows percentages at the Redfish Island survey site; **C** shows percentages at the East Bay survey site; **D** shows percentages at the Hannah's Reef survey site; **E** shows percentages at the Clear Lake entrance survey site; and **F** shows the percentages at the Trinity Bay survey site. All survey sites display mostly silty or sandy sediments within the bay.

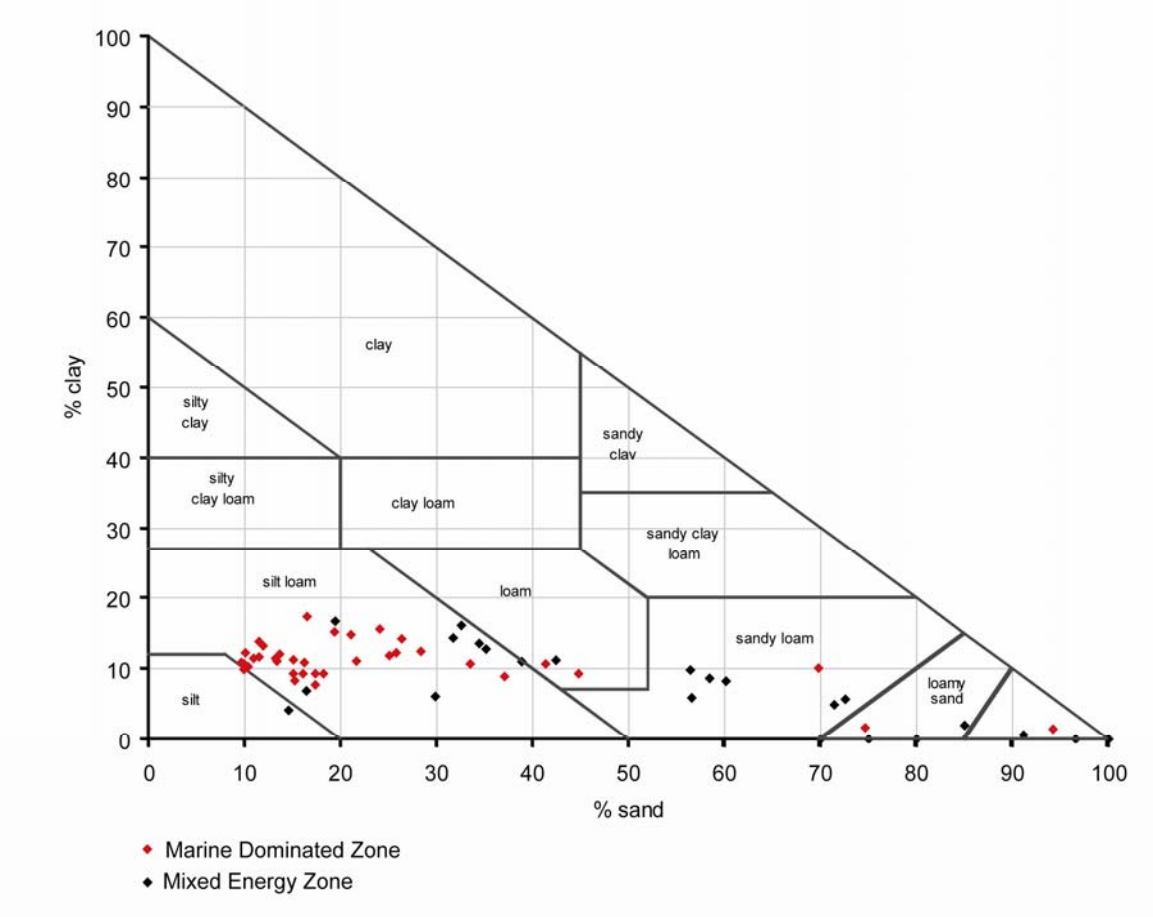

Figure 31. Ternary diagram with overlapping Sheppard's Classification. Showa the differences in sand/silt/clay percentages between the marine dominated zone and the mixed energy zone.

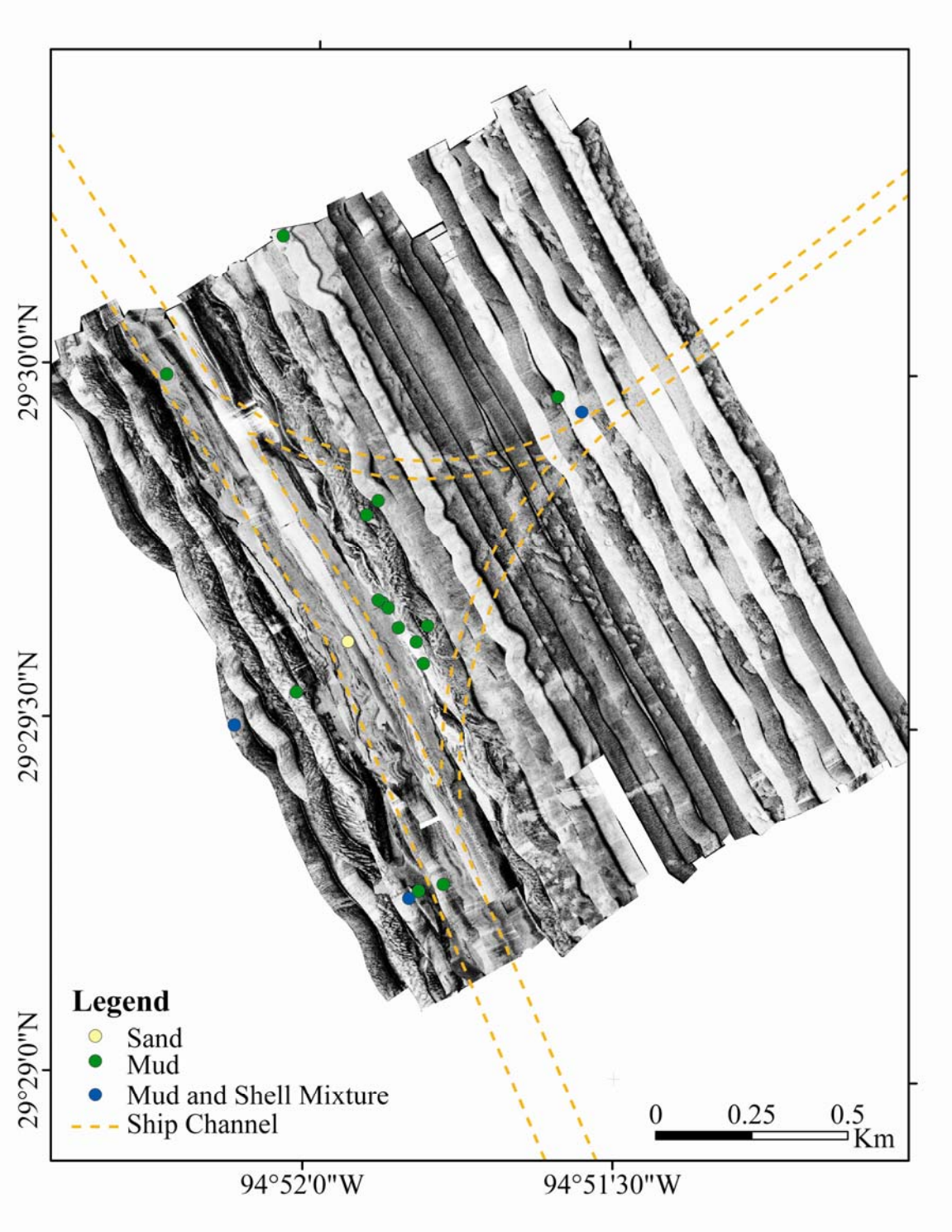

Figure 32. Surface sediment map from the Redfish Island survey area.

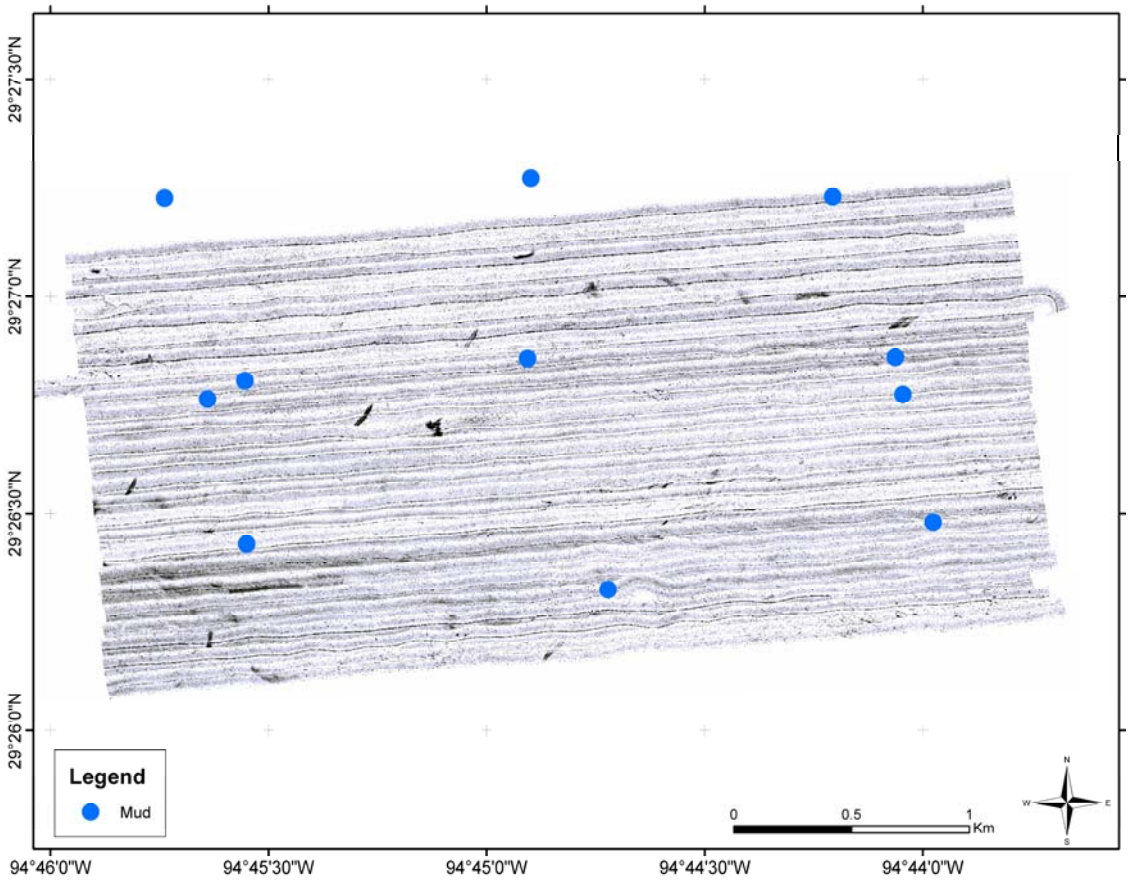

Figure 33. Sediment types of surface samples from the East Bay survey site.

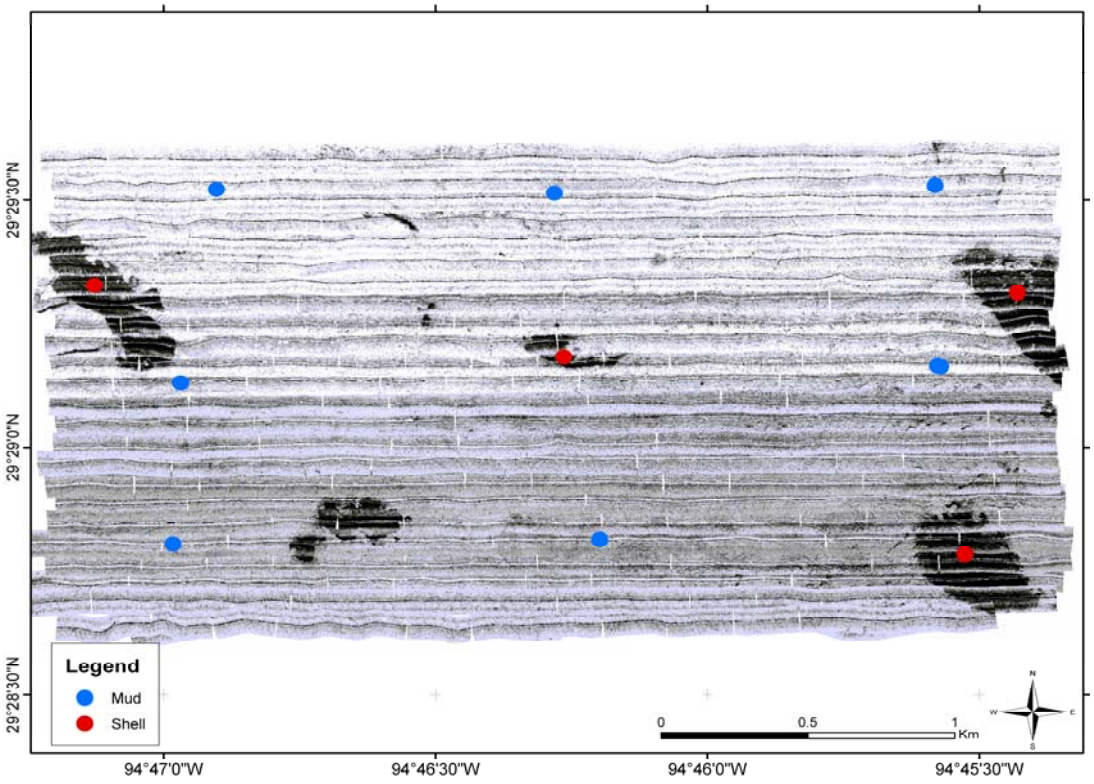

Figure 34. Sediment types of surface samples from the Hannah's Reef survey area.

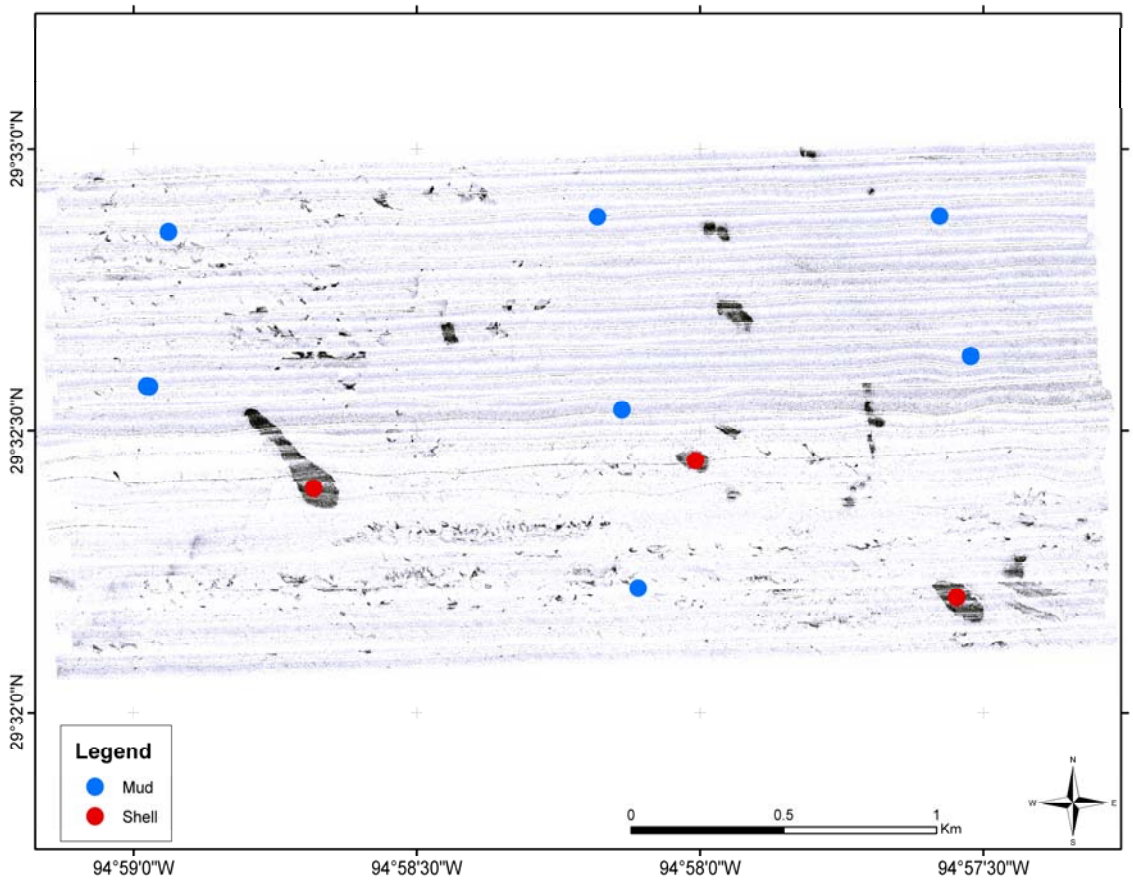

Figure 35. Sediment types of surface samples from the Clear Lake entrance survey area.

The majority of the sediment samples in the on-channel survey sites and a few of the ones in the off-channel survey sites display bimodal distribution of sediment sizes. Bimodal distribution was recorded in samples taken from 40 cm cores, displaying bimodal sediment distribution through the entire length of the core (Figure 37). This suggests that the sediments are being deposited from two separate sources, most likely marine and fluvial sediments (Appendix D).

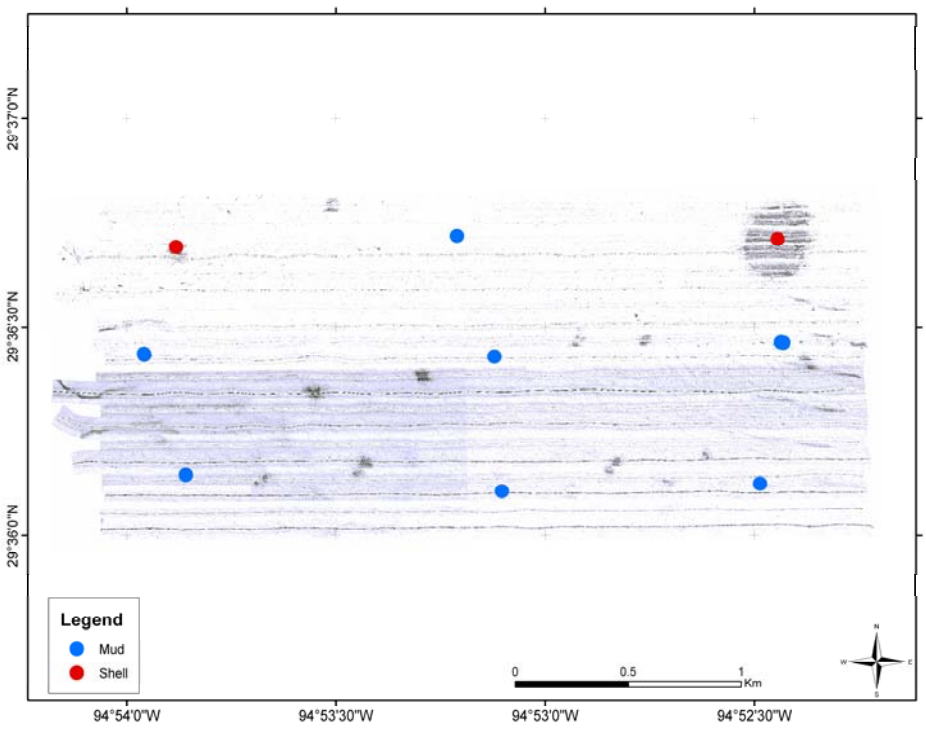

Figure 36. Sediment types of surface samples from the Trinity Bay survey area.

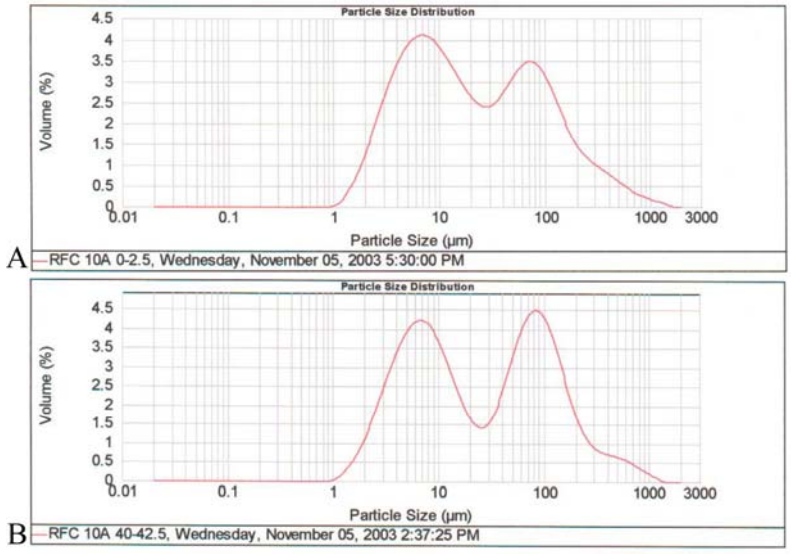

Figure 37. Particle size graphs of Redfish core 10 showing bimodal distribution. Graphs show distribution in the surface sediment (**A)** and at 40 cm (**B)** due to both fluvial and marine input into the bay. This core was collected away from dredge spoils, eliminating the possibility that the bimodal distribution is a result of channel dredging.

DISCUSSION

In this study, I examined sonar data displaying the distribution of bay bottom sediments and anthropogenic impacts in Galveston Bay. I expected to image bay bottom sediment changes as we moved from the southern part of the bay north, going from a high energy environment to a low energy environment (Dalrymple et al. 1992, Nichols et al. 1991). Due to the proximity of the Bolivar Survey to docks, I expected to locate numerous anthropogenic impacts with the highest concentration of impacts in the area.

Bay bottom classification varied with the type of marine environment in which the survey area was located. All but one survey site displayed high and low returns; however the bay bottom sediments varied greatly. In the Bolivar Roads survey area, high return originates from the coarse marine shell debris comprising the Bolivar flood tidal delta, whereas high returns in the other survey areas are due to large areas of oyster shells (Figures 2, 13, 14, 15). Sand was sampled in the Bolivar Roads survey area where low backscatter was observed, while silty loam was collected areas of low backscatter in the remaining survey sites. Therefore, the side-scan sonar, along with surface sediment samples, imaged 5 distinct bottom types: marine derived shell debris, shell debris and mud, sand, bay-fill mud (silty loam), and oyster reefs (*Crassostrea virginica*) (Figure 28).

Bay bottom sediment distribution maps display a wide variety of bay bottom types. SRT 1 is indicative of bay fill sediments and is located through the axis of the Trinity incised valley as mapped by Smyth et al. (1988). The parallel stratigraphy that terminates at a stronger reflector at depth represent the slow filling of the bay by fine grained sediments after sea level stabilized at its present level (Figure 17). SRT 2 in the Bolivar

Roads area is believed to represent sediments from the flood tidal delta, which are reworked by currents and waves. This interpretation is based on the tilted seismic horizons in the chirp record and the sandy sediment and mud lenses found in the core collected in the area (Figure 17). SRT 2 in the Redfish Island area is located along the axis of the ship channel and represents a thin layer of sediments (SRT 1) left over after dredging the chip channel. SRT 3 shows no internal structure and is correlated to areas of coarse, angular sediment also on the flood tidal delta. Surface sediment samples in these areas consisted of angular shell debris, implying that the currents in the Bolivar Roads area are strong enough to remove fine grained sediment, leaving a lag deposit of coarse shell debris (Figure 21). SRT 3 in the Redfish Island area correlated with stiff silty sediment found in an area of dredge spoils, which reduced the penetration of the chirp signal. SRT 4 is found in areas of high side-scan sonar backscatter where oyster shells were collected in grab samples. These areas usually show mounded topography or very strong reflections at the bay bottom/water interface and are locations of current *Crassostrea virginica* oyster reefs. SRT 5, 6, and 7 are located around areas where oyster mounds occur and appear related to the current oyster formations. It appears that these bottom types are either buried oyster beds or a hard surface. In most instances of current mounded topography (SRT 4), SRT 5 or 6 can be traced to the base of current oyster reefs. SRT 8 appears along the flanks of the incised valley and most likely represents coarse sediments deposited along the coastline in shallow waters (Figure 17).

The side-scan and chirp records reflect the “tripartite” model built by Dalrymple et al. 1992 with respect to grain size variations and relative energy. The Bolivar Roads survey area lies at the mouth of the estuary and consist of the bay’s largest flood-tidal delta

consisting of the estuaries coarsest sediments. This area corresponds to Dalrymaple's marine dominated zone which is influenced mostly by waves and tidal currents. The geophysical and geological data collected in this area agree with Dalrymaple's model. The side-scan sonar records displayed high acoustic returns and the chirp sonar showed shallow penetration or acoustic reverberation with strong bay-bottom returns, both representative of coarse sediment. The gravity core and grab samples from the area showed coarse, marine sediments deposited due to wave and tidal action within the bay.

The remaining five survey sites are located in what Dalrymple refers to as the "central basin". This area is minimally influenced by wave and tidal energy, allowing fine grained sediments to settle out of suspension. My geophysical and geological data corresponded to this model. The side-scan sonar recorded low acoustic returns in the absence biological influence (oyster beds). The parallel laminated sediments fading out toward the shorelines are representative of the finer grained, open basin sediments in this area and are due to the slow filling of the bay. The geologic samples corresponded to the geophysical data as the majority of the sample contained fine-grained silt and organics. The third part of Dalrymple's model, the river-dominated zone, was not included in this study.

Two general types of impacts were seen on the bay bottom, debris and sediment disruption. The side-scan records show that, as expected, most debris type anthropogenic impacts are found along the flanks and within the ship channel areas (Figures 5, 8). In these areas the majority of impacts appear to be debris from passing ships or probable sunken boats (Figures 5, 11). The exception to this is the area flanking the HSC in the Redfish Island area. This location contains numerous indicators of sediment disruption

by oyster and shell dredging, which displays many circular grooves and depressions in the bay bottom (Figure 11). Other sediment disruption impacts seen in the area are dredge spoils which have failed and are flowing back into the ship channel and depressions (Figures 9, 10).

The remaining four survey areas display impacts mostly associated with sediment disruption. These impacts appear to be associated with shrimp trawling and are visible as long, parallel grooves in the bay bottom (Figure 16). Shrimp boats were trawling in the areas during the surveys, leading us to believe that many of the marks visible in the side-scan sonar images are recent.

The study indicates that human activity, and the resultant anthropogenic impacts, decreases as you move away from the HSC and areas of oyster leases. All debris type impacts were located on the on-channel survey sites while none were found in the off-channel sites, leading to the speculation that either the debris found on the bay floor in Galveston Bay is from vessels using the HSC. However, smaller vessels (i.e. sport fishing boats) may deposit debris on the bay bottom smaller than the effective resolution of the side-scan sonar.

Comparison of imaged oyster beds with those mapped by Powell et al. (1995) show the difference in resolution of the two surveys and/or the change in oyster productivity in the survey areas due to differences in equipment and line spacing. In the Hannah's Reef survey area, the previous oyster reef study seemed to over-estimate the size of the oyster reefs (Figure 38). Figures 39 and 40 show the opposite as more oyster reefs were discovered in this area than previously known. Using side-scan sonar to map oyster reefs presented a better representation of the oyster reef locations and size in the bay.

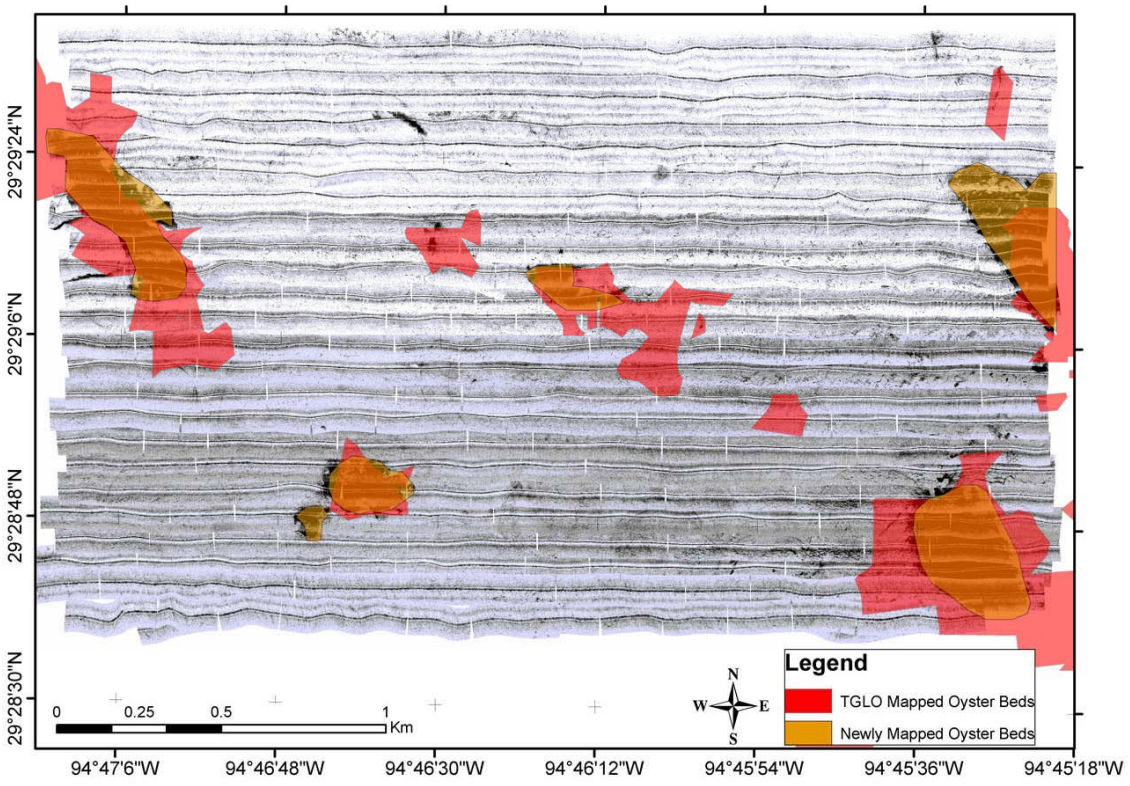

Figure 38. Oyster distribution in the Hannah's Reef area. Map shows locations and sizes of both previously mapped oyster beds (red shading) and newly mapped oyster beds (yellow shading).

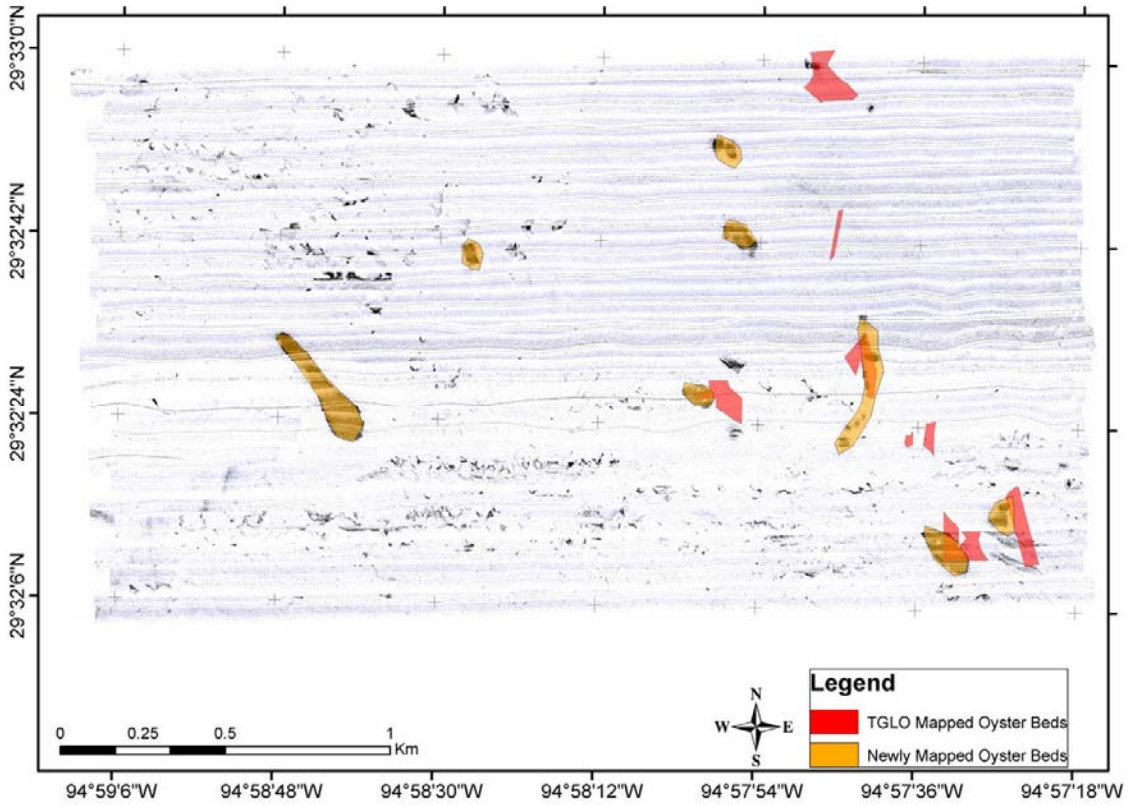

Figure 39. Oyster distribution in the Clear Lake entrance area. Map shows locations and sizes of both previously mapped oyster beds (red shading) and newly mapped oyster beds (yellow shading).

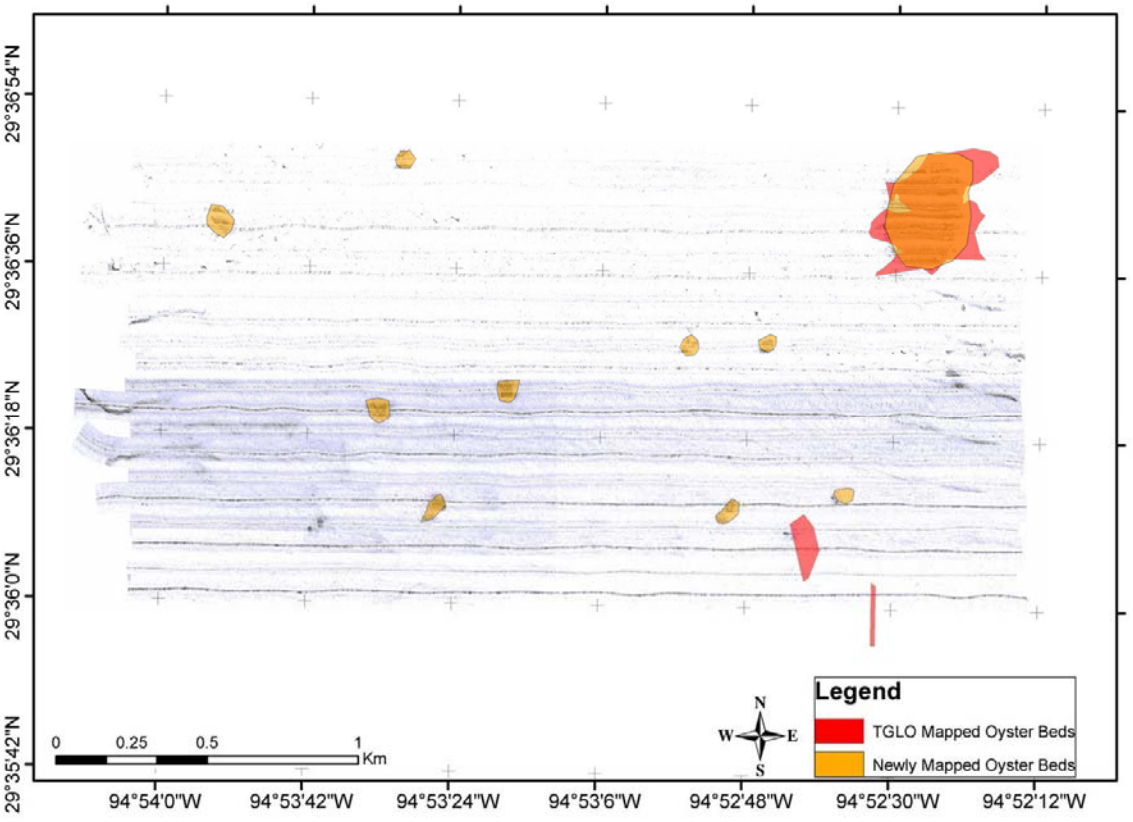

Figure 40. Oyster distribution the Trinity Bay area. Map shows locations and sizes of both previously mapped oyster beds (red shading) and newly mapped oyster beds (yellow shading).

Chirp records displayed mostly sediment disruption type impacts due to either the removal of sediment during channel dredging as seen in both the Bolivar Roads and Redfish Island survey area (Figure 41), shell mining as seen only in the Redfish Island area (Figure 42), or by the addition of sediment along the flanks of the ship channel as dredge spoils are created, also only seen in the Redfish Island survey area (Figure 43). Some man-made, metallic objects were also imaged in the chirp records. One chirp line in Redfish Island displayed a series of hyperbolic reflections, indicative of a buried pipeline running through the survey area (Figure 44).

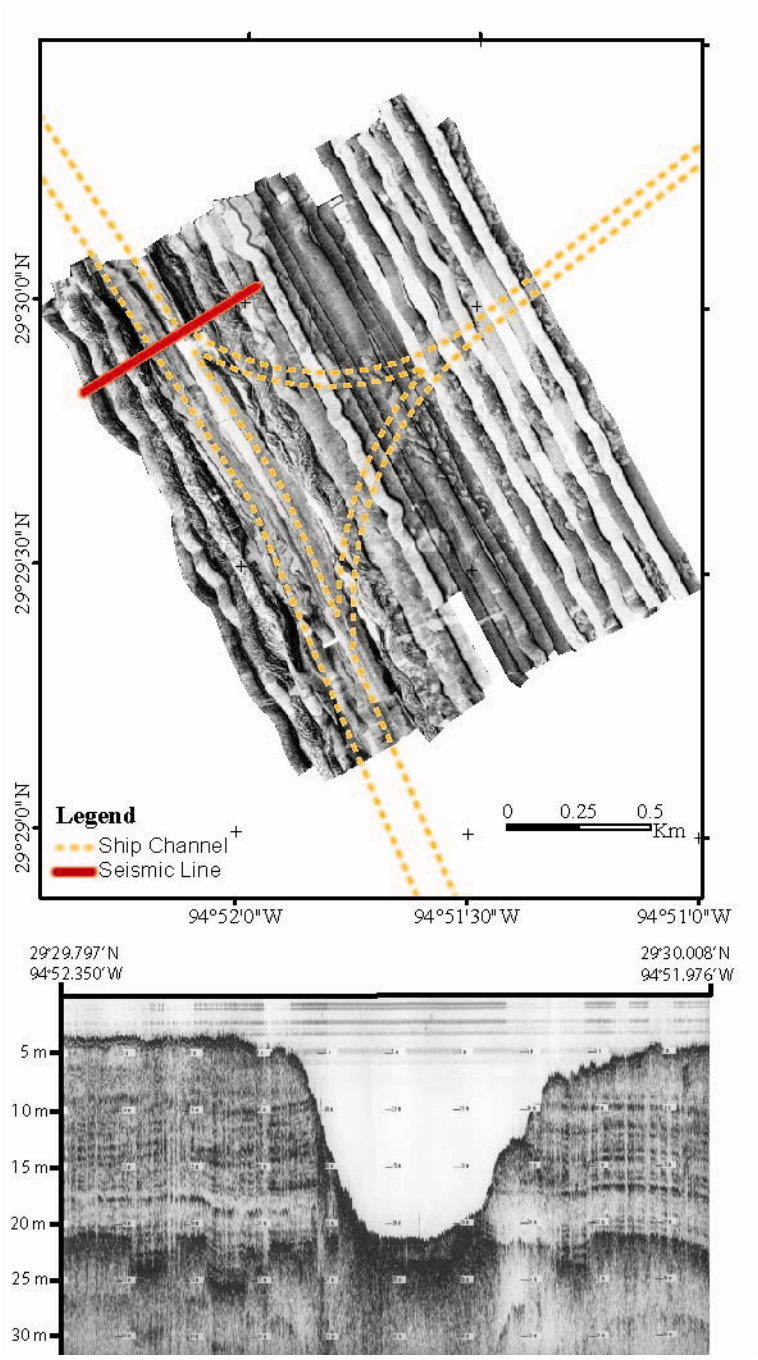

Figure 41. Chirp sonar image showing dredged area of the Houston Ship Channel. The red line on the map above shows the location of the chirp profile below.

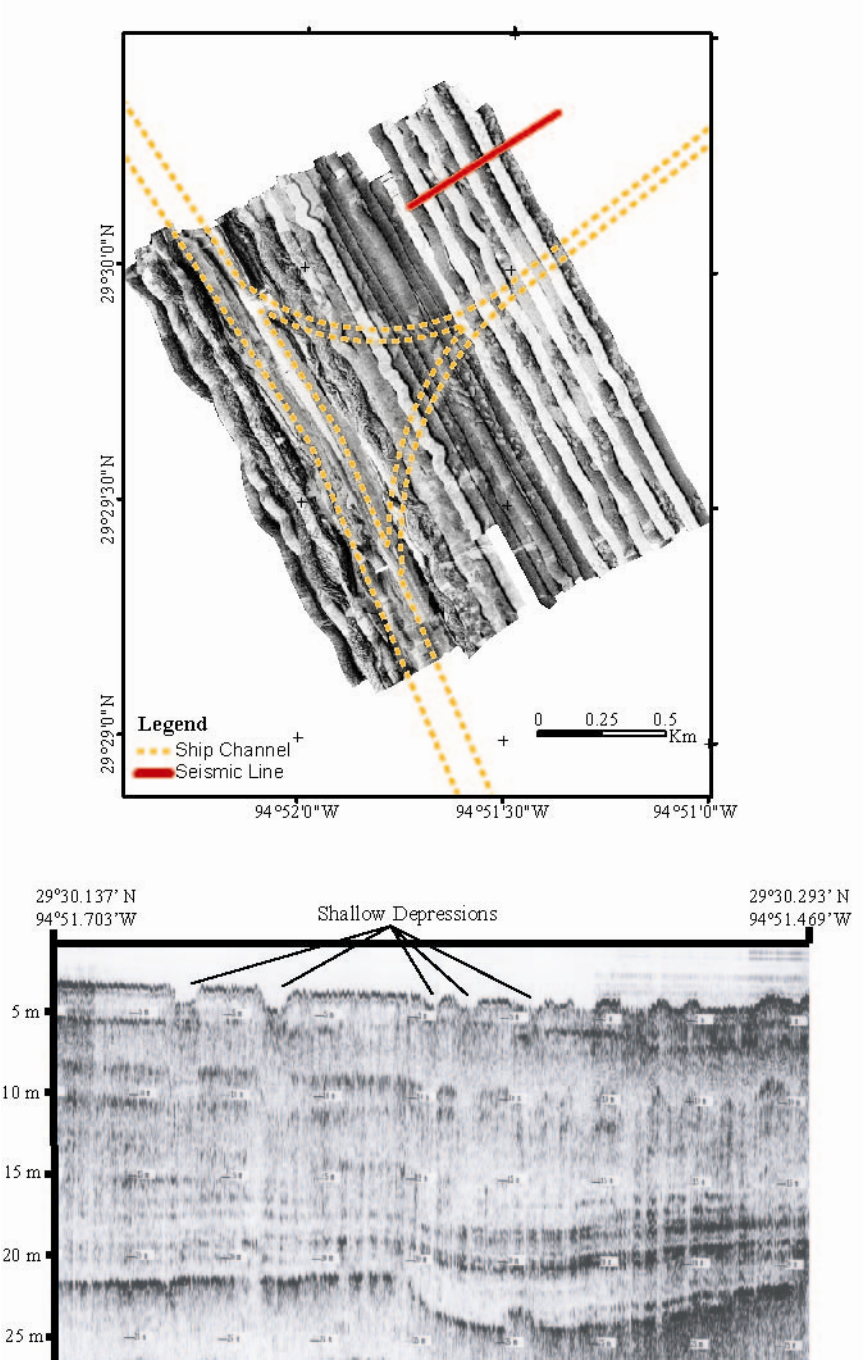

Figure 42. Chirp sonar image showing shell mining effects on the bay bottom. The red line on the map above shows the location of the chirp profile below.

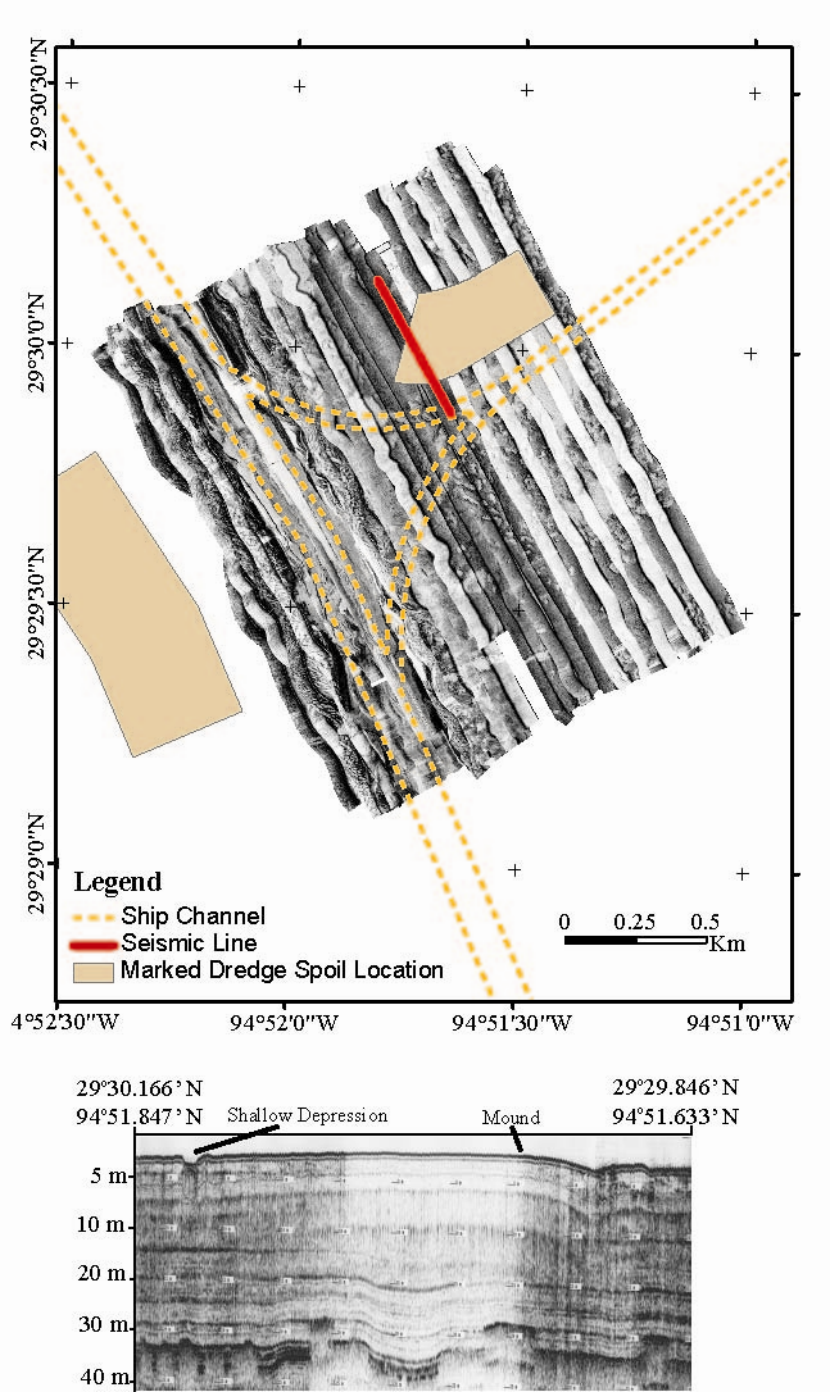

Figure 43. Chirp sonar image showing a dredge spoil. Image from the Redfish Island area. The red line on the map above shows the location of the chirp profile below.

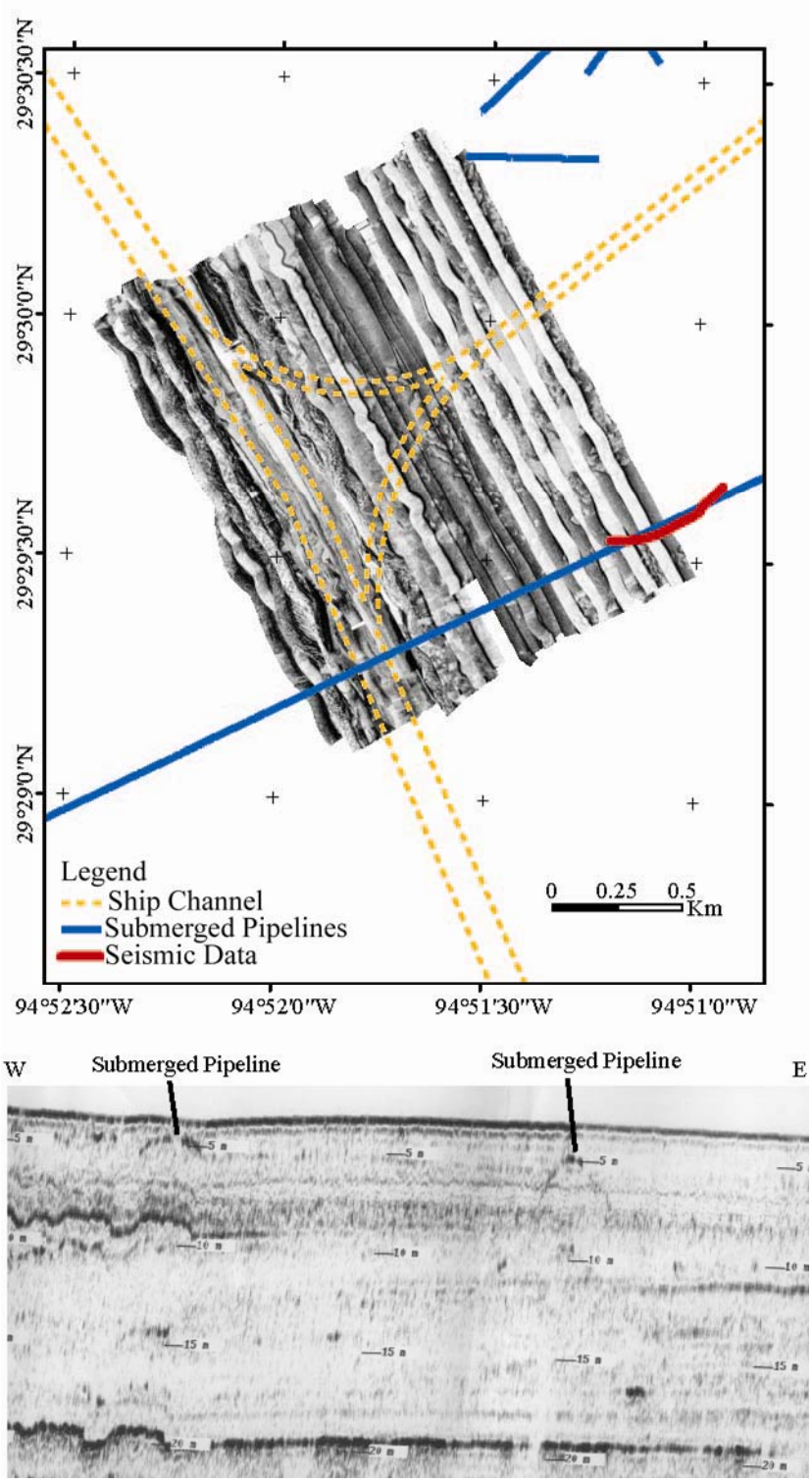

Figure 44. Chirp image of a buried pipeline in the Redfish Island area. The red line on the map above shows the location of the chirp profile below.

CONCLUSIONS

The primary objective of the survey was to use high-resolution geophysical equipment to map sediment distribution and anthropogenic impacts. Both the side-scan and chirp data revealed differences in bottom types. Three side-scan backscatter intensities were mapped in the side-scan sonar mosaics and eight bottom reflection types were interpreted from the sub-bottom data. The bottom types from the side-scan mosaics allowed for the differentiation between soft, bay fill mud, sand, shell debris and oyster beds. Chirp data from the Bolivar Roads and Redfish Island survey areas were classified into three separate bottom reflection types whereas the records in the other survey sites were divided into five types. Horizontal, parallel reflectors were displayed along the center of the Trinity incised valley and areas of weak or no reflectors were seen along its flanks. The parallel reflectors are indicative of bay fill sediments, while the flanks of the incised valley appear to contain coarser sediment which reduced acoustic penetration.

Three survey areas with currently existing oyster reefs displayed bottom types 4, 5, 6, and 7. It is not known if these strong reflectors are buried oyster reefs or a buried hard bottom and without deeper cores we cannot come to a solid conclusion. However, it is apparent that these bottom types are associated with current oyster beds, as the reflectors can be traced upward through the sediment column to the base of current oyster mounds and beds, and frequent buried mounds are seen at the same depth and are interpreted as buried oyster reefs.

Two types of impacts were seen on the bay bottom, debris and sediment disruption. Debris in the bay is concentrated in and around the ship channel and consists of objects

such as cylinders, pipes, and sunken boats. Areas of sediment disruption due to shrimp and oyster trawlers are scattered throughout the bay and were present in all six survey areas. The greatest density of trawl marks was imaged in the Bolivar Roads, Redfish Island, and Hannah's Reef survey sites. Another type of sediment disruption seen in the survey areas are those due to channel dredging and dredge spoil placement. Dredge spoils were present in the Redfish Island survey area and seemed to flow to the west.

REFERENCES CITED

Barnhardt, W. A., J.T. Kelley, S.M. Dickson, and D.F. Belknap, 1998, Mapping the Gulf of Maine with side-scan sonar: A new bottom-type classification for complex seafloor: Journal of Coastal Research, v. 14, no. 2, p. 646-659.

Cochrane, G. R., and K. D. Lafferty, 2002, Use of acoustic classification of sidescan sonar data for mapping benthic habitat in the Northern Channel Islands, California: Continental Shelf Research, v. 22, p. 683-690.

Dalrymple, R. W., B. A. Zaitlin, and R. Boyd, 1992, Estuarine facies models: Conceptual basis and stratigraphic implications: Journal of Sedimentary Research, v. 62, p. 1130-1146.

Dellapenna, T.M., S.A. Kuehl, and L.C. Schaffner, 1998, Sea-bed mixing and particle residence times in biologically and physically dominated estuarine systems: A comparison of Lower Chesapeake Bay and the York River Subestuary: Estuarine, Coastal and Shelf Science, v. 46, p. 777-795.

Eittreim, S. L., R. J. Anima, and A. J. Stevenson, 2001, Seafloor geology of the Monterey Bay area continental shelf: Marine Geology, v. 181, p. 3-34.

Lankford, R. R., and J. J. W. Rogers, 1969, Holocene Geology of the Galveston Bay Area: Houston, Houston Geological Society.

Lee, S. H., S. K. Chough, G. G. Back, and Y. B. Kim, 2002, Chirp (2-7-kHz) echo characters of the South Korea Plateau, East Sea: Styles of mass movement and sediment gravity flow: Marine Geology, v. 184, p. 227-247.

Nichols, M. M., G.H. Johnson, and P.C. Peebles, 1991, Modern sediment and facies model for a microtidal coastal plain estuary, The James River, Virginia: Journal of Sedimentary Petrology, v. 61, no. 6, p. 883-899.

Powell, E. N., J. Song, M. S. Ellis, and E. A. Wilson-Ormond, 1995, The status and long-term trends of oyster reefs in Galveston Bay, Texas: Journal of Shellfish Research, v. 14, p. 439-457.

Rodriguez, A. B., J. B. Anderson, and J. Bradford, 1998, Holocene tidal deltas of the trinity incised valley: Analogs for exploration and production: Gulf Coast Association of Geological Societies Transactions, v. 47, p. 373-380.

Smith, G. F., E.B. Roach, and D.G. Bruce, 2003, The location, composition, and origin of oyster bars in mesohaline Chesapeake Bay: Estuarine, Coastal and Shelf Science, v. 56, p. 391-409.

Smyth, W. C., J. B. Anderson, and M. A. Thomas, 1988, Seismic facies analysis of entrenched valley-fill: A case study in the Galveston Bay area, Texas: Gulf Coast Association of Geological Societies Transactions, v. 38, p. 385-394.

Wright, L.D., D. B. Prior, C.H. Hobbs, R. J. Byrne, J. D. Boon, L. C. Schaffner, and M. D. Green, 1987, Spatial variability of bottom types in the lower Chesapeake Bay and adjoining estuaries and inner shelf: Estuarine, Coastal Shelf Science, v. 26, p. 765-784.

APPENDIX A

Table 1: Survey Site Parameters

Site	NW Corner	NW Corner	SE Corner	SE Corner	Num. Tracks	Track Length (km)	Long side (km)	Short side (km)	Survey area (km^2)
Bolivar Roads	29° 21.82'	94° 48.89'	29° 21.27'	94° 46.49'	50	141	3.3	1.7	6.1
Redfish Island	29° 29.98'	94° 52.46'	29° 29.47'	94° 50.99'	39	74.4	2	1.6	3.1
East Bay	29° 27.08'	94° 45.96'	29° 26.29'	94° 43.68'	31	104.8	3.5	1.9	6.7
Hannah's Reef	29° 29.58'	94° 47.23'	29° 28.69'	94° 45.34'	28	69.2	3.1	1.8	5.3
Clear Lake	29° 32.94'	94° 59.18'	29° 32.14'	94° 57.27'	27	77.8	3.1	1.8	5.3
Trinity Bay	29° 36.79'	94° 54.08'	29° 36.02'	94° 52.23'	20	58.9	2.8	1.5	4.3

APPENDIX B

Table 2: Anthropogenic Impacts at Bolivar Roads

Latitude	Longitude	Type
N	W	
29.3456	94.7856	Object
29.3534	94.7815	Object
29.3542	94.7917	Hole/Groove
29.3600	94.8001	Object
29.3631	94.8009	Object
29.3744	94.7949	Object
29.3490	94.7861	Object
29.3525	94.7825	Object
29.3591	94.8003	Object
29.3596	94.8018	Object
29.3621	94.8066	Object
29.3701	94.7953	Object
29.3651	94.792	Object

Table 3: Anthropogenic Impacts at Red Island

Latitude	Longitude	Type
N	W	
29.4909	94.8620	Hole/Groove
29.4956	94.8617	Object
29.4979	94.8659	Hole/Groove
29.4992	94.8564	Hole/Groove
29.4871	94.8624	Object
29.4873	94.8634	Object
29.4879	94.8645	Object
29.4887	94.8630	Hole/Groove
29.4897	94.8651	Hole/Groove
29.4901	94.8638	Object
29.4903	94.8669	Hole/Groove
29.4912	94.8518	Hole/Groove
29.4918	94.8515	Hole/Groove
29.4919	94.8637	Object
29.4934	94.8637	Hole/Groove
29.4938	94.8687	Hole/Groove
29.4939	94.8547	Hole/Groove
29.4945	94.8541	Hole/Groove
29.4947	94.8546	Hole/Groove
29.4951	94.8650	Object
29.4951	94.8539	Hole/Groove
29.4959	94.8579	Hole/Groove
29.4960	94.8693	Object
29.4962	94.8538	Hole/Groove
29.4967	94.8547	Hole/Groove
29.4990	94.8600	Hole/Groove
29.4994	94.8598	Hole/Groove

APPENDIX C

Table 4: Surface Sediment Samples at Bolivar Roads

* Estimated percentage due to grain size restrictions of Malvern.

Sample ID	Type	Latitude	Longitude	Sand %	Silt %	Clay %	Material
BRC-1	Core	29° 21.85'	94° 47.95'	14.58	81.30	4.12	Silt
BRC-2	Core	29° 21.42'	94° 47.24'	16.45	76.63	6.92	Silt Loam
BRC-3	Core	29° 21.44'	94° 47.23'	91.09	8.35	0.56	Sand
BRC-4	Core	29° 21.08'	94° 47.14'	70*	30	0	Shell Debris
BRC-5	Core	29° 21.16'	94° 46.60'	96.50	3.44	0.06	Sand
BRC-6	Core	29° 20.83'	94° 47.15'	N/A	N/A	N/A	
BRC-7	Core	29° 20.96'	94° 47.03'	N/A	N/A	N/A	
BRC-8	Core	29° 21.19'	94° 46.73'	N/A	N/A	N/A	
BRG-1	Grab	29° 21.44'	94° 47.18'	42.49	46.25	11.26	Loam
BRG-2	Grab	29° 21.40'	94° 47.37'	31.68	53.92	14.40	Silt Loam
BRG-3	Grab	29° 21.99'	94° 47.62'	100*	0	0	Shell Debris
BRG-4	Grab	29° 21.23'	94° 47.76'	100*	0	0	Shell Debris
BRG-5	Grab	29° 21.64'	94° 48.06'	72.55	21.71	5.73	Sandy Loam
BRG-6	Grab	29° 21.91'	94° 47.30'	100*	0	0	Shell Debris
BRG-7	Grab	29° 21.81'	94° 47.81'	29.91	63.89	6.20	Silt Loam
BRG-8	Grab	29° 21.93'	94° 47.56'	100*	0	0	Shell Debris
BRG-9	Grab	29° 22.06'	94° 47.40'	19.39	63.97	16.64	Silt Loam
BRG-10	Grab	29° 22.46'	94° 47.85'	80*	20	0	Shell Debris
BRG-11	Grab	29° 22.45'	94° 47.89'	75*	25	0	Shell Debris
BRG-12	Grab	29° 22.24'	94° 47.94'	100*	0	0	Shell Debris
BRG-13	Grab	29° 22.17'	94° 48.15'	100*	0	0	Shell Debris
BRG-14	Grab	29° 21.86'	94° 48.34'	60.13	31.62	8.26	Sandy Loam
BRG-15	Grab	29° 21.72'	94° 48.06'	35.13	52.10	12.77	Silt Loam
BRG-16	Grab	29° 21.62'	94° 47.82'	100*	0	0	Shell Debris
BRG-17	Grab	29° 21.54'	94° 47.60'	100*	0	0	Shell Debris
BRG-18	Grab	29° 21.49'	94° 47.40'	32.51	51.38	16.11	Silt Loam
BRG-19	Grab	29° 21.45'	94° 47.32'	56.37	33.86	9.77	Sandy Loam
BRG-20	Grab	29° 21.47'	94° 46.95'	84.94	13.17	1.88	Loamy Sand
BRG-21	Grab	29° 21.60'	94° 47.05'	71.46	23.71	4.83	Sandy Loam
BRG-22	Grab	29° 21.55'	94° 47.28'	100*	0	0	Shell Debris
BRG-23	Grab	29° 21.37'	94° 47.42'	100*	0	0	Shell Debris
BRG-24	Grab	29° 21.21'	94° 47.50'	100*	0	0	Shell Debris
BRG-25	Grab	29° 20.99'	94° 47.51'	100*	0	0	Shell Debris
BRG-26	Grab	29° 21.24'	94° 47.67'	38.79	50.13	11.08	Silt Loam
BRG-27	Grab	29° 21.41'	94° 47.73'	100*	0	0	Shell Debris
BRG-28	Grab	29° 21.64'	94° 47.75'	80*	20	0	Shell Debris
BRG-29	Grab	29° 21.83'	94° 47.78'	34.42	52.02	13.56	Silt Loam
BRG-30	Grab	29° 22.04'	94° 47.84'	58.39	32.93	8.68	Shell Debris
BRG-31	Grab	29° 22.24'	94° 47.86'	100*	0	0	Shell Debris
BRG-32	Grab	29° 22.43'	94° 47.83'	56.60	37.51	5.89	Sandy Loam

Table 5: Surface Sediment Samples at Redfish Island

Sample ID	Type	Latitude	Longitude	Sand %	Silt %	Clay %	Material
RFC-1	Core	29° 29.26'	94° 51.82'	16.66	65.95	17.39	Silt Loam
RFC-2	Core	29° 29.25'	94° 51.84'	70*	20	10	Shell Debris
RFC-3	Core	29° 29.61'	94° 51.83'	25.96	61.78	12.27	Silt Loam
RFC-4	Core	29° 29.63'	94° 51.86'	N/A	N/A	N/A	Silt Loam
RFC-5	Core	29° 29.67'	94° 51.89'	N/A	N/A	N/A	Silt Loam
RFC-6	Core	29° 29.67'	94° 51.89'	19.48	65.35	15.16	Silt Loam
RFC-7	Core	29° 29.92'	94° 52.35'	70*	20	10	Shell Debris
RFC-8	Core	29° 30.18'	94° 52.06'	74.78	23.61	1.61	Loamy Sand
RFC-9	Core	29° 29.79'	94° 51.91'	N/A	N/A	N/A	Silt Loam
RFC-10	Core	29° 29.81'	94° 51.90'	28.50	59.11	12.39	Silt Loam
RFG-1	Grab	29° 29.99'	94° 52.24'	26.51	59.40	14.09	Silt Loam
RFG-2	Grab	29° 29.49'	94° 52.12'	N/A	N/A	N/A	Silt Loam
RFG-3	Grab	29° 29.54'	94° 52.02'	24.22	60.23	15.55	Silt Loam
RFG-4	Grab	29° 29.61'	94° 51.94'	94.48	4.24	1.28	Sand
RFG-5	Grab	29° 29.66'	94° 51.88'	25.23	62.97	11.81	Silt Loam
RFG-6	Grab	29° 29.58'	94° 51.82'	21.24	64.09	14.67	Silt Loam
RFG-7	Grab	29° 29.94'	94° 51.57'	N/A	N/A	N/A	Silt Loam
RFG-8	Grab	29° 29.96'	94° 51.61'	37.18	53.98	8.84	Silt Loam
RFG-9	Grab	29° 29.27'	94° 51.78'	44.94	45.85	9.21	Loam
RFG-10	Grab	29° 29.64'	94° 51.81'	41.47	47.81	10.72	Loam

Table 6: Surface Sediment Samples at East Bay

Sample ID	Type	Latitude	Longitude	Sand %	Silt %	Clay %	Material
EBC1A	Core	29° 26.86'	94° 44.06'	N/A	N/A	N/A	Silt Loam
EBC1B	Core	29° 26.77'	94° 44.05'	N/A	N/A	N/A	Silt Loam
EBC2A	Core	29° 26.76'	94° 45.64'	N/A	N/A	N/A	Silt Loam
EBC2B	Core	29° 26.81'	94° 45.55'	N/A	N/A	N/A	Silt Loam
EBG1	Grab	29° 27.23'	94° 45.74'	15.14	73.69	11.17	Silt Loam
EBG2	Grab	29° 26.43'	94° 45.55'	11.08	77.55	11.37	Silt Loam
EBG3	Grab	29° 26.32'	94° 44.72'	11.61	76.69	11.69	Silt Loam
EBG4	Grab	29° 26.86'	94° 44.91'	13.31	75.25	11.44	Silt Loam
EBG5	Grab	29° 27.27'	94° 44.90'	13.73	74.22	12.06	Silt Loam
EBG6	Grab	29° 27.23'	94° 44.21'	13.47	75.42	11.12	Silt Loam
EBG7	Grab	29° 26.48'	94° 43.98'	11.53	74.70	13.77	Silt Loam

Table 7: Surface Sediment Samples at Hannah's Reef

Sample ID	Type	Latitude	Longitude	Sand %	Silt %	Clay %	Material
HRC1A	Core	29° 29.16'	94° 45.57'	N/A	N/A	N/A	Silt Loam
HRC1B	Core	29° 29.17'	94° 45.58'	N/A	N/A	N/A	Silt Loam
HRC2A	Core	29° 29.13'	94° 46.97'	N/A	N/A	N/A	Silt Loam
HRC2B	Core	29° 29.13'	94° 46.97'	N/A	N/A	N/A	Silt Loam
HRG1	Grab	29° 28.80'	94° 46.98'	17.46	73.34	9.20	Silt Loam
HRG2	Grab	29° 29.33'	94° 47.13'	N/A	N/A	N/A	Shell Debris
HRG3	Grab	29° 29.52'	94° 46.90'	N/A	N/A	N/A	Shell Debris
HRG4	Grab	29° 29.51'	94° 46.28'	15.32	76.47	8.21	Silt Loam
HRG5	Grab	29° 29.18'	94° 46.26'	N/A	N/A	N/A	Shell Debris
HRG6	Grab	29° 28.81'	94° 46.20'	18.30	72.51	9.19	Silt Loam
HRG7	Grab	29° 28.78'	94° 45.53'	N/A	N/A	N/A	Shell Debris
HRG8	Grab	29° 29.31'	94° 45.43'	N/A	N/A	N/A	Shell Debris
HRG9	Grab	29° 29.53'	94° 45.58'	10.17	77.71	12.12	Silt Loam

Table 8: Surface Sediment Samples at the Clear Lake Entrance Site

Sample ID	Type	Latitude	Longitude	Sand %	Silt %	Clay %	Material
CLC1A	Core	29° 32.58'	94° 58.97'	N/A	N/A	N/A	Silt Loam
CLC1B	Core	29° 32.58'	94° 58.98'	N/A	N/A	N/A	Silt Loam
CLC2A	Core	29° 32.63'	94° 57.52'	N/A	N/A	N/A	Silt Loam
CLC2B	Core	29° 32.63'	94° 57.52'	N/A	N/A	N/A	Silt Loam
CLG1	Grab	29° 32.21'	94° 53.48'	10.00	79.46	10.54	Silt Loam
CLG2	Grab	29° 32.40'	94° 58.68'	N/A	N/A	N/A	Shell Debris
CLG3	Grab	29° 32.85'	94° 58.94'	9.79	79.37	10.90	Silt Loam
CLG4	Grab	29° 32.88'	94° 58.18'	16.30	72.90	10.79	Silt Loam
CLG5	Grab	29° 32.54'	94° 58.14'	12.00	74.83	13.17	Silt Loam
CLG6	Grab	29° 32.87'	94° 58.18'	N/A	N/A	N/A	Shell Debris
CLG7	Grab	29° 32.22'	94° 58.11'	10.40	79.45	10.16	Silt Loam
CLG8	Grab	29° 32.20'	94° 57.55'	N/A	N/A	N/A	Shell Debris
CLG9	Grab	29° 32.88'	94° 57.58'	16.23	74.61	9.16	Silt Loam

Table 9: Surface Sediment Samples from the Trinity Bay Survey Site

Sample ID	Type	Latitude	Longitude	Sand %	Silt %	Clay %	Material
TBC1A	Core	29° 36.43'	94° 53.96'	N/A	N/A	N/A	Silt Loam
TBC1B	Core	29° 36.44'	94° 53.96'	N/A	N/A	N/A	Silt Loam
TBC2A	Core	29° 36.46'	94° 52.43'	N/A	N/A	N/A	Silt Loam
TBC2B	Core	29° 36.46'	94° 52.44'	N/A	N/A	N/A	Silt Loam
TBG1	Grab	29° 32.15'	94° 53.86'	17.49	74.79	7.72	Silt Loam
TBG2	Grab	29° 36.69'	94° 53.88'	N/A	N/A	N/A	Shell Debris
TBG3	Grab	29° 36.72'	94° 53.21'	21.68	67.22	11.10	Silt Loam
TBG4	Grab	29° 36.43'	94° 53.12'	33.67	55.77	10.56	Silt Loam
TBG5	Grab	29° 32.11'	94° 53.10'	15.12	75.59	9.30	Silt Loam
TBG6	Grab	29° 36.13'	94° 52.49'	10.05	80.02	9.93	Silt
TBG7	Grab	29° 36.71'	94° 52.44'	N/A	N/A	N/A	Shell Debris

APPENDIX D

GRAIN SIZE GRAPHS

BOLIVAR ROADS CORE 1 SURFACE SAMPLE

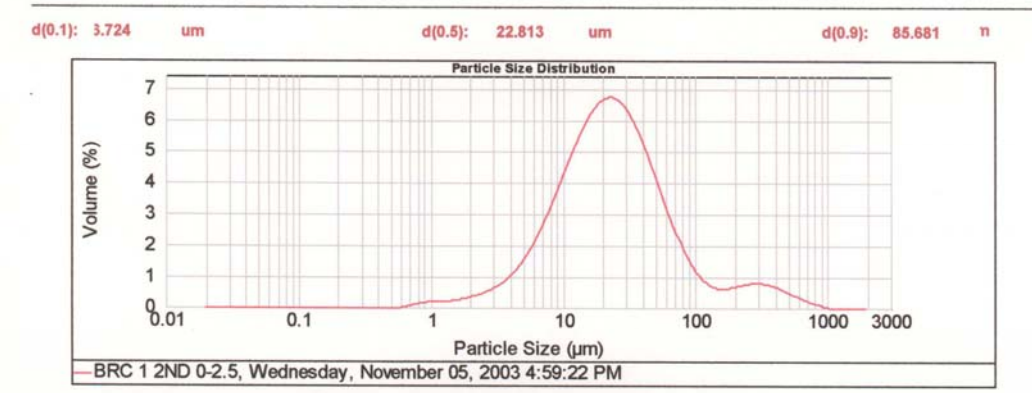

Percentage between 0.00 µm and 3.90 µm : 4.12%
Percentage between 3.90 µm and 63.00 µm : 81.30%
Percentage between 63.00 µm and 2000.00 µm : 14.58%

BOLIVAR ROADS CORE 2 SURFACE SAMPLE

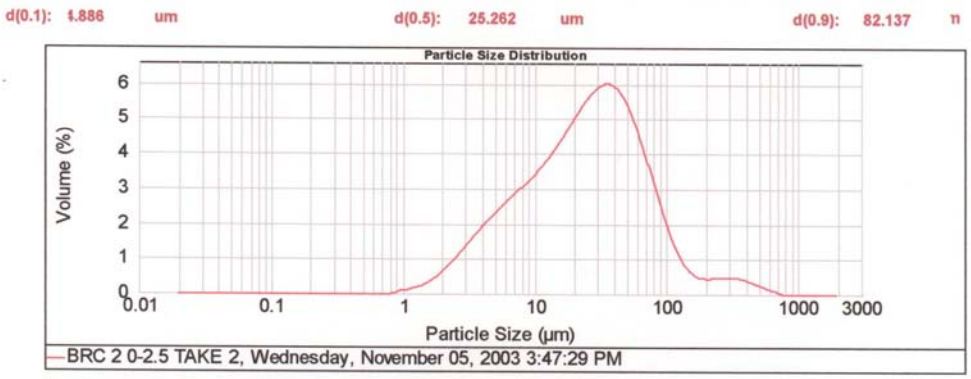

Percentage between 0.00 µm and 3.90 µm : 6.92%
Percentage between 3.90 µm and 63.00 µm : 76.63%
Percentage between 63.00 µm and 2000.00 µm : 16.45%

BOLIVAR ROADS CORE 5 SURFACE SAMPLE

d(0.1): 136.253 um d(0.5): 241.109 um d(0.9): 411.756 n

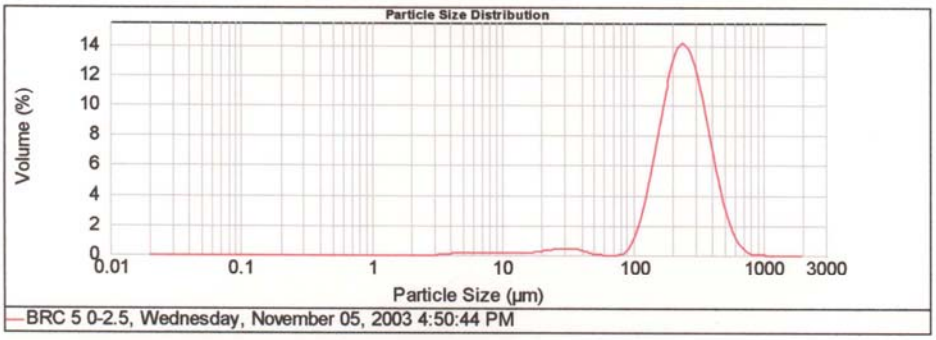

Percentage between 0.00 µm and 3.90 µm : 0.06%
Percentage between 3.90 µm and 63.00 µm : 3.44%
Percentage between 63.00 µm and 2000.00 µm : 96.50%

BOLIVAR ROADS GRAB 1 SURFACE SAMPLE

d(0.1): 3.628 um d(0.5): 22.350 um d(0.9): 258.981 n

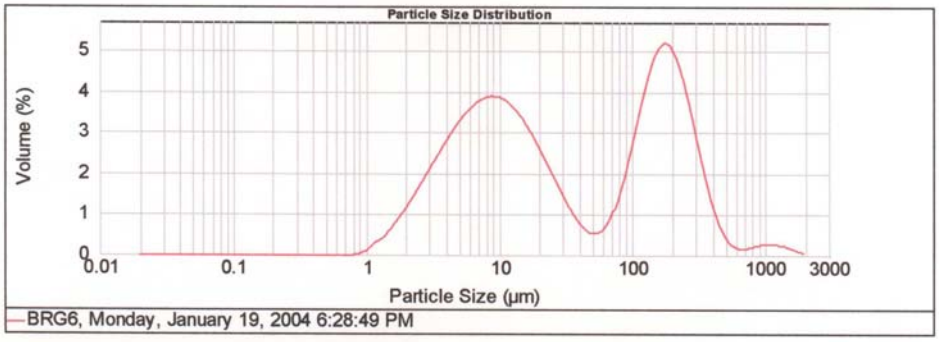

Percentage between 0.00 µm and 3.90 µm : 11.26%
Percentage between 3.90 µm and 63.00 µm : 46.25%
Percentage between 63.00 µm and 2000.00 µm : 42.49%

BOLIVAR ROADS GRAB 2 SURFACE SAMPLE

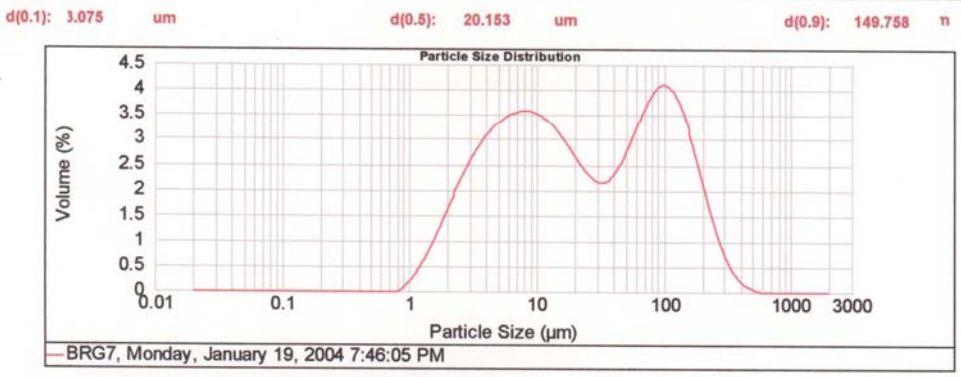

Percentage between 0.00 µm and 3.90 µm : 14.40%
Percentage between 3.90 µm and 63.00 µm : 53.92%
Percentage between 63.00 µm and 2000.00 µm : 31.68%

BOLIVAR ROADS GRAB 5 SURFACE SAMPLE

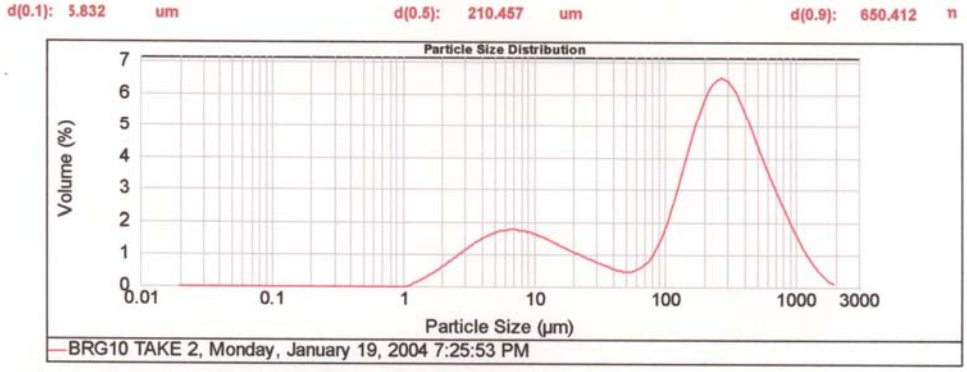

Percentage between 0.00 µm and 3.90 µm : 5.73%
Percentage between 3.90 µm and 63.00 µm : 21.71%
Percentage between 63.00 µm and 2000.00 µm : 72.55%

BOLIVAR ROADS GRAB 7 SURFACE SAMPLE

d(0.1): 5.199 um d(0.5): 26.920 um d(0.9): 212.807 n

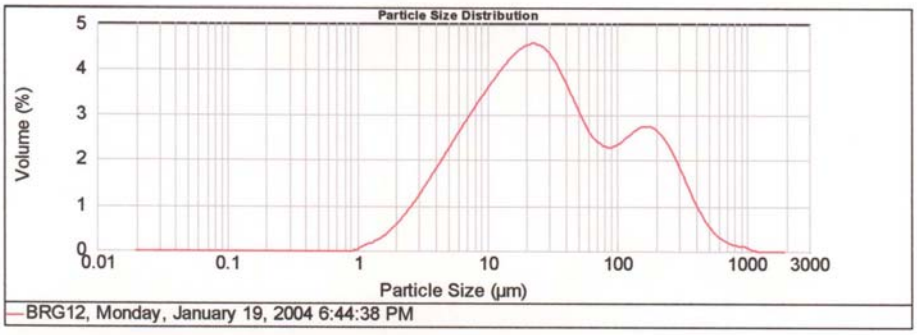

Percentage between 0.00 µm and 3.90 µm : 6.20%
Percentage between 3.90 µm and 63.00 µm : 63.89%
Percentage between 63.00 µm and 2000.00 µm : 29.91%

BOLIVAR ROADS GRAB 9 SURFACE SAMPLE

d(0.1): 2.831 um d(0.5): 15.127 um d(0.9): 102.292 n

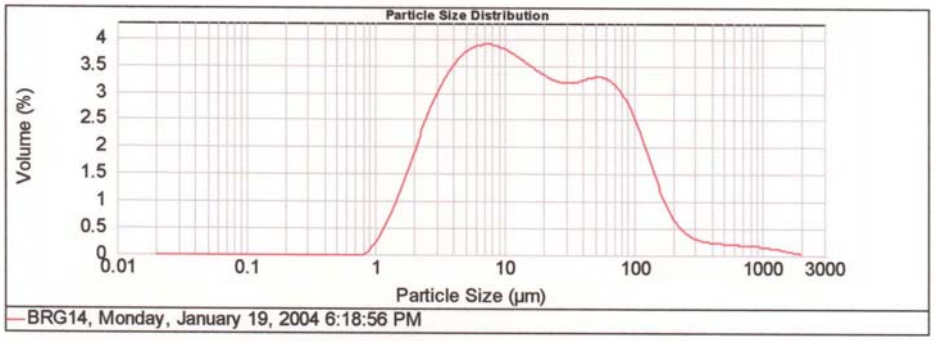

Percentage between 0.00 µm and 3.90 µm : 16.64%
Percentage between 3.90 µm and 63.00 µm : 63.97%
Percentage between 63.00 µm and 2000.00 µm : 19.39%

BOLIVAR ROADS GRAB 14 SURFACE SAMPLE

d(0.1): 4.417 um d(0.5): 117.345 um d(0.9): 360.804 n

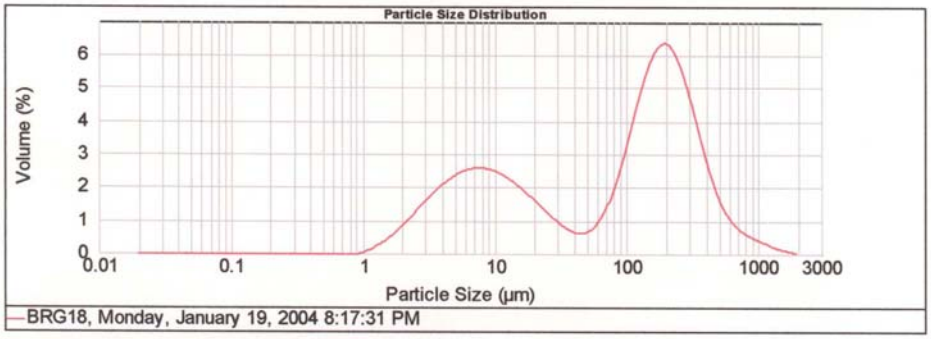

Percentage between 0.00 µm and 3.90 µm : 8.26%
Percentage between 3.90 µm and 63.00 µm : 31.62%
Percentage between 63.00 µm and 2000.00 µm : 60.13%

BOLIVAR ROADS GRAB 15 SURFACE SAMPLE

d(0.1): 3.389 um d(0.5): 17.459 um d(0.9): 200.422 n

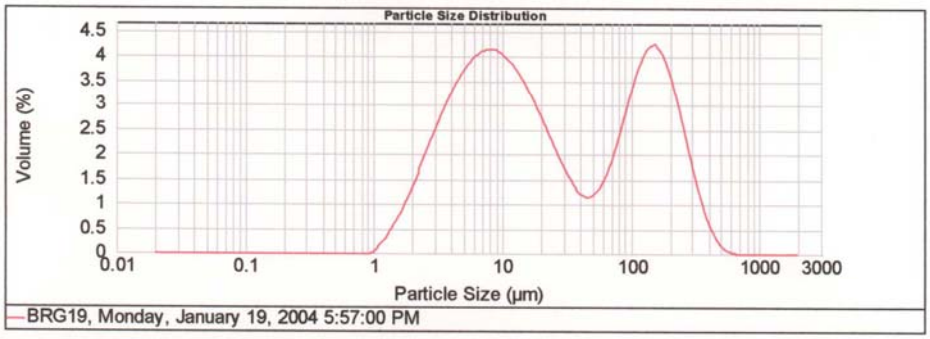

Percentage between 0.00 µm and 3.90 µm : 12.77%
Percentage between 3.90 µm and 63.00 µm : 52.10%
Percentage between 63.00 µm and 2000.00 µm : 35.13%

BOLIVAR ROADS GRAB 18 SURFACE SAMPLE

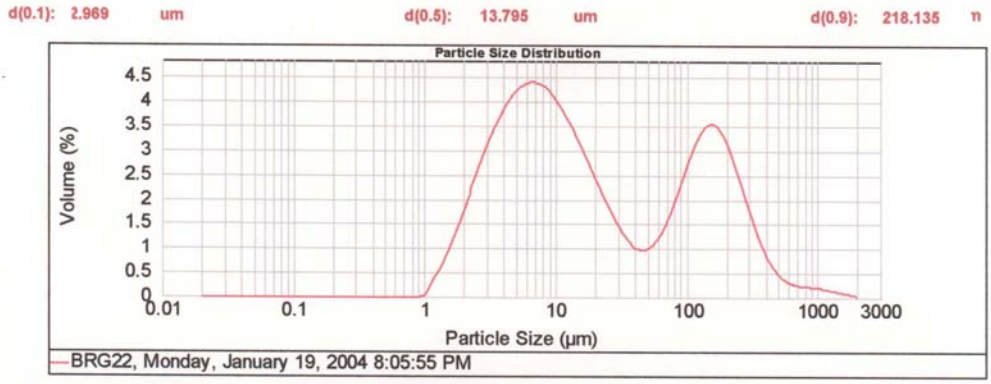

Percentage between 0.00 µm and 3.90 µm : 16.11%
Percentage between 3.90 µm and 63.00 µm : 51.38%
Percentage between 63.00 µm and 2000.00 µm : 32.51%

BOLIVAR ROADS GRAB 19 SURFACE SAMPLE

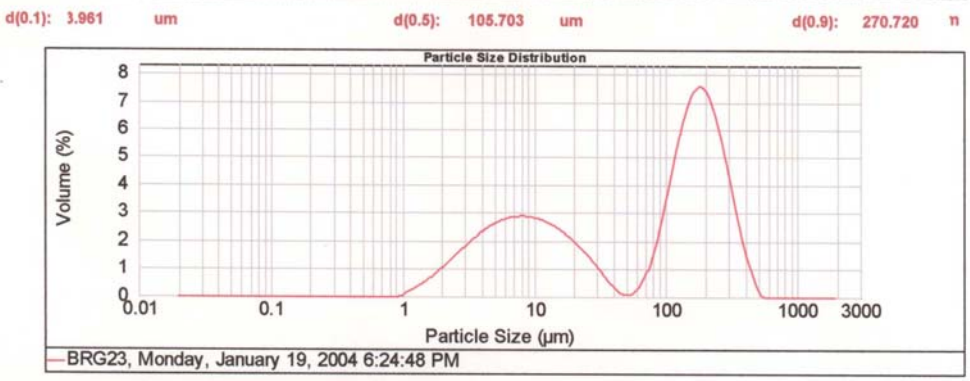

Percentage between 0.00 µm and 3.90 µm : 9.77%
Percentage between 3.90 µm and 63.00 µm : 33.86%
Percentage between 63.00 µm and 2000.00 µm : 56.37%

BOLIVAR ROADS GRAB 20 SURFACE SAMPLE

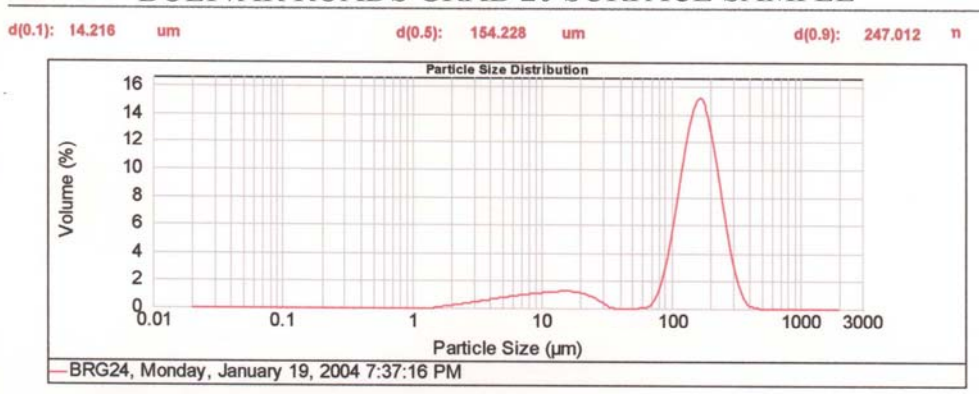

Percentage between 0.00 µm and 3.90 µm : 1.88%
Percentage between 3.90 µm and 63.00 µm : 13.17%
Percentage between 63.00 µm and 2000.00 µm : 84.94%

BOLIVAR ROADS GRAB 21 SURFACE SAMPLE

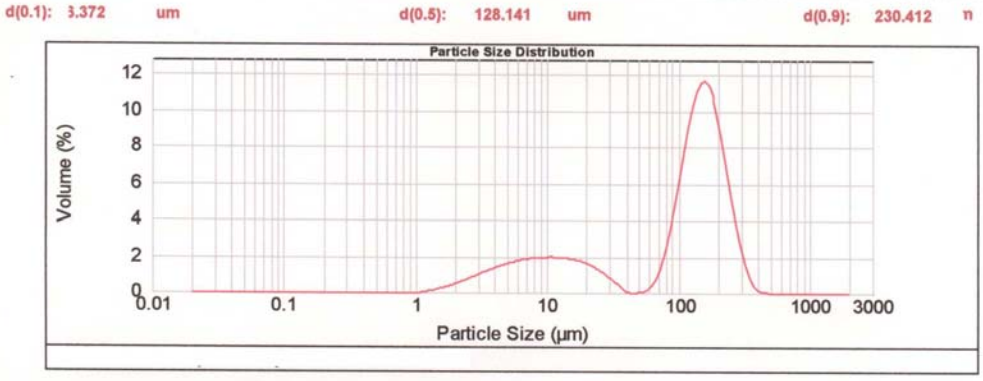

Percentage between 0.00 µm and 3.90 µm : 4.83%
Percentage between 3.90 µm and 63.00 µm : 23.71%
Percentage between 63.00 µm and 2000.00 µm : 71.46%

BOLIVAR ROADS GRAB 26 SURFACE SAMPLE

d(0.1): 3.692 um d(0.5): 19.479 um d(0.9): 264.895 n

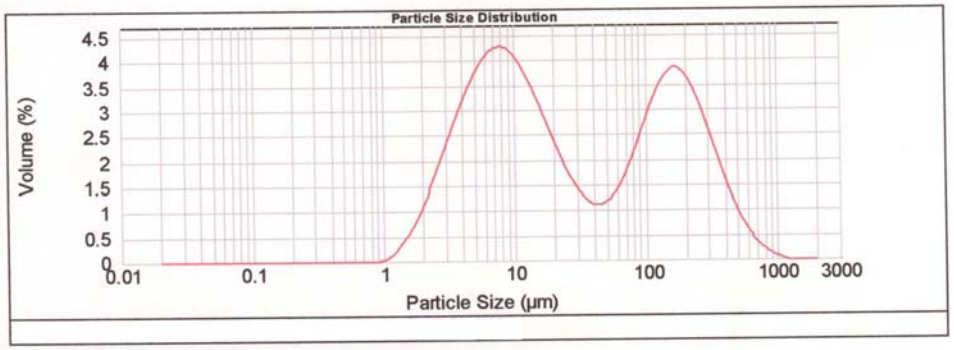

Percentage between 0.00 µm and 3.90 µm : 11.08%
Percentage between 3.90 µm and 63.00 µm : 50.13%
Percentage between 63.00 µm and 2000.00 µm : 38.79%

BOLIVAR ROADS GRAB 29 SURFACE SAMPLE

d(0.1): 3.215 um d(0.5): 20.373 um d(0.9): 203.969 n

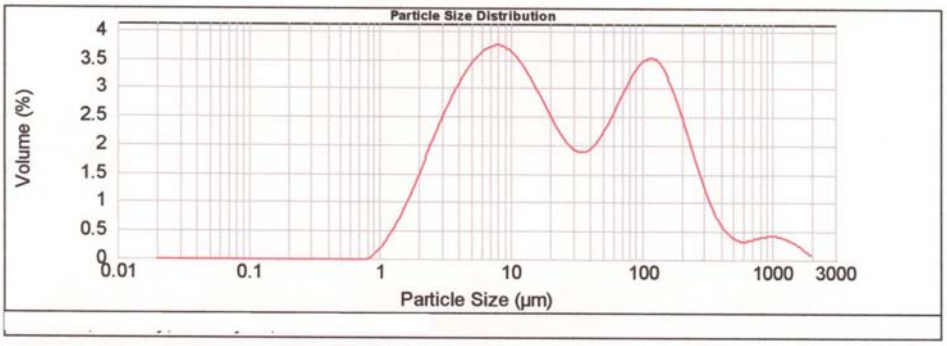

Percentage between 0.00 µm and 3.90 µm : 13.56%
Percentage between 3.90 µm and 63.00 µm : 52.02%
Percentage between 63.00 µm and 2000.00 µm : 34.42%

BOLIVAR ROADS GRAB 30 SURFACE SAMPLE

d(0.1): 4.254 um d(0.5): 105.752 um d(0.9): 293.683 n

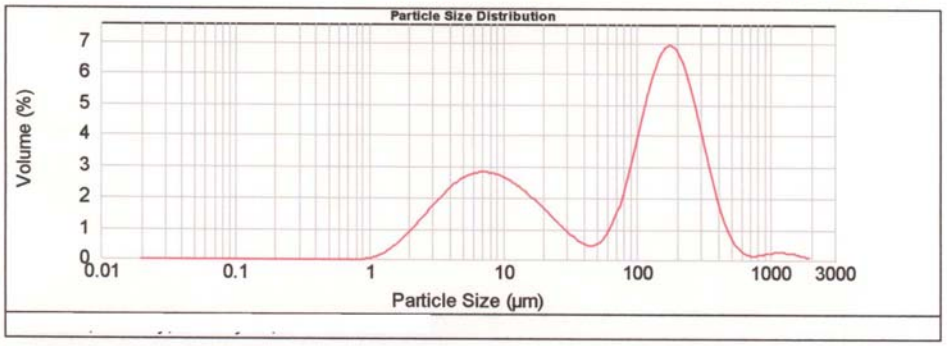

Percentage between 0.00 µm and 3.90 µm : 8.68%
Percentage between 3.90 µm and 63.00 µm : 32.93%
Percentage between 63.00 µm and 2000.00 µm : 58.39%

BOLIVAR ROADS GRAB 32 SURFACE SAMPLE

d(0.1): 5.213 um d(0.5): 103.171 um d(0.9): 311.605 n

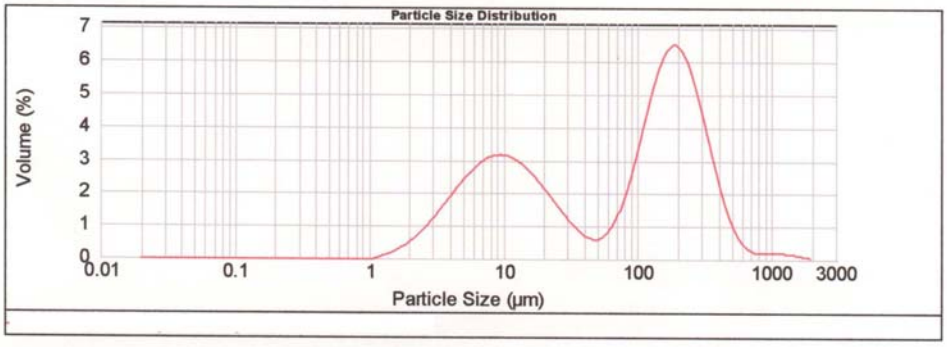

Percentage between 0.00 µm and 3.90 µm : 5.89%
Percentage between 3.90 µm and 63.00 µm : 37.51%
Percentage between 63.00 µm and 2000.00 µm : 56.60%

REDFISH ISLAND CORE 1 SURFACE SAMPLE

d(0.1): 2.898 um d(0.5): 10.682 um d(0.9): 129.496 n

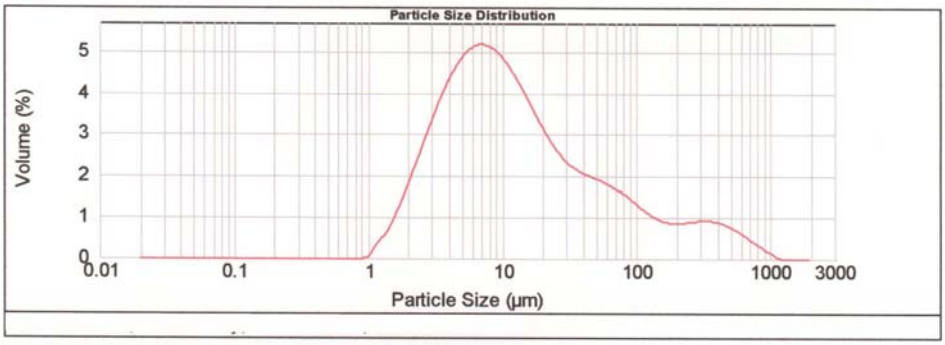

Percentage between 0.00 µm and 3.90 µm : 17.39%
Percentage between 3.90 µm and 63.00 µm : 65.95%
Percentage between 63.00 µm and 2000.00 µm : 16.66%

REDFISH ISLAND CORE 3 SURFACE SAMPLE

d(0.1): 102.967 um d(0.5): 213.056 um d(0.9): 354.824 n

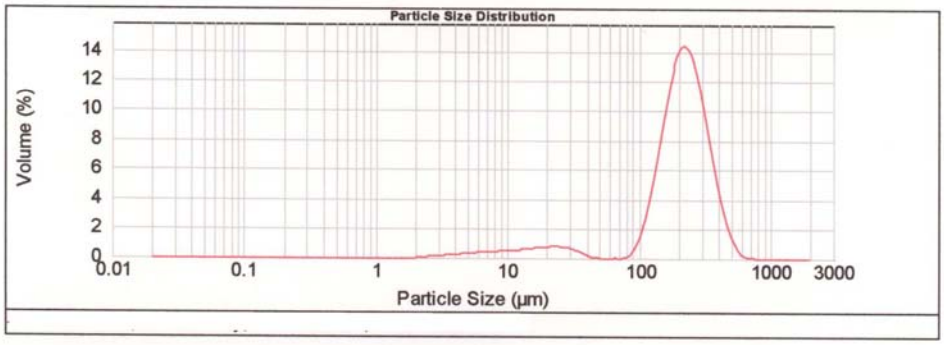

Percentage between 0.00 µm and 3.90 µm : 0.56%
Percentage between 3.90 µm and 63.00 µm : 8.35%
Percentage between 63.00 µm and 2000.00 µm : 91.09%

REDFISH ISLAND CORE 6 SURFACE SAMPLE

d(0.1): 3.142 um d(0.5): 12.479 um d(0.9): 145.746 n

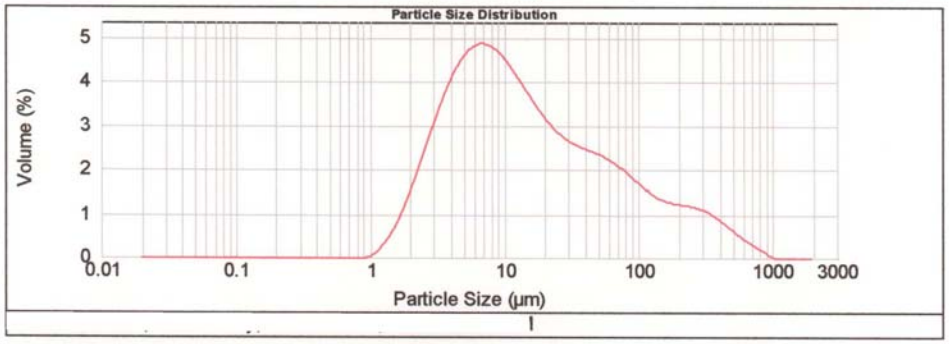

Percentage between 0.00 µm and 3.90 µm : 15.16%
Percentage between 3.90 µm and 63.00 µm : 65.35%
Percentage between 63.00 µm and 2000.00 µm : 19.48%

REDFISH ISLAND CORE 8 SURFACE SAMPLE

d(0.1): 13.951 um d(0.5): 97.656 um d(0.9): 188.547 n

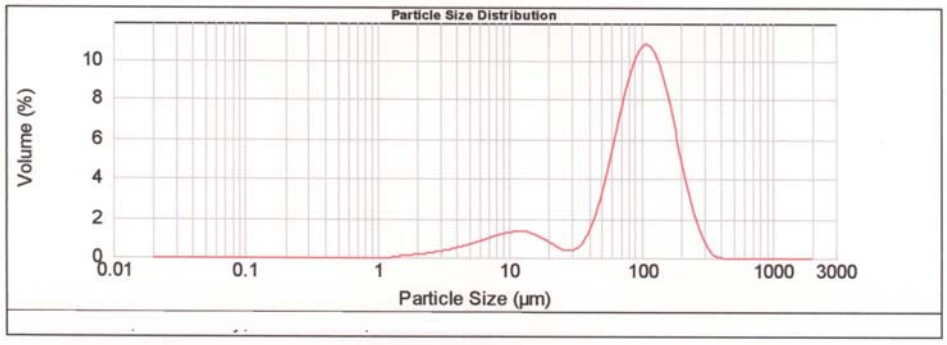

Percentage between 0.00 µm and 3.90 µm : 1.61%
Percentage between 3.90 µm and 63.00 µm : 23.61%
Percentage between 63.00 µm and 2000.00 µm : 74.78%

REDFISH ISLAND CORE 10 SURFACE SAMPLE

d(0.1): 3.477 um d(0.5): 18.715 um d(0.9): 164.324 n

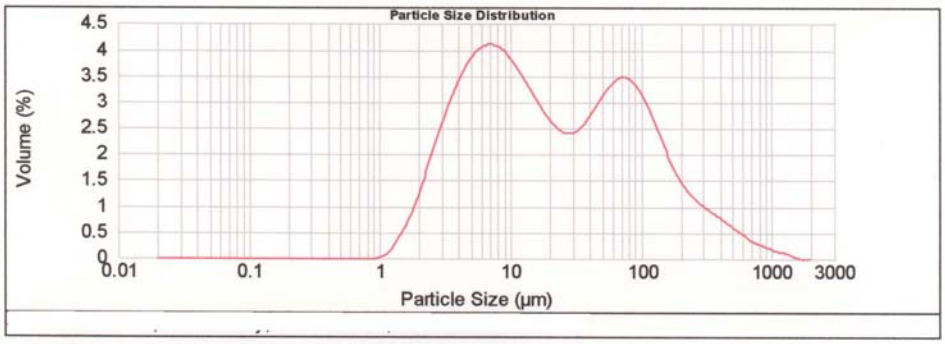

Percentage between 0.00 µm and 3.90 µm : 12.39%
Percentage between 3.90 µm and 63.00 µm : 59.11%
Percentage between 63.00 µm and 2000.00 µm : 28.50%

REDFISH ISLAND GRAB 1 SURFACE SAMPLE

d(0.1): 3.156 um d(0.5): 18.134 um d(0.9): 125.090 n

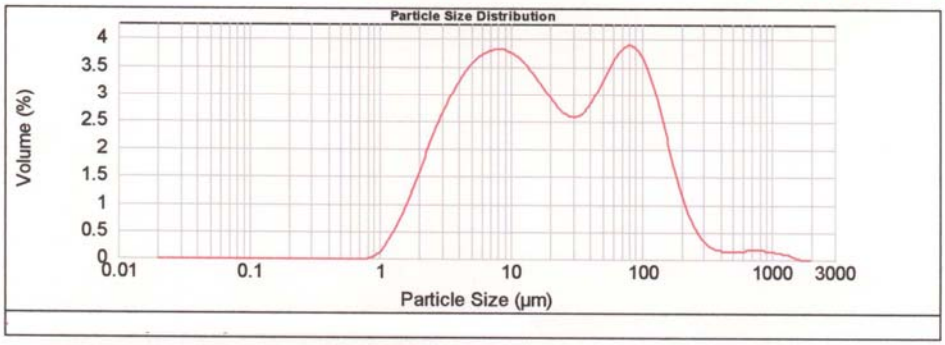

Percentage between 0.00 µm and 3.90 µm : 14.09%
Percentage between 3.90 µm and 63.00 µm : 59.40%
Percentage between 63.00 µm and 2000.00 µm : 26.51%

REDFISH ISLAND GRAB 4 SURFACE SAMPLE

d(0.1): 76.166 um d(0.5): 131.314 um d(0.9): 216.218 n

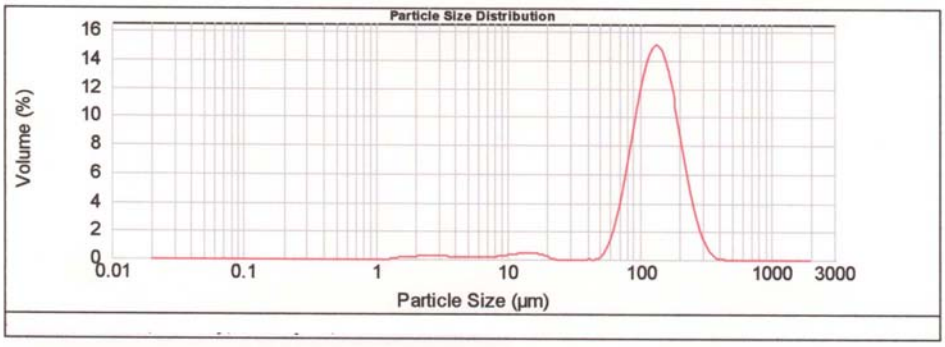

Percentage between 0.00 µm and 3.90 µm : 1.28%
Percentage between 3.90 µm and 63.00 µm : 4.24%
Percentage between 63.00 µm and 2000.00 µm : 94.48%

REDFISH ISLAND GRAB 5 SURFACE SAMPLE

d(0.1): 3.538 um d(0.5): 17.209 um d(0.9): 126.376 n

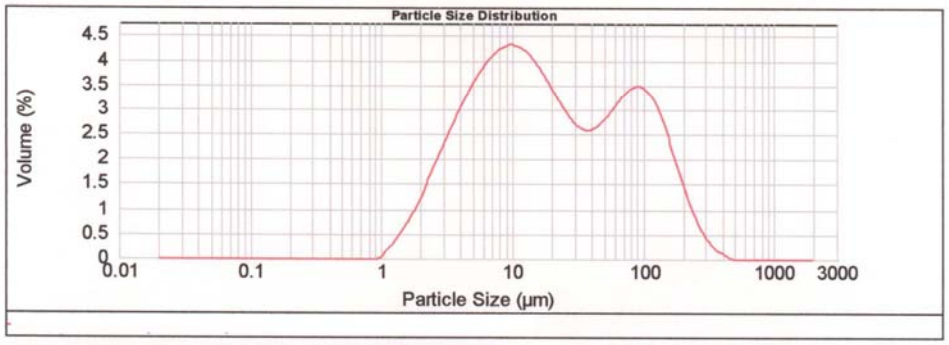

Percentage between 0.00 µm and 3.90 µm : 11.81%
Percentage between 3.90 µm and 63.00 µm : 62.97%
Percentage between 63.00 µm and 2000.00 µm : 25.23%

REDFISH ISLAND GRAB 6 SURFACE SAMPLE

d(0.1): 3.074 um d(0.5): 16.375 um d(0.9): 104.970 n

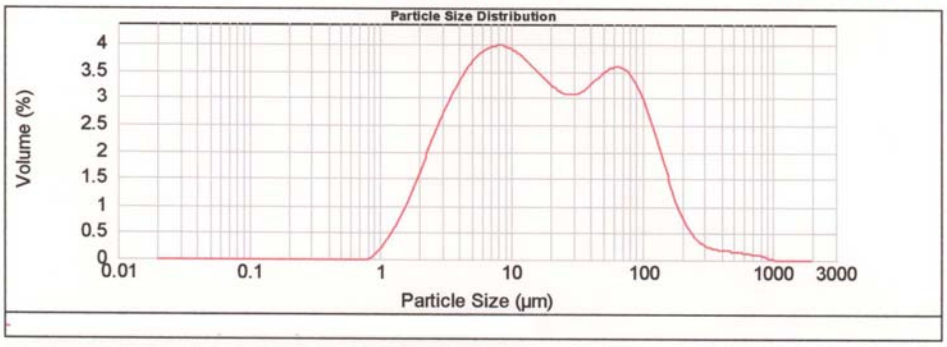

Percentage between 0.00 µm and 3.90 µm : 14.67%
Percentage between 3.90 µm and 63.00 µm : 64.09%
Percentage between 63.00 µm and 2000.00 µm : 21.24%

REDFISH ISLAND GRAB 8 SURFACE SAMPLE

d(0.1): 4.197 um d(0.5): 30.275 um d(0.9): 160.256 n

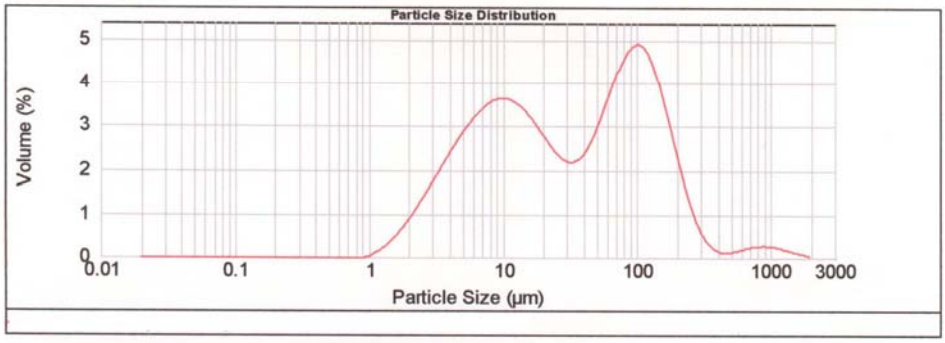

Percentage between 0.00 µm and 3.90 µm : 8.84%
Percentage between 3.90 µm and 63.00 µm : 53.98%
Percentage between 63.00 µm and 2000.00 µm : 37.18%

REDFISH ISLAND GRAB 9 SURFACE SAMPLE

d(0.1): 4.122 um d(0.5): 53.128 um d(0.9): 262.636 n

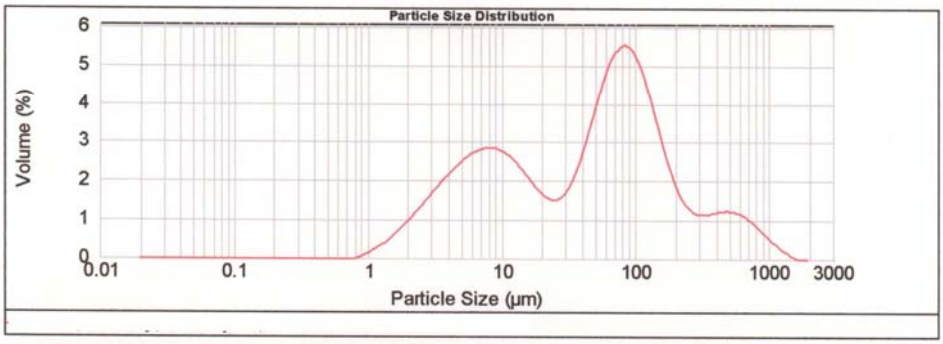

Percentage between 0.00 µm and 3.90 µm : 9.21%
Percentage between 3.90 µm and 63.00 µm : 45.85%
Percentage between 63.00 µm and 2000.00 µm : 44.94%

REDFISH ISLAND GRAB 10 SURFACE SAMPLE

d(0.1): 3.719 um d(0.5): 46.749 um d(0.9): 193.491 n

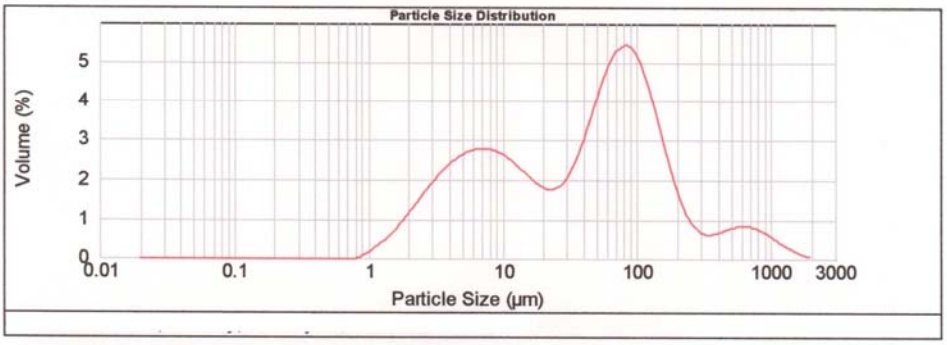

Percentage between 0.00 µm and 3.90 µm : 10.72%
Percentage between 3.90 µm and 63.00 µm : 47.81%
Percentage between 63.00 µm and 2000.00 µm : 41.47%

EAST BAY GRAB 1 SURFACE SAMPLE

d(0.1): 3.686 um d(0.5): 12.545 um d(0.9): 104.204 n

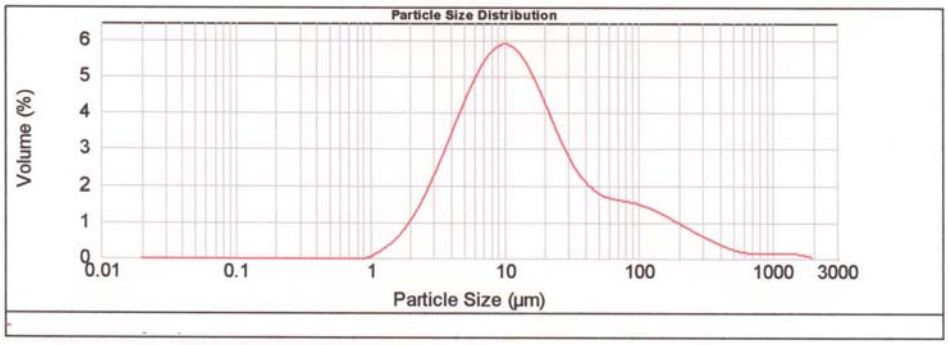

Percentage between 0.00 µm and 3.90 µm : 11.17%
Percentage between 3.90 µm and 63.00 µm : 73.69%
Percentage between 63.00 µm and 2000.00 µm : 15.14%

EAST BAY GRAB 2 SURFACE SAMPLE

d(0.1): 3.656 um d(0.5): 12.392 um d(0.9): 67.953 n

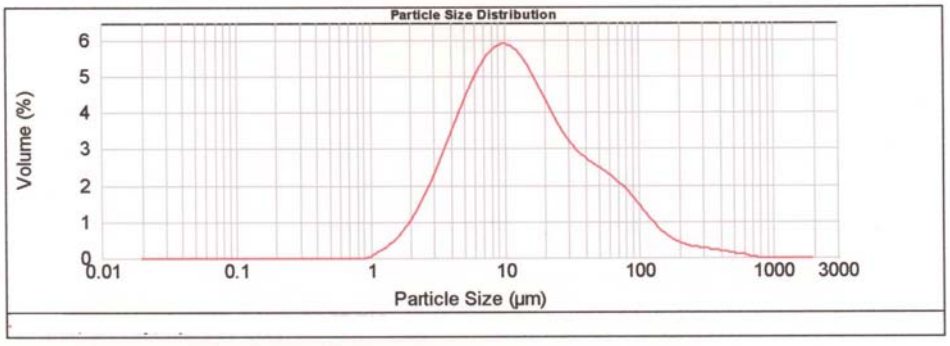

Percentage between 0.00 µm and 3.90 µm : 11.37%
Percentage between 3.90 µm and 63.00 µm : 77.55%
Percentage between 63.00 µm and 2000.00 µm : 11.08%

EAST BAY GRAB 3 SURFACE SAMPLE

d(0.1): 3.622 um d(0.5): 11.340 um d(0.9): 74.874 n

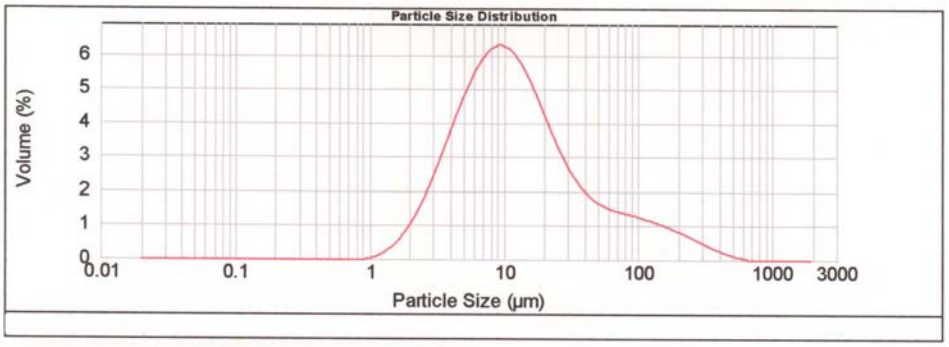

Percentage between 0.00 µm and 3.90 µm : 11.69%
Percentage between 3.90 µm and 63.00 µm : 76.69%
Percentage between 63.00 µm and 2000.00 µm : 11.61%

EAST BAY GRAB 4 SURFACE SAMPLE

d(0.1): 3.638 um d(0.5): 12.285 um d(0.9): 90.037 n

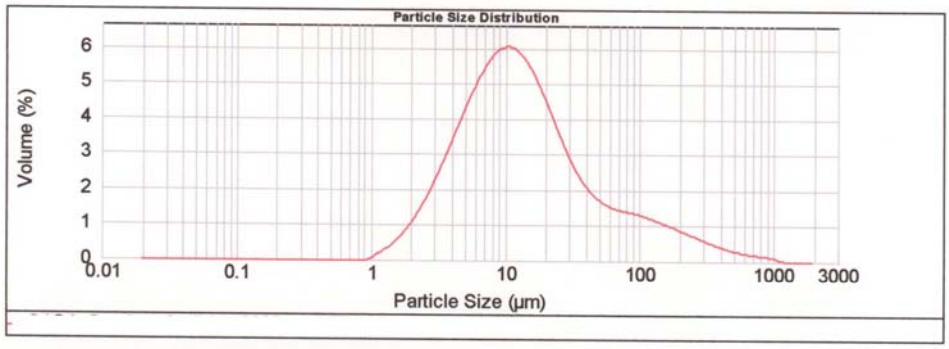

Percentage between 0.00 µm and 3.90 µm : 11.44%
Percentage between 3.90 µm and 63.00 µm : 75.25%
Percentage between 63.00 µm and 2000.00 µm : 13.31%

EAST BAY GRAB 5 SURFACE SAMPLE

d(0.1): 3.549 um d(0.5): 11.695 um d(0.9): 90.273 n

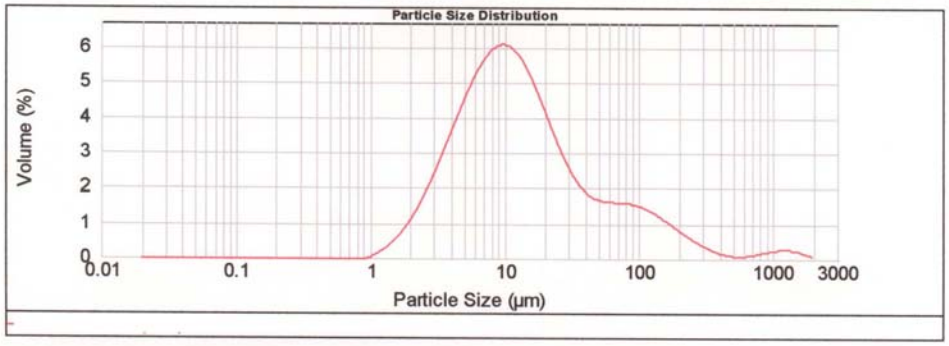

Percentage between 0.00 µm and 3.90 µm : 12.06%
Percentage between 3.90 µm and 63.00 µm : 74.22%
Percentage between 63.00 µm and 2000.00 µm : 13.73%

EAST BAY GRAB 6 SURFACE SAMPLE

d(0.1): 3.702 um d(0.5): 12.260 um d(0.9): 89.556 n

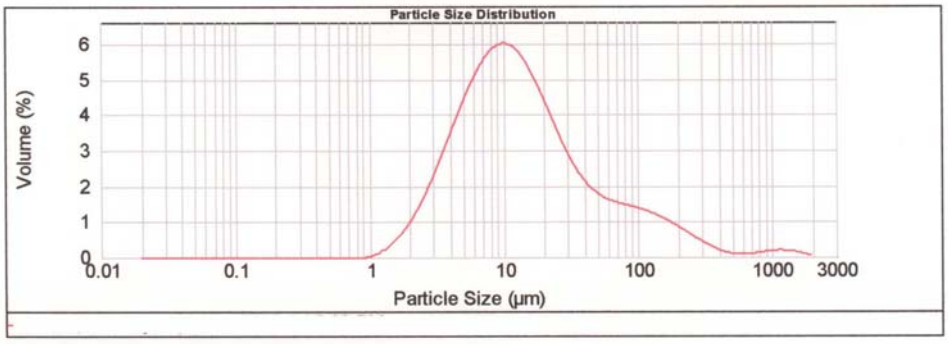

Percentage between 0.00 µm and 3.90 µm : 11.12%
Percentage between 3.90 µm and 63.00 µm : 75.42%
Percentage between 63.00 µm and 2000.00 µm : 13.47%

EAST BAY GRAB 7 SURFACE SAMPLE

d(0.1): 3.627 um d(0.5): 12.236 um d(0.9): 97.739 n

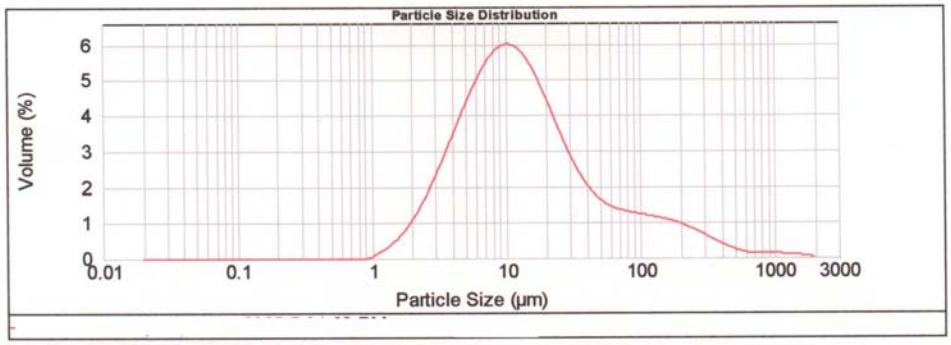

Percentage between 0.00 µm and 3.90 µm : 11.53%
Percentage between 3.90 µm and 63.00 µm : 74.70%
Percentage between 63.00 µm and 2000.00 µm : 13.77%

HANNAH'S REEF GRAB 1 SURFACE SAMPLE

d(0.1): 4.077 um d(0.5): 15.134 um d(0.9): 105.715 n

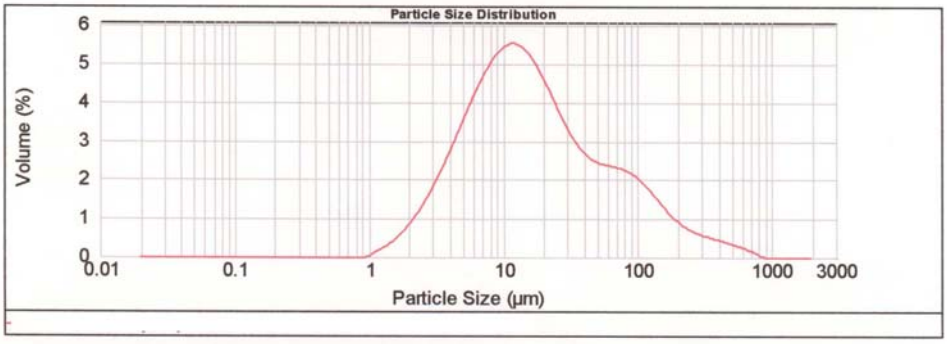

Percentage between 0.00 µm and 3.90 µm : 9.20%
Percentage between 3.90 µm and 63.00 µm : 73.34%
Percentage between 63.00 µm and 2000.00 µm : 17.46%

HANNAH'S REEF GRAB 4 SURFACE SAMPLE

d(0.1): 1.294 um d(0.5): 14.128 um d(0.9): 92.165 n

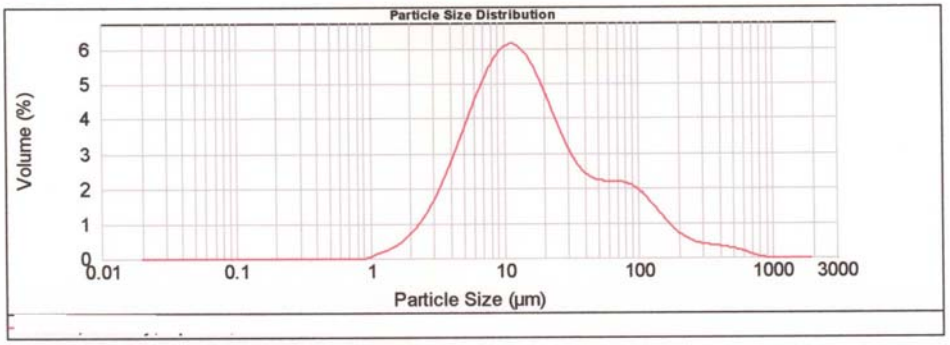

Percentage between 0.00 µm and 3.90 µm : 8.21%
Percentage between 3.90 µm and 63.00 µm : 76.47%
Percentage between 63.00 µm and 2000.00 µm : 15.32%

HANNAH'S REEF GRAB 6 SURFACE SAMPLE

d(0.1): 1.064 um d(0.5): 13.979 um d(0.9): 119.593 n

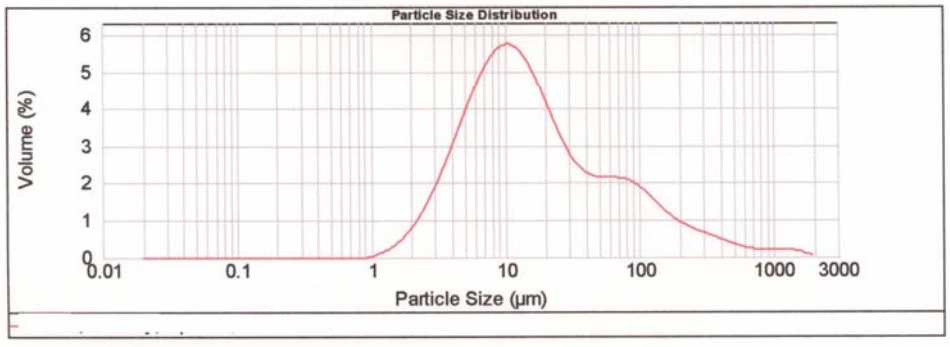

Percentage between 0.00 µm and 3.90 µm : 9.19%
Percentage between 3.90 µm and 63.00 µm : 72.51%
Percentage between 63.00 µm and 2000.00 µm : 18.30%

HANNAH'S REEF GRAB 9 SURFACE SAMPLE

d(0.1): 3.562 um d(0.5): 10.792 um d(0.9): 64.267 n

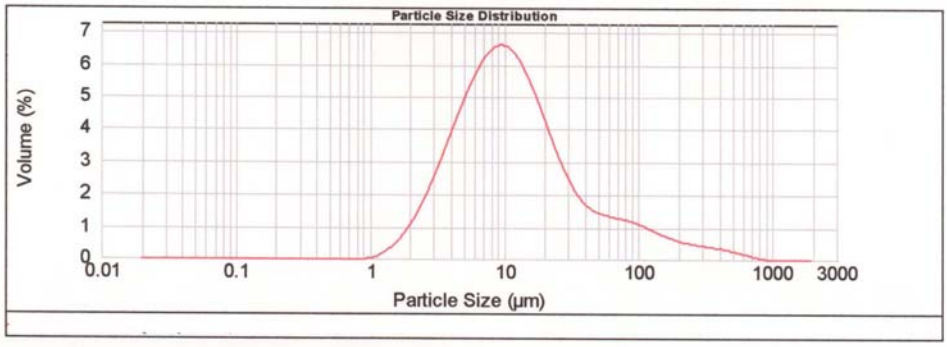

Percentage between 0.00 µm and 3.90 µm : 12.12%
Percentage between 3.90 µm and 63.00 µm : 77.71%
Percentage between 63.00 µm and 2000.00 µm : 10.17%

CLEAR LAKE ENTRANCE GRAB 1 SURFACE SAMPLE

d(0.1): 3.804 um d(0.5): 11.661 um d(0.9): 62.995 n

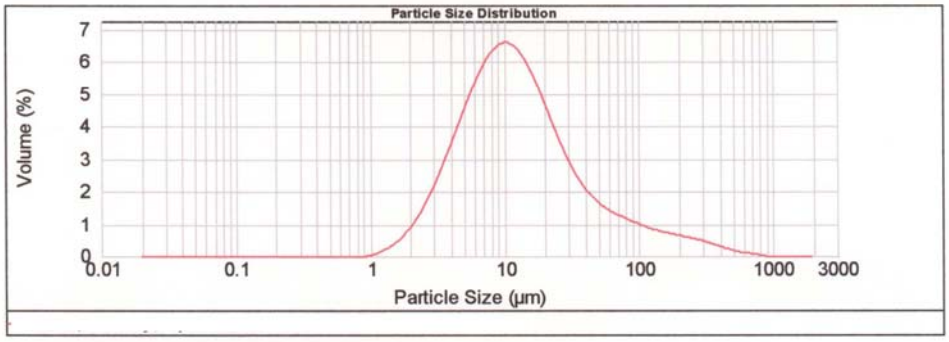

Percentage between 0.00 µm and 3.90 µm : 10.54%
Percentage between 3.90 µm and 63.00 µm : 79.46%
Percentage between 63.00 µm and 2000.00 µm : 10.00%

CLEAR LAKE ENTRANCE GRAB 3 SURFACE SAMPLE

d(0.1): 3.748 um d(0.5): 11.561 um d(0.9): 61.788 n

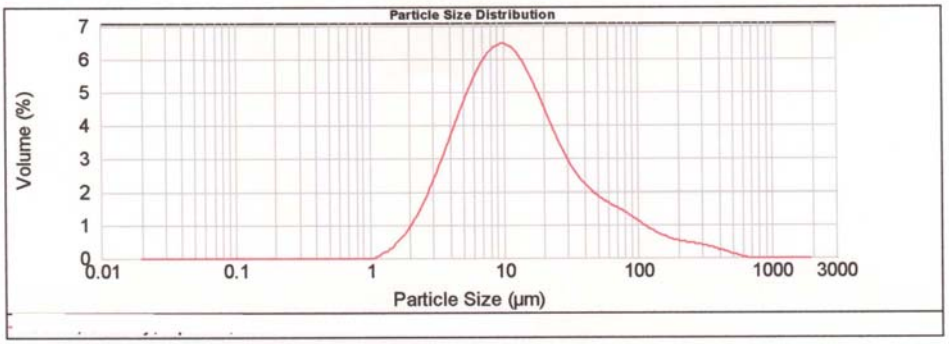

Percentage between 0.00 µm and 3.90 µm : 10.90%
Percentage between 3.90 µm and 63.00 µm : 79.31%
Percentage between 63.00 µm and 2000.00 µm : 9.79%

CLEAR LAKE ENTRANCE GRAB 3 SURFACE SAMPLE

d(0.1): 3.748 um d(0.5): 11.561 um d(0.9): 61.788 n

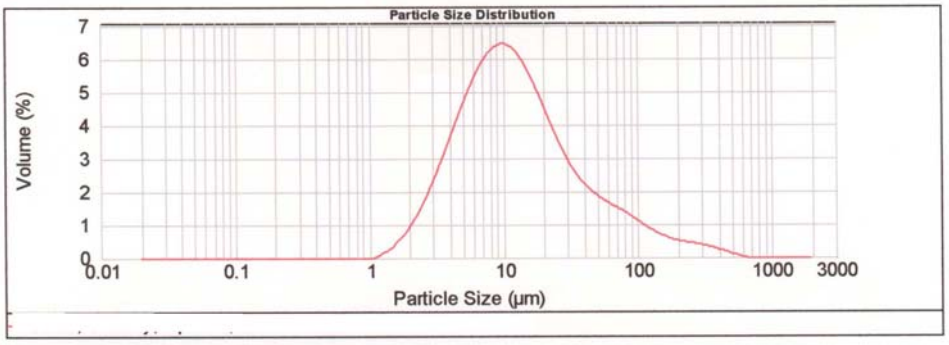

Percentage between 0.00 µm and 3.90 µm : 10.90%
Percentage between 3.90 µm and 63.00 µm : 79.31%
Percentage between 63.00 µm and 2000.00 µm : 9.79%

CLEAR LAKE ENTRANCE GRAB 4 SURFACE SAMPLE

d(0.1): 3.755 um d(0.5): 12.837 um d(0.9): 115.203 n

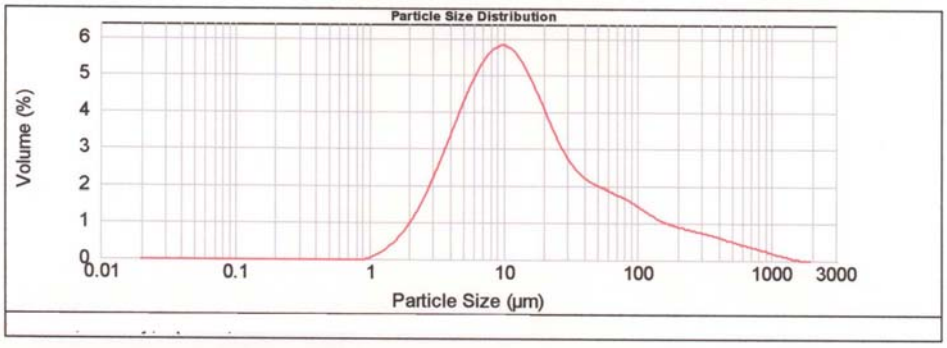

Percentage between 0.00 µm and 3.90 µm : 10.79%
Percentage between 3.90 µm and 63.00 µm : 72.92%
Percentage between 63.00 µm and 2000.00 µm : 16.30%

CLEAR LAKE ENTRANCE GRAB 5 SURFACE SAMPLE

d(0.1): 3.389 um d(0.5): 11.563 um d(0.9): 74.302 n

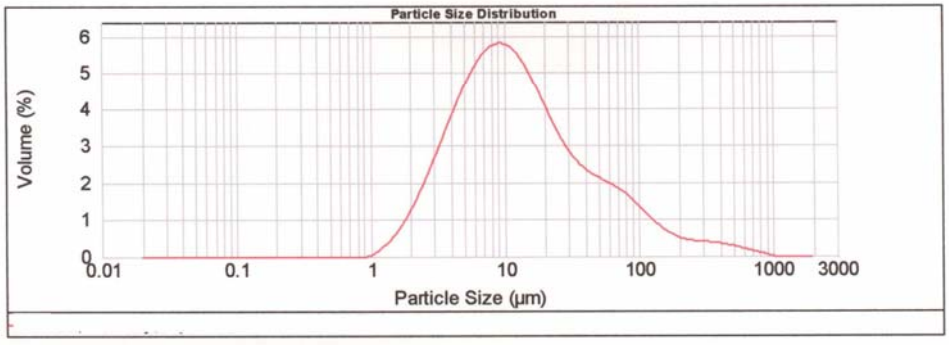

Percentage between 0.00 µm and 3.90 µm : 13.17%
Percentage between 3.90 µm and 63.00 µm : 74.83%
Percentage between 63.00 µm and 2000.00 µm : 12.00%

CLEAR LAKE ENTRANCE GRAB 7 SURFACE SAMPLE

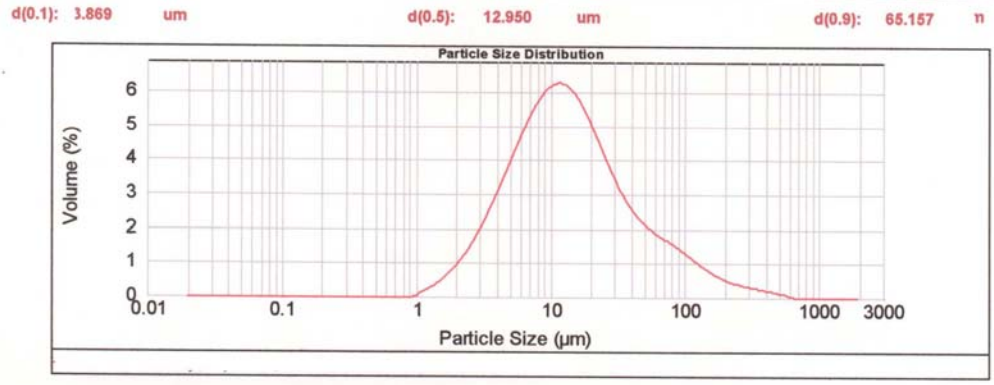

Percentage between 0.00 µm and 3.90 µm : 10.16%
Percentage between 3.90 µm and 63.00 µm : 79.45%
Percentage between 63.00 µm and 2000.00 µm : 10.40%

CLEAR LAKE ENTRANCE GRAB 9 SURFACE SAMPLE

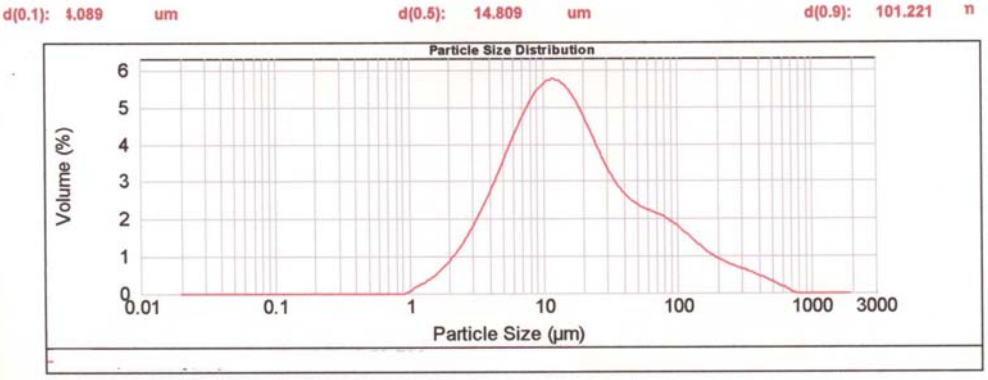

Percentage between 0.00 µm and 3.90 µm : 9.16%
Percentage between 3.90 µm and 63.00 µm : 74.61%
Percentage between 63.00 µm and 2000.00 µm : 16.23%

TRINTY BAY GRAB 1 SURFACE SAMPLE

d(0.1): 1.487 um d(0.5): 15.336 um d(0.9): 109.840 n

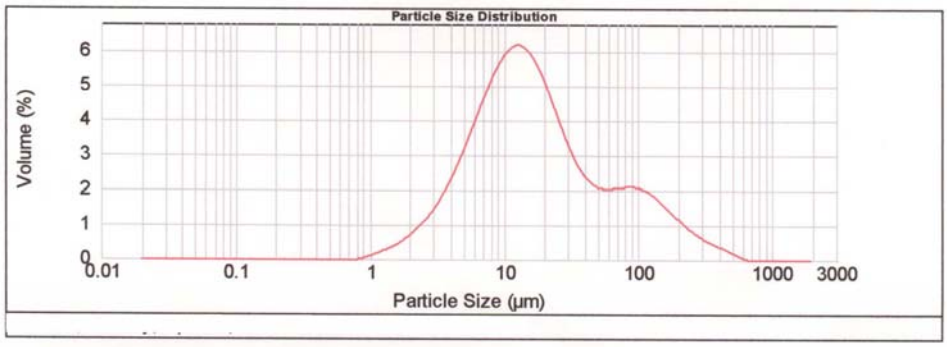

Percentage between 0.00 µm and 3.90 µm : 7.72%
Percentage between 3.90 µm and 63.00 µm : 74.79%
Percentage between 63.00 µm and 2000.00 µm : 17.49%

TRINITY BAY GRAB 3 SURFACE SAMPLE

d(0.1): 3.694 um d(0.5): 14.599 um d(0.9): 125.558 n

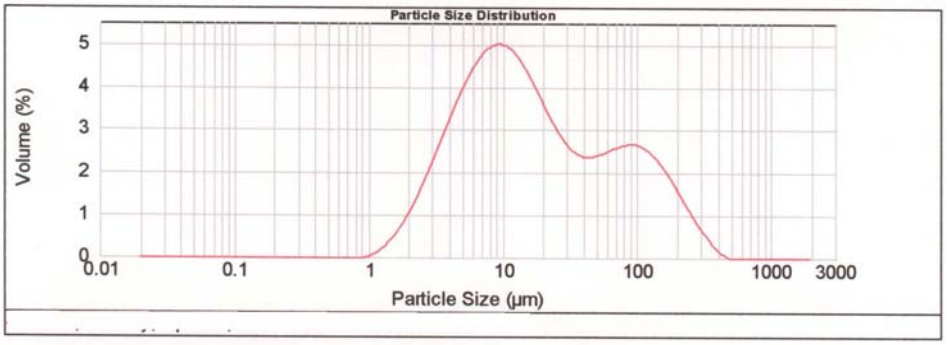

Percentage between 0.00 µm and 3.90 µm : 11.10%
Percentage between 3.90 µm and 63.00 µm : 67.22%
Percentage between 63.00 µm and 2000.00 µm : 21.68%

TRINITY BAY GRAB 4 SURFACE SAMPLE

d(0.1): 3.779 um d(0.5): 20.703 um d(0.9): 166.004 n

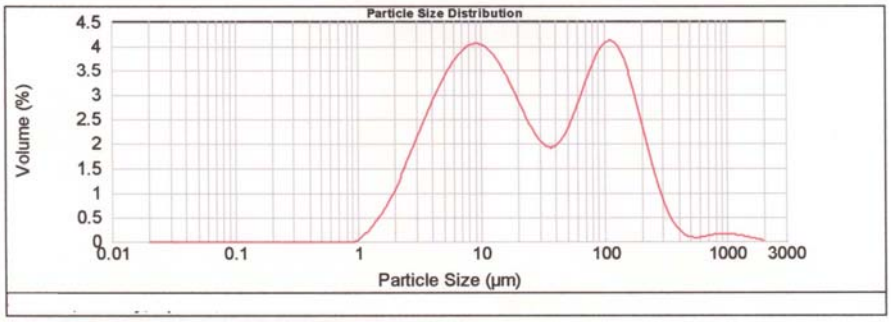

Percentage between 0.00 µm and 3.90 µm : 10.56%
Percentage between 3.90 µm and 63.00 µm : 55.77%
Percentage between 63.00 µm and 2000.00 µm : 33.67%

TRINITY BAY GRAB 5 SURFACE SAMPLE

d(0.1): 4.035 um d(0.5): 12.933 um d(0.9): 97.492 n

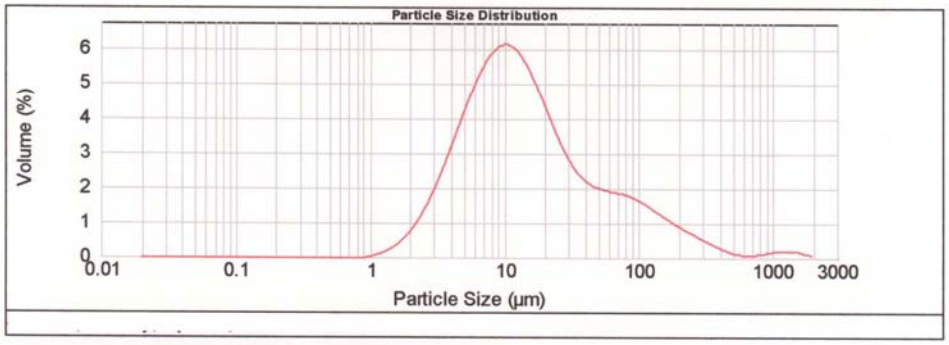

Percentage between 0.00 µm and 3.90 µm : 9.30%
Percentage between 3.90 µm and 63.00 µm : 75.59%
Percentage between 63.00 µm and 2000.00 µm : 15.12%

TRINITY BAY GRAB 6 SURFACE SAMPLE

d(0.1): 3.914 um d(0.5): 12.562 um d(0.9): 63.337 n

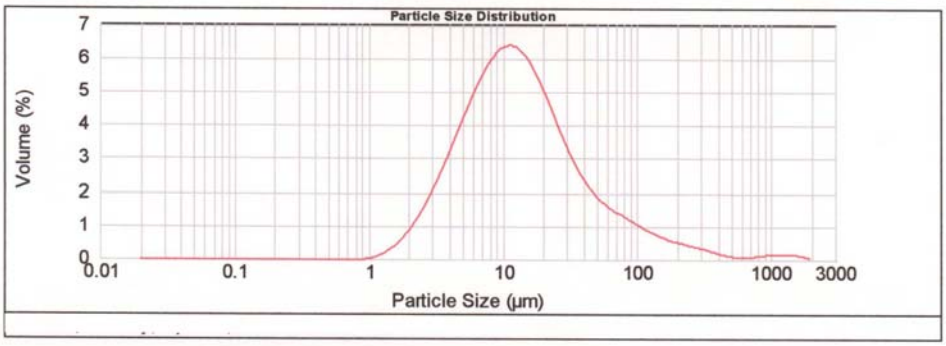

Percentage between 0.00 µm and 3.90 µm : 9.93%
Percentage between 3.90 µm and 63.00 µm : 80.02%
Percentage between 63.00 µm and 2000.00 µm : 10.05%

APPENDIX E

X-RADIOGRAPHS OF CORE SAMPLES

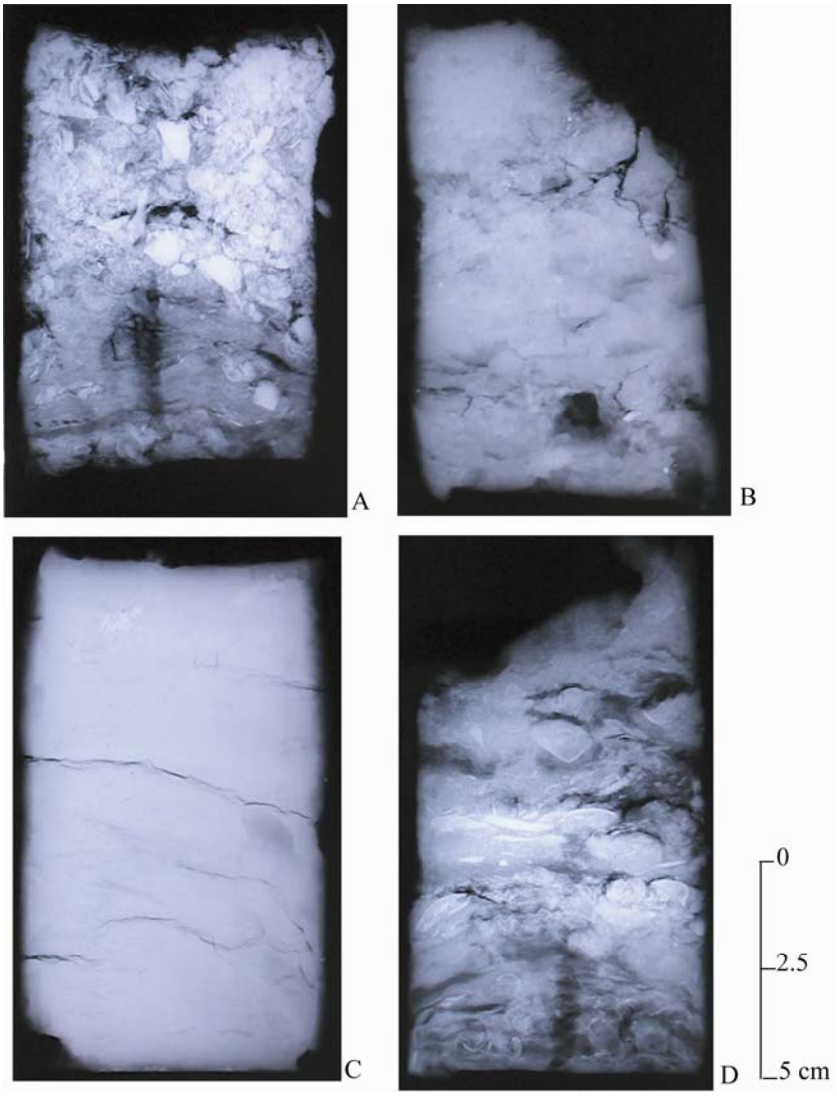

Figure 1: X-radiographs from cores in the Bolivar Roads survey area. **A** shows abundant shell debris. **B** shows sediment with little or no internal structure. **C** shows a core of dense material with no internal structures. **D** shows some layering with abundant marine shell debris.

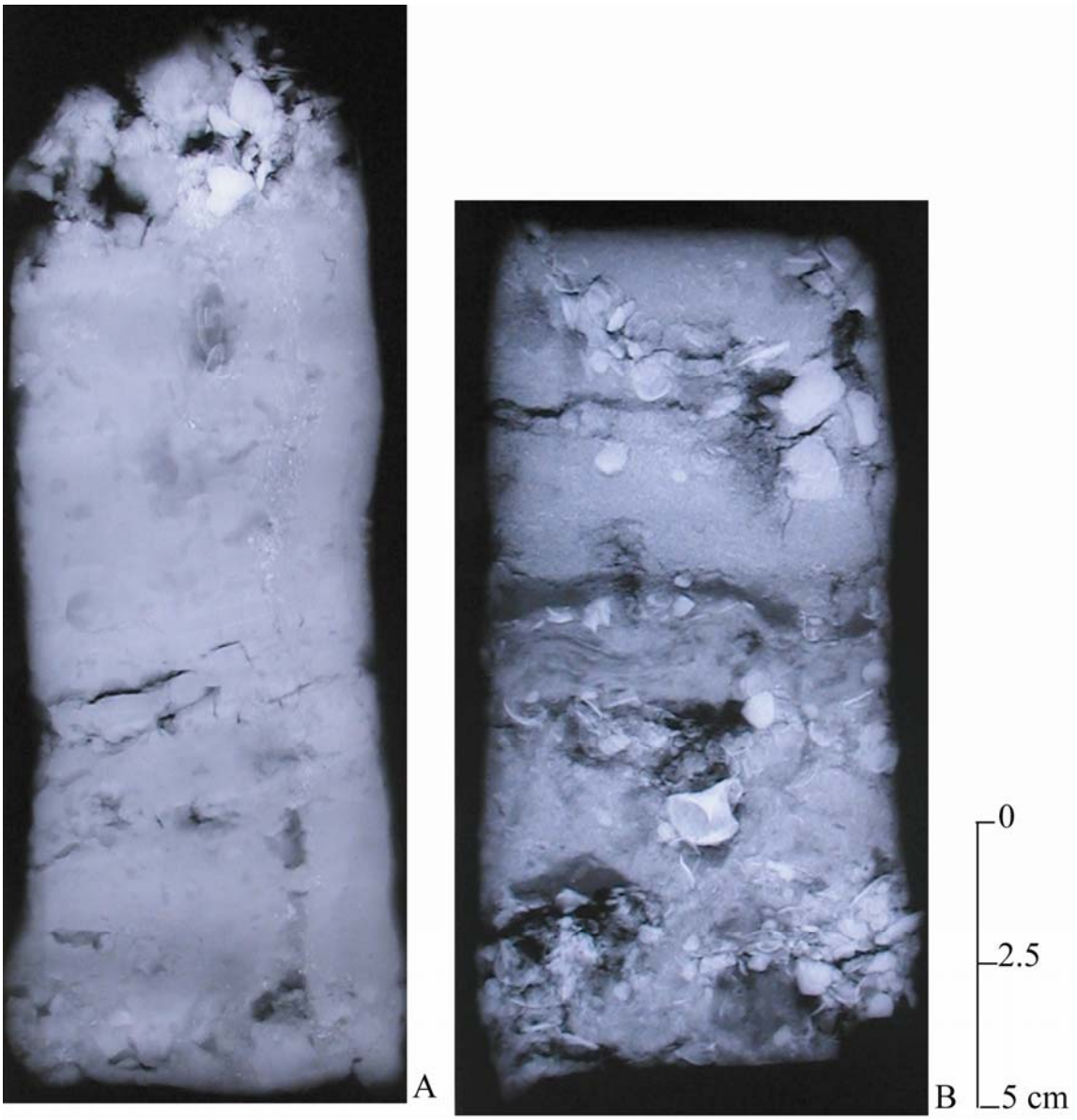

Figure 2: X-radiographs from cores in the Bolivar Roads survey area. **A** shows shell debris in the upper two cm of the core followed by coarse sediment showing no stratification. **B** shows sediment with some stratification and abundant marine shell debris.

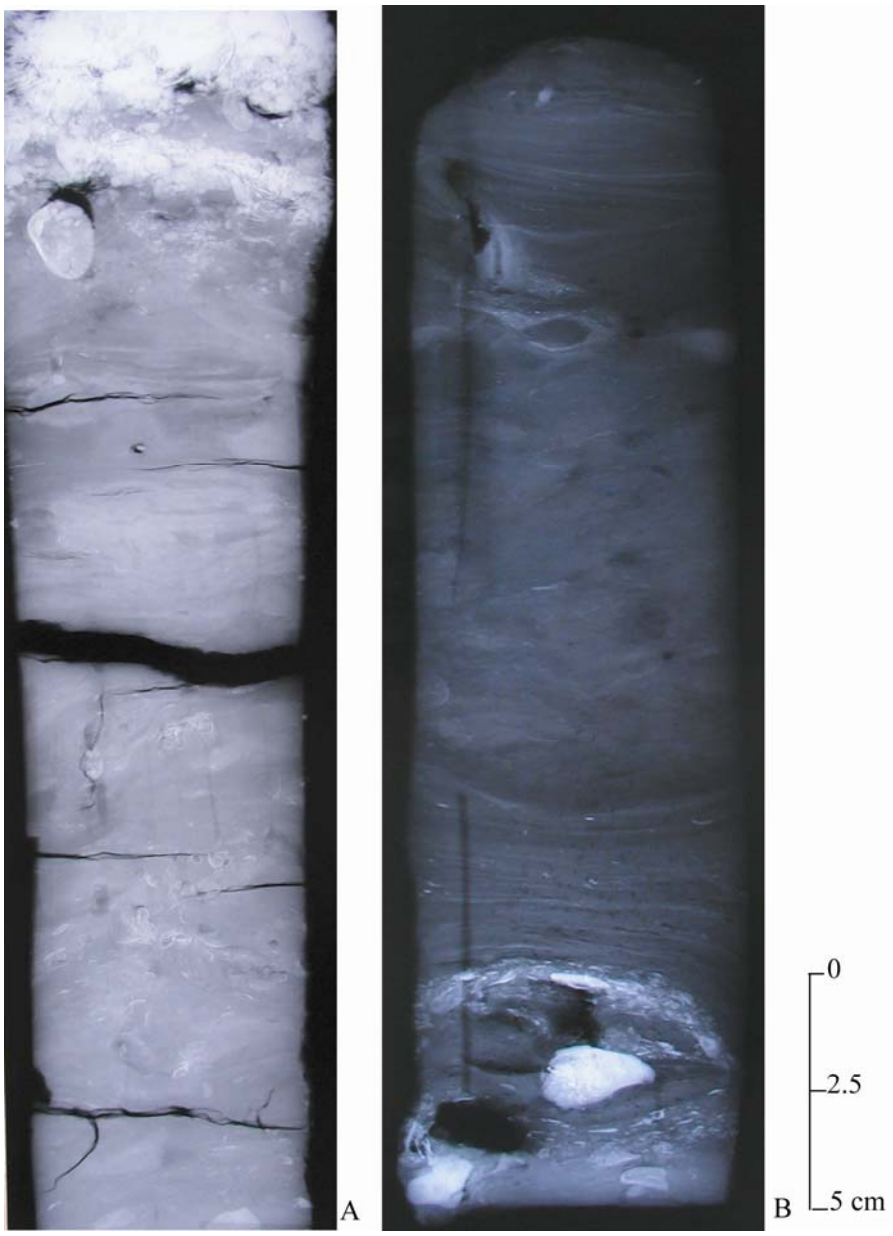

Figure 3: X-radiographs from cores in Bolivar Roads and Redfish Island survey area. **A** shows a core from the Bolivar Roads area with shell debris in the upper three cm of the core followed by coarse sediment with mild stratification and bioturbation displayed as dark circular and linear features in the core. The black section in the middle represents a crack in the core (i.e. area of no sediment). **B** shows a core from the Redfish Island survey area, displaying finer sediment which is highly stratified in the upper 5 cm and lower 8 cm with a highly bioturbated, non-stratified section in the middle. The lower three cm contains oyster shell debris.

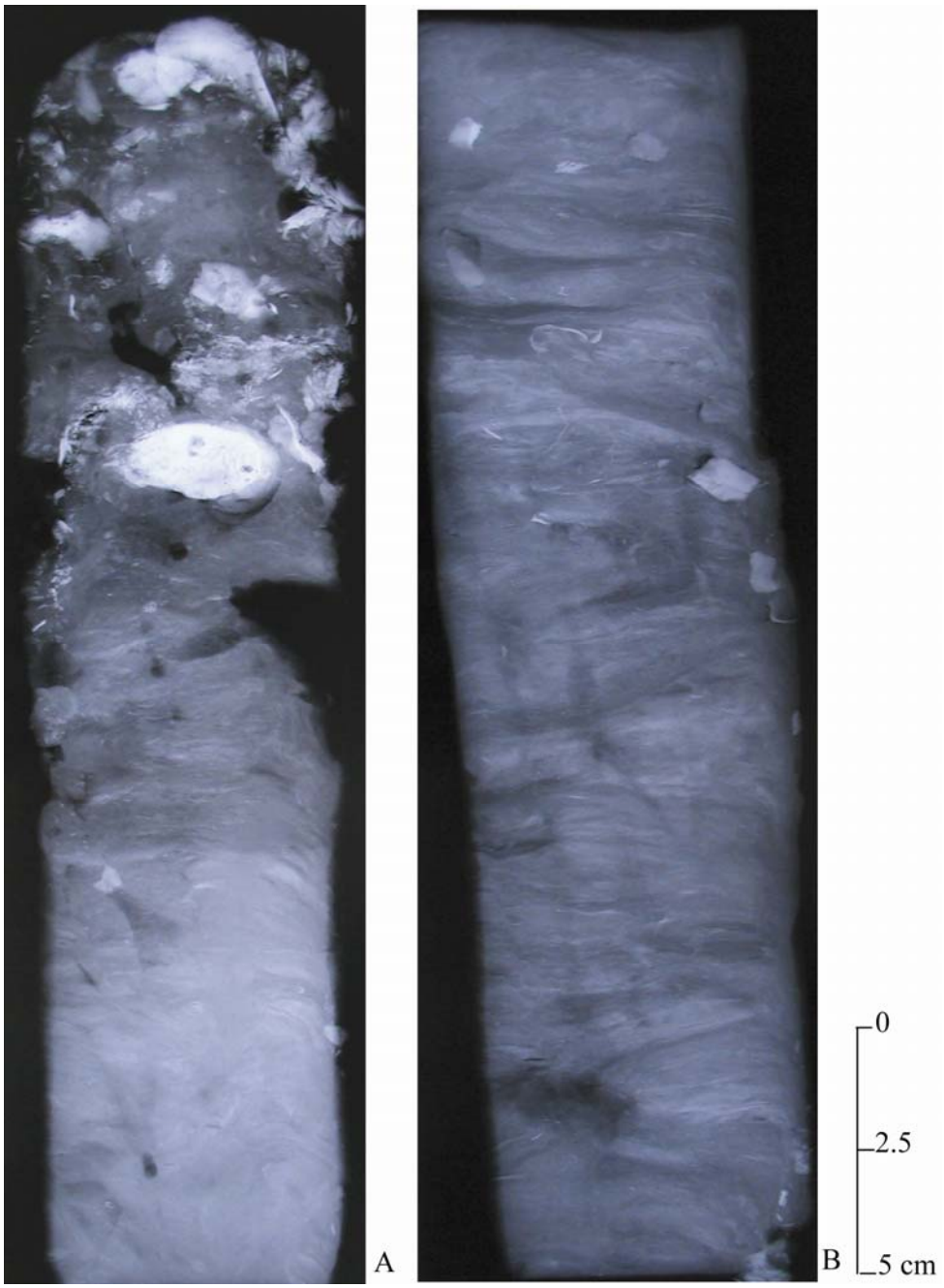

Figure 4: X-radiographs from a long core divided into two parts from the Redfish Island survey area. **A** shows the upper section of the core and contains oyster shell debris in the upper ten cm of the core followed by fine, bioturbated sediment and little stratification. **B** shows the lower section of the core with intermittent oyster shells and bioturbated, stratified sediment.

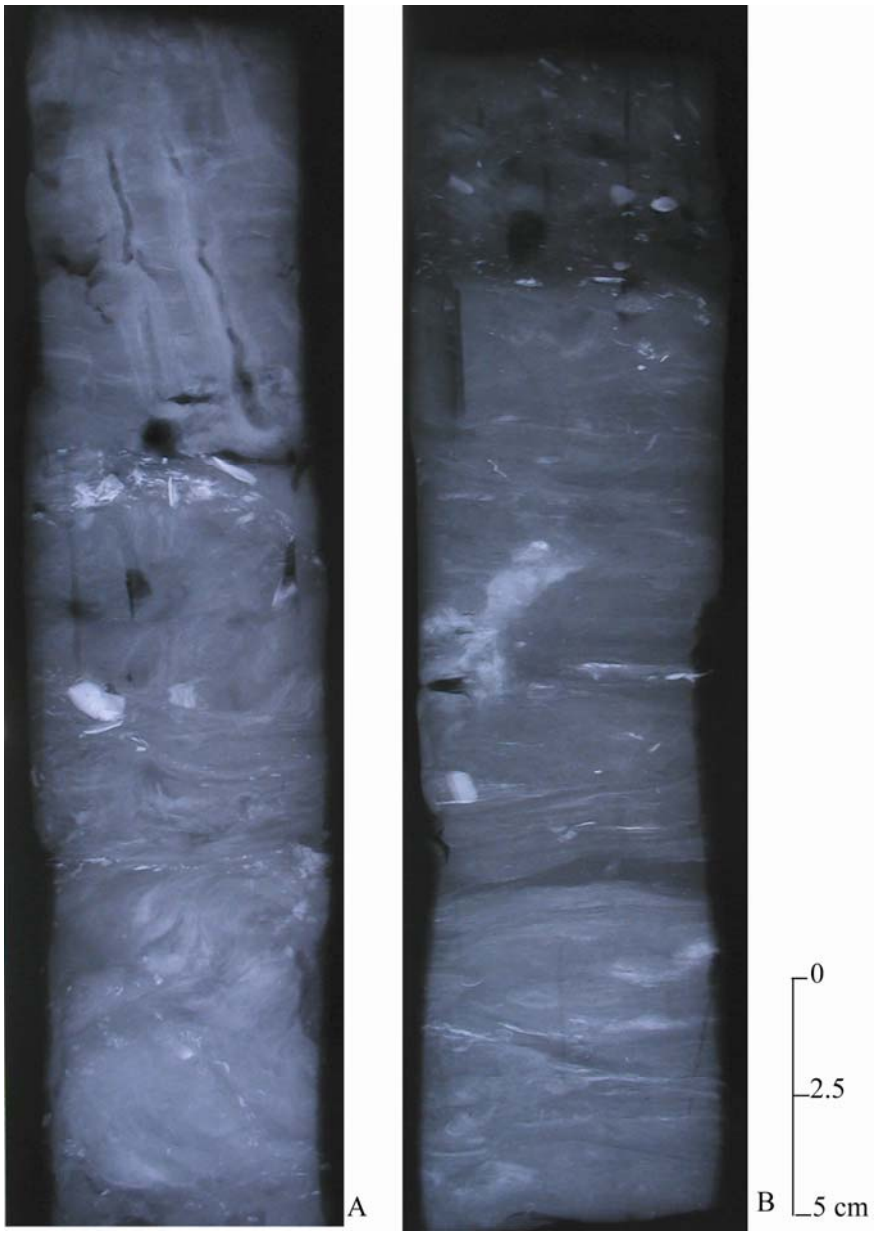

Figure 5: X-radiographs from a long core divided into two parts from the Redfish Island survey area. **A** shows the upper section of the core and contains intermittent oyster shell debris followed by fine, highly bioturbated sediment and little or no stratification. **B** shows the lower section of the core with intermittent oyster shells and bioturbated, weakly stratified sediment.

Figure 6: X-radiograph from a core from the Redfish Island survey area showing the no stratification and intermittent oyster shell debris. The black area in the center of the image is an anomaly caused by an air bubble trapped between the core and the x-ray tray.

VITA

Donald Shea Maddox attended Millsaps College in Jackson, MS, where he fulfilled the requirements for a B.S. in Geology. He attended Texas A&M University where he obtained a Master of Science in Geophysics. After completion of his M.S., he remained at Texas A&M University in order to earn his Ph.D. in Geology. He can be reached at 15423 Chestnut Falls Dr., Cypress, TX 77433.

PUBLICATIONS

- Maddox, D.S., W.W. Sager, and T. Dellapenna, 2005. Side-scan sonar imaging of bay bottom sediment and anthropogenic impacts in Galveston Bay, TX. Gulf Coast Association of Geological Societies Transactions, in press.
- Maddox, D.S., W.W. Sager, and T. Dellapenna, 2005. Side-scan sonar imaging of bay bottom sediment and anthropogenic impacts in Galveston Bay, TX: GSA Abstracts with Programs, vol. 37, no. 3.
- Maddox, D.S., W.W. Sager, and T. Dellapenna, 2004. Mapping bottom type and anthropogenic impacts on sediments in Galveston Bay, TX: GSA Abstracts with Programs, vol. 36, no. 1.
- Maddox, D.S., W.W. Sager, and T. Dellapenna, 2004. Mapping bottom type and anthropogenic impacts on sediments in Galveston Bay, Texas: 14th Annual Texas GIS Forum and Training Conference, April 2004.